



SAN FRANCISCO BAY AREA PRECIPITATION IN A WARMER WORLD

Volume 2 Future Precipitation Intensity,
Duration, and Frequency



Foreword by Brian Strong, Chief Resilience Officer:

Building a climate-resilient San Francisco requires us to understand and plan for current and future environmental hazards. Data and projections about the likely impacts of climate change can be used in the planning process to provide us with key information to establish policies for a climate-resilient city and to implement adaptive measures that can help protect our residents.

San Francisco's research into climate change impacts began in the early 2000's, as the City initially sought data on how a warming climate would affect our water supply. Since that time, we have been working on many different facets of climate change, including developing climate focused data sources to enable forward thinking decision making. As one example, we have already developed sufficient data to help us better understand how we can adapt to rising seas through the development of the [2014 Sea Level Rise Guidance for Capital Projects](#), [2016 Sea Level Rise Action Plan](#), and [2020 Sea Level Rise Vulnerability and Consequence Assessment](#).

Another priority has been to better understand the frequency and strength of precipitation events and how they may affect inland flooding. To do so, San Francisco undertook a unique, first of its kind in the nation climate modeling collaboration between a municipality, climate scientists at Lawrence Berkeley National Laboratory (LBNL), and climate consultants at Pathways Climate Institute to create a research team that focused on a better understanding of future precipitation events through climate modeling. Using supercomputing resources at LBNL's National Energy Research Scientific Computing Center (NERSC), the research team found that the effect of climate change on future storms is predicted to be significant, leading to more powerful events unleashing substantially more water. This initially resulted in a report published in [April 2022](#). This two-volume report (*San Francisco Bay Area Precipitation In A Warmer World, Volume 1: State of the Science and Volume 2: Future Precipitation Intensity, Duration, and Frequency*) provides groundbreaking scientific data on precipitation events for use by the entire City as we develop planning tools and policies to adapt to a changing climate with increasingly extreme storms. These two volumes highlight that both large and small storms are increasing in intensity.

The City agencies that funded these studies include the San Francisco Public Utilities Commission, San Francisco Office of Resilience and Capital Planning, San Francisco International Airport, and the Port of San Francisco. They are joined by other City agencies that will be using this data into develop and improve resilience plans.

The results of Citywide climate change research projects illustrate how San Francisco must think holistically about how to manage increased rainfall, sea level rise, drought, extreme heat, and other climate induced events. Toward that end we created the ClimateSF program which brings together key City agencies whose services could be critically impacted by climate change. These agencies are taking collective action through planning, policy, and guidance, championing a coordinated vision on climate resilience that streamlines City responses and promotes an equitable, safe, and healthy city for generations to come. The precipitation information in these volumes is fundamental to our ability to create meaningful solutions.

While this Extreme Precipitation study analyzed future potential rainfall in San Francisco, it can be modified and used throughout the Bay Area to enhance the region’s understanding of precipitation under a warming climate. The study’s findings may not be relevant outside of the Bay Area, therefore use of the study’s findings beyond the Bay Area is not recommended without independent scientific verification.



Brian Strong
Chief Resilience Officer
City and County of San Francisco



SAN FRANCISCO BAY AREA PRECIPITATION IN A WARMER WORLD

Volume 2: Future Precipitation Intensity,
Duration, and Frequency

Contents

Acknowledgments	01
Executive Summary	03
Measuring and Defining Storms	11
From Research to Application	16
Future Condition IDF Curves for 2050 and 2100	28
Other Climate Variables	40
Closing Thoughts	45
References	46



Acknowledgments

Stakeholder Committee



Anna Roche (Chair)
Sarah Minick
San Francisco Public Utilities Commission



Erin Cooke
Eugene Ling
Rinaldi Wibowo
Colton Yee
San Francisco International Airport



Brian Strong
Sandra Hamlat
Melissa Higbee
Office of Resilience and Capital Planning



Brad Benson
Matthew Wickens
Steven Reel
Port of San Francisco

Lead Authors



Michael Mak
James Neher
Christine L. May
Juliette Finzi Hart
Pathways Climate Institute



Michael Wehner
Lawrence Berkeley National Laboratory



Additional Acknowledgments

We would like to thank all the City and County of San Francisco staff that participated on the stakeholder committee and supported this effort.

Thank you to Susan Leal, Urban Water Works for her peer reviews of presentations, early submittals, and this report and as well as her commitment to support the critical translation of research-based climate science to actionable science to inform decision making.

We would especially like to thank Professor Christina Patricola, Iowa State University, for completing the Weather Research and Forecasting (WRF) modeling for both historical and future conditions. The WRF modeling and the analysis of the simulations used resources of the National Energy Research Scientific Computing Center (NERSC; <https://www.nersc.gov>; DOI: 10.13039/100017223), a U.S. Department of Energy Office of Science User Facility located at Lawrence Berkeley National Laboratory, operated under Contract No. DE-AC02-05CH11231. This work used the Extreme Science and Engineering Discovery Environment (XSEDE) computing resource Stampede2, which is supported by National Science Foundation grant number ACI-1548562, through allocations ATM190012 and ATM190016. The authors acknowledge the Texas Advanced Computing Center (TACC; <http://www.tacc.utexas.edu>) at The University of Texas at Austin for providing HPC resources that have contributed to the research results reported within this document.

Suggested Citation

Mak M, Neher J, May CL, Finzi Hart J, Wehner M. 2023. San Francisco Bay Area Precipitation in Warmer World. Volume 2: Future Precipitation Intensity, Duration, and Frequency. Prepared for the City and County of San Francisco.

Executive Summary



Background

For decades, climate scientists have warned of more intense storms that will occur more frequently. Recent scientific research highlights that today's extreme storm events are a mere preview of what is to come as the climate continues to warm. The San Francisco Bay Area (Bay Area) has experienced damage and disruption from numerous extreme storm events that delivered heavy precipitation and other severe storm conditions, such as strong winds and storm surge. These extreme precipitation events are expected to increase in intensity with climate change, increasing the likelihood of flooding, particularly when coupled with sea level rise.

For San Francisco, understanding how large storms might change under a warming climate was identified as a priority action for the City departments in the 2016 Sea Level Rise Action Plan (San Francisco, 2016). The San Francisco Public Utilities Commission (SFPUC), the Port of San Francisco (Port), the San Francisco International Airport (SFO), and the City and County of San Francisco's Office of Resilience and Capital Planning all have an interest in understanding how future storms could impact the City's residents, business activities, its critical infrastructure, and its natural resources. With funding from the four agencies, Pathways Climate Institute and Lawrence Berkeley National Laboratory (LBNL) completed this Extreme Precipitation Study to provide information that San Francisco can use to provide actionable information that San Francisco can use to prepare for future extreme precipitation.

The findings from this study are presented in two volumes to meet the needs of decision-makers and practitioners. Developed for City decision makers, Volume 1 provides an overview of the state of the science of extreme precipitation for San Francisco and the greater Bay Area region. Volume 2 (this volume) presents a suite of updated Intensity-Duration-Frequency (IDF) curves that incorporate projected changes in future precipitation through the end of the century. IDF curves describe the relationship between the probability of a certain amount of rain falling (intensity), for a certain amount of time (duration), and how often this combination will impact their area of interest (frequency).

For the purposes of these Guidebooks, and as defined by the National Oceanic and Atmospheric Administration National Severe Storms Laboratory, flooding "is an overflowing of water onto land that is normally dry. Floods can happen during heavy rains, when ocean waves come on shore, when snow melts quickly, or when dams or levees break. Damaging flooding may happen with only a few inches of water, or it may cover a house to the rooftop. Floods can occur within minutes or over a long period, and may last days, weeks, or longer. Floods are the most common and widespread of all weather-related natural disasters."

The findings and IDF curves presented use the highest emissions scenario evaluated by the Intergovernmental Panel on Climate Change (IPCC), which is associated with 4 to 5 degrees Celsius of warming by 2100 (IPCC, 2021). Volume 2 also provides a scaling mechanism whereby the results can be translated to any future warming scenario.

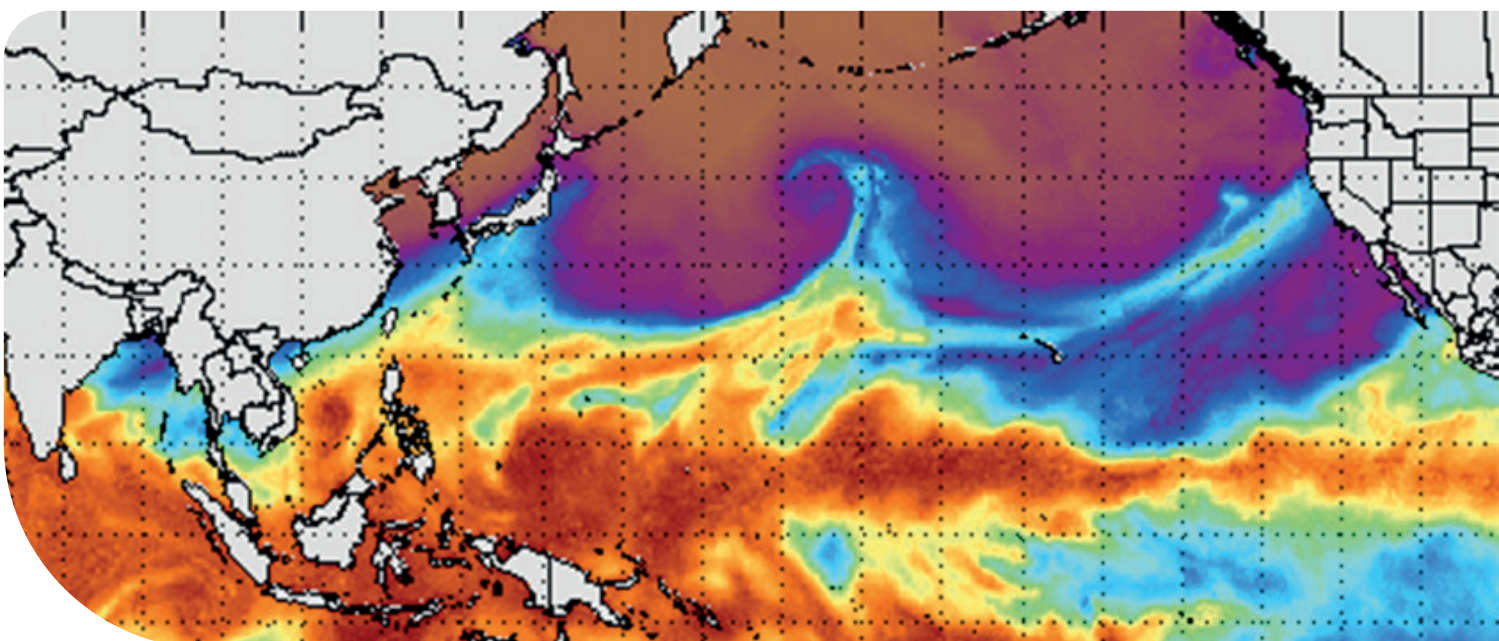
Bay Area Precipitation

The Bay Area has a Mediterranean climate, with about 75% of its annual average rainfall between November and March, and little to no rainfall occurring in summer. The Bay Area oscillates between extremes, with periods of below average annual rainfall (e.g., drought conditions) interspersed with years with above average annual rainfall. Two storm types bring rainfall to the Bay Area:

- **Extratropical cyclones (ETCs)** develop offshore and can bring cloudiness and mild showers to severe gales, thunderstorms, blizzards, and heavy rain.
- **Atmospheric rivers (ARs)** originate in the tropics and can bring light beneficial rain to torrential downpours and high winds.

Each storm type can occur on its own, or they can occur in combination, which represents the most common storm type affecting the West Coast (Zhang et al., 2019). A single AR event can also co-occur with a series of back-to-back ETCs. AR events can be associated with a series of back-to-back extratropical cyclones (Dacre & Pinto, 2020), as occurred during the early winter storms in 2022-2023. When an ETC is accompanied by a rapid atmospheric pressure drop, explosive cyclogenesis occurs. The rapid pressure drop creates a “bomb cycle” which is often associated with strong winds, heavy rains, and severe weather conditions (Sanders & Gyakum, 1980; Zhu & Newell, 1994).

The goal of the Extreme Precipitation Study was to understand how these storm types might change with a warming climate and how these changes impact rainfall projections.



Source: CalWater 2015

Volume 1 Findings



Volume 1 provides background on the current state of the science and defines key storm characteristics, presents the selected historical storms, and describes how these storms and storm types will change over time. Volume 1 also compares the findings to both the October 2021 Bomb Cyclone and the series of early winter 2022-2023 storms that made national headlines and caused widespread flooding throughout the Bay Area and much of California.

Based on the modeling, ARs and ETCs are likely to get more intense and severe as the climate warms (Patricola et al., 2022). Across all storms, storm duration increased, ranging from 9 – 24% increase in duration by 2050 and from 18 – 55% increase in duration by the end of century, both relative to historic conditions. ETCs, as well as the combination of ARs and ETCs, produced the greatest increase in total precipitation, ranging from 7 – 17% by 2050 and 26 – 37% by 2100, both relative to historic conditions (Patricola et al., 2022). The changes were also evaluated using the AR category (Cat) scale (akin to hurricane intensity scales we see during hurricane season) that provides predictive ranks, on a scale of 1 – 5, to incoming ARs based on integrated water vapor, the amount of moisture a storm system holds, and duration of event (Ralph et al., 2019). The scale ranges from Cat 1 (primarily beneficial) to Cat 5 (primarily hazardous). Rhoades et al (2020) showed an end-of-century shift from ARs being “mostly or primarily beneficial” to “mostly or primarily hazardous”. This shift is observed in the modeled storms. For all six storms modeled by LBNL, the AR categories increased in a warmer future, with some storms exceeding the Cat 1 – 5 scale and requiring an extension of the scale as high as 8.

In addition to analyzing the characteristics of how storms may change under a warming climate; we can also analyze the shorter duration intensities within the storms. Short-duration rainfall, such as the 1-hour or 3-hour duration, are more applicable to urban flooding and flash floods (Ayat et al., 2022). Analysis of the modeled storms reveals that the short durations are increasing at a faster rate than longer durations and storm totals. For example, the 5-year, 3-hour duration is projected to increase by 20% by 2050 and 56% by 2100, and the 100-year, 3-hour duration is projected to increase by 26% by 2050 and 67% by 2100 (Table 1). As the duration increases, the projected increase in precipitation decreases. For example, the 5-year, 24-hour duration is projected to increase by 17% by 2050 and 41% by 2100, and the 100-year, 24-hour duration is projected to increase by 22% by 2050 and 51% by 2100 (Table 2).

The change in storms can also be viewed as a change in storm frequency. For example, today's 5-year, 3-hour event could become a 2-year, 3-hour event by 2050, and a 1-year, 3-hour event by 2100. Today's 5-year, 24-hour event could become a 3-year, 24-hour event by 2050, and a 1.5-year, 24-hour event by 2100. Similarly, today's 100-year, 24-hour rainfall event could become a 40-year, 24-hour event by 2050, and a 20-year, 24-hour event by 2100.

	5-year, 3-hour		100-year, 3-hour	
	Inches	% Increase	Inches	% Increase
Historical	1.3	n/a	2.3	n/a
2050	1.5	20%	2.8	26%
2100	2.0	56%	3.8	67%

Table 1. Summary of total rainfall accumulation and percent change from historical in 5-year and 100-year return interval events for short-term (3-hour) duration for 2050 and 2100.

	5-year, 24-hour		100-year, 24-hour	
	Inches	% Increase	Inches	% Increase
Historical	3.0	n/a	5.8	n/a
2050	3.6	17%	7.1	22%
2100	4.3	41%	8.8	51%

Table 2. Summary of total rainfall accumulation and percent change from historical in 5-year and 100-year return interval events for long-term (24-hour) duration for 2050 and 2100.

Volume 2 Findings

Flooding and the intensification of storms have dominated news headlines in recent years, as the long-predicted impacts of climate change are becoming increasingly apparent across California, the U.S., and the globe. Irrespective of the type of storm, e.g., beneficial or hazardous, AR or ETC, or a combination of both, all storms associated with precipitation can be described by three intrinsic properties:

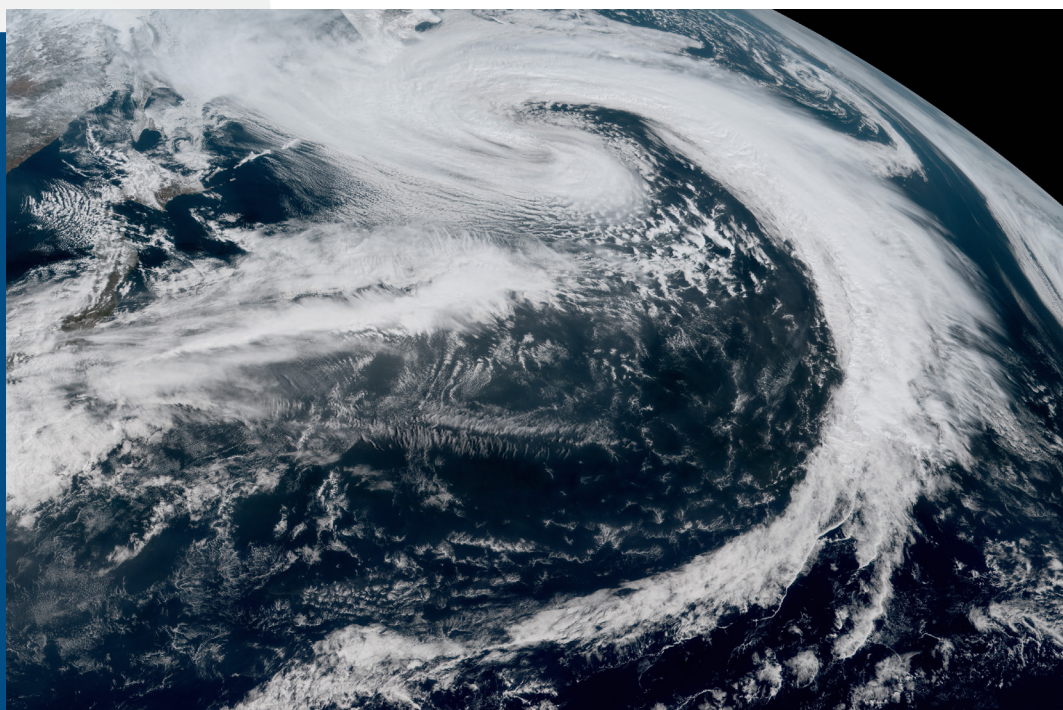
- **Intensity (I)** describes the amount of rainfall per unit of time (often expressed as inches / hour).
- **Duration (D)** describes the amount of time over which the rain falls (usually measured in minutes, hours, or days).
- **Frequency (F)** describes the probability of an event (e.g., intensity and duration) occurring with a given year or years (often expressed by return intervals).

With sufficient historical rainfall observations, IDF curves are created for a specific location for a specific rain gage. IDF curves describe the relationship between the probability of a certain amount of rain falling (intensity), for a certain amount of time (duration), and how often this combination will impact their area of interest (frequency). The longer the historic record, the more robust and or accurate – the resulting IDF curves would be. IDF curves allow a practitioner to quickly estimate how much precipitation may fall in a given duration and return period, as well as how sensitive that estimate is to changes in duration or return period. Unfortunately, IDF curves based on historical observations do not account for climate change and the increases in extreme precipitation that are already occurring. The development of robust future condition IDF curves for San Francisco and SFO are the primary focus of this assessment.

Using a hybrid methodology that combines best available climate science with the state-of-the-art regional climate modeling completed by LBNL, future condition IDF curves were developed that capture the changes observed across different durations. Scaling factors for scaling historical condition IDF curves for Bay Area communities are presented in this Guidebook, Volume 2, with location specific future condition IDF curves provided for the San Francisco (SF) Downtown and SFO weather stations (i.e., rain gages). An example is provided to demonstrate how different communities (within the broader Bay Area region) can use the scaling factors to derive their own location specific future condition IDF curves.

The future conditions IDF curves presented here are developed assuming a SSP5-8.5 climate future, which is the highest greenhouse gas emissions scenario considered by the Intergovernmental Panel on Climate Change (IPCC, 2021). However, the findings can be scaled to other climate scenarios, such as SSP3-7.0 and SSP2-4.5, if required for risk-based decision making or sensitivity analysis. The scaling approach also provides robustness as climate science evolves and emission trajectories are updated in future IPCC reports, as the scaling approach will still hold valid.

A future with higher static sea levels will exacerbate flooding from extreme precipitation. Initial modeling of wind, atmospheric pressure, and the ensuing waves and storm surge did not yield any immediately discernible patterns. However, the regional climate modeling was optimized for precipitation. More refined regional climate modeling that focuses on these different atmospheric components is needed to understand the compounding nature of extreme precipitation and other future atmospheric and oceanographic conditions.



Source: NOAA



Photo: Intersection of Valley Street and Church Street in San Francisco, CA, on December 31, 2022.

Photo Credit: 311 data and photos submitted by the public

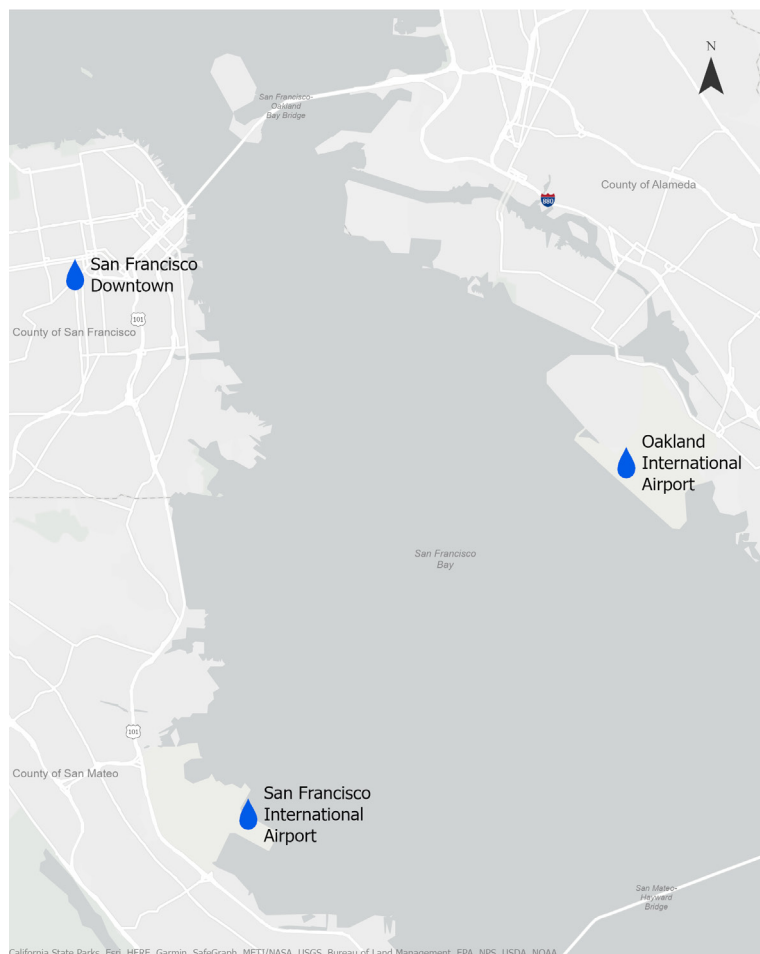
Measuring and Defining Storms

Understanding Storm Characteristics

Irrespective of the type of storm that impacts a community, e.g., AR versus ETC or a combination of both, all storms associated with precipitation can be described by three intrinsic properties:

- **Intensity (I)** describes the amount of rainfall per unit of time (often expressed as inches / hour).
- **Duration (D)** describes the amount of time over which the rain falls (usually measured in minutes, hours, or days).
- **Frequency (F)** describes the probability of an event (e.g., intensity and duration) occurring with a given year or years (often expressed by return intervals).

The recent series of storms that inundated the Bay Area during early winter 2022-2023 provide useful examples to demonstrate the different storm components and how they interact to yield different impacts on the ground throughout the broader Bay Area.



Map: Rainfall gages at San Francisco International Airport, Oakland International Airport, and Downtown San Francisco

Precipitation Intensity




Figure 1 presents the precipitation intensity (in inches per hour (in/hr) of rainfall) at three rain gages near San Francisco – the SF Downtown rain gage, SFO rain gage, and the Oakland International Airport (OAK) rain gage. The figures present the precipitation that fell during the series of storms between December 26, 2022 through January 16, 2023. While many news outlets reported nine distinct AR events, for the purpose of this discussion, the color-coding in Figure 1 divides the rainfall into five separate storm events, each separated by 34 hours of no precipitation. When examining the atmospheric pressure (Figure 18), it is possible to discern nine different low-pressure systems. These low-pressure bars are included in grey bands in Figure 1 for reference. But, for this Guidebook, we limit the discussion to the five distinctive and successive storms as five different storm events, referred as Storms 1- 5.

One can observe considerable variability in precipitation intensity within and across the different storm events, as well as across the geographies, as seen by the many different peaks and valleys on Figure 1, with Storm 2 by far the most intense of events across the three stations. During Storm 2, the most intense rainfall was recorded at the SF Downtown station (Figure 1a). During Storm 3, the highest peak intensity was recorded at the OAK station (relative to SF Downtown and SFO), and during Storm 5 the highest peak intensity was recorded the SFO rain gage (relative to the rain gages at SF Downtown and OAK).

These location-specific precipitation data demonstrate how variable and localized precipitation can be within the Bay Area. If this analysis was extended to San Jose in the South Bay and/or Vallejo in the North Bay, the variation in precipitation would increase further. As with the real estate adage, when working to understand the impact of a single storm within a given region, it all comes down to “location, location, location.” These localized storm impacts reaffirm the need for regional-scale climate modeling (such as that completed for this study) that can elucidate different topographical features that can influence both the storm track and amount of precipitation that falls, to provide more refined projections of future precipitation trends across the Bay Area.

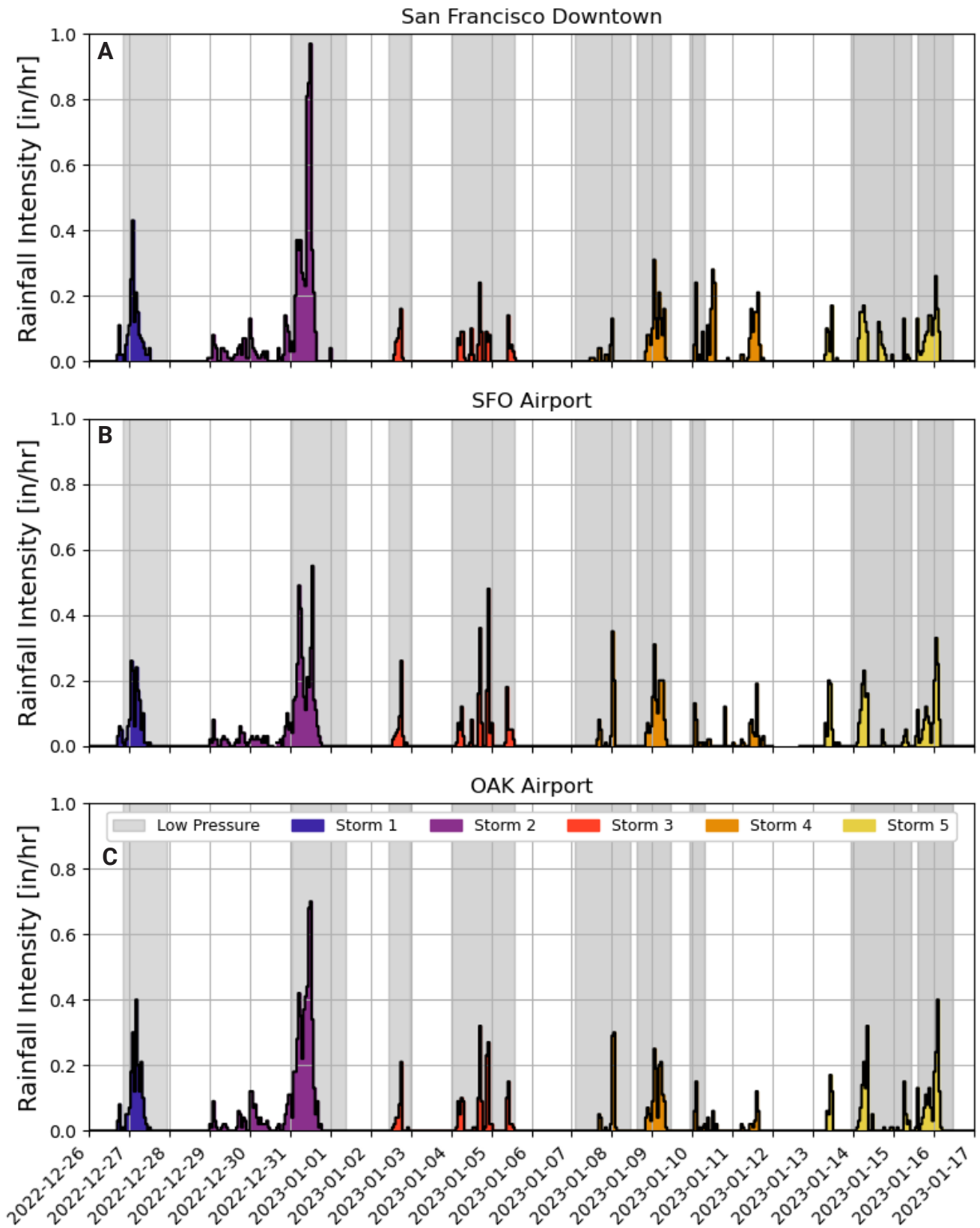


Figure 1. Rainfall Intensity at three Bay Area rain gages: (A) SF Downtown, (B) SFO, and (C) OAK

Precipitation Duration and Return Period

Figure 2 presents that maximum rainfall for each duration, for each storm, across the three rain gage locations, and Figure 3 presents the corresponding return period (based on the historical record using the National Oceanic and Atmospheric Administration (NOAA) Atlas 14). Similar to Figure 1, the highest rainfall across all durations, for the three locations, occurred during Storm 2.

At SF Downtown, the 3-hour and 12-hour durations had return periods of ~300-years (Figure 3a). At the SF Downtown rain gage, the 6-hour duration had a return period of about 200 years, and the 24-hour duration had return period of about 100 years. The heaviest precipitation at the San Francisco rain gage fell during a 6-hour period that corresponded with low Bay water levels. Except for Storm 2, the other storms had return periods of 2 years or less. However, the serial nature of storms can create flooding conditions far worse than if each storm occurred in isolation (Fish et al., 2022). As evidenced by the 13 ARs (to date) during 2022-2023. As the climate continues to warm, years with multiple AR episodes will increase, the ARs will be warmer and hold more water vapor leading to potential heavier rainfall events, and the AR season is expected to lengthen (Dettinger et al., 2011).

At the SFO gage, Storm 2 was less intense, with the 12-hour duration just above a 25-year return period, and a 2-day duration of a ~10-year return period (Figure 3b). The return periods for Storms 3, 4 and 5 were slightly higher as measured at the SFO rain gage than at the SF Downtown rain gage, but still largely below the 2-year return period. At the OAK rain gage, Storm 2 was more closely correlated with the SF Downtown rain gage. The precipitation at the OAK rain gage was about 0.3 to 0.5 inches less across all durations than the SF Downtown rain gage, resulting in lower return periods. Only the 12-hour duration exceeded the 100-year return period, and the 6-hour and 24-hour durations were about a 50-year return period.

The differences in Storm 2 across these stations highlights that the maximum rainfall band was centered directly over San Francisco and headed over the SF Bay towards Oakland. SFO, which is about 10 miles south of San Francisco, was located outside of the maximum rainfall band for Storm 2.

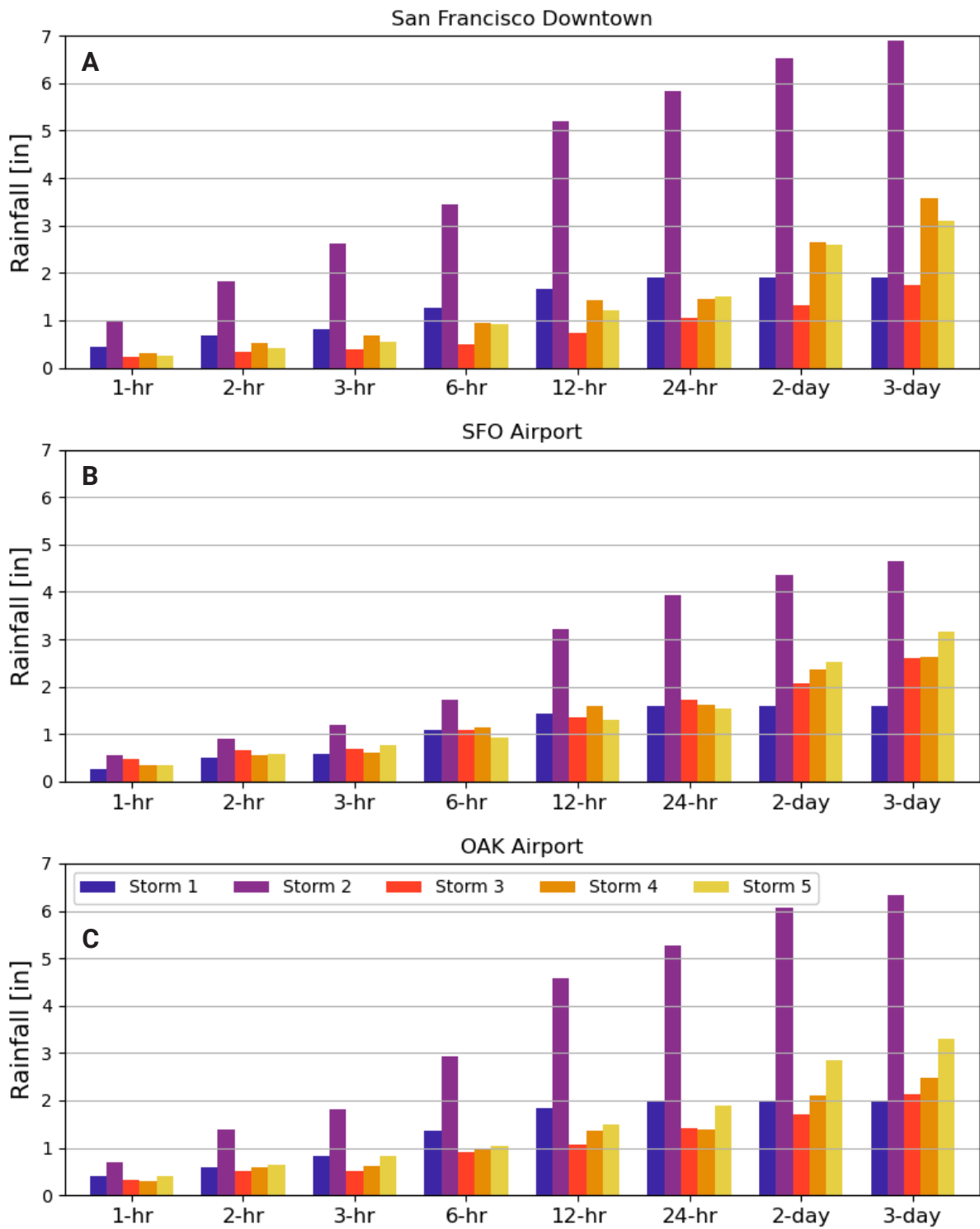


Figure 2. Rainfall totals by duration at three Bay Area rain gages: (A) SF Downtown, (B) SFO, and (C) OAK

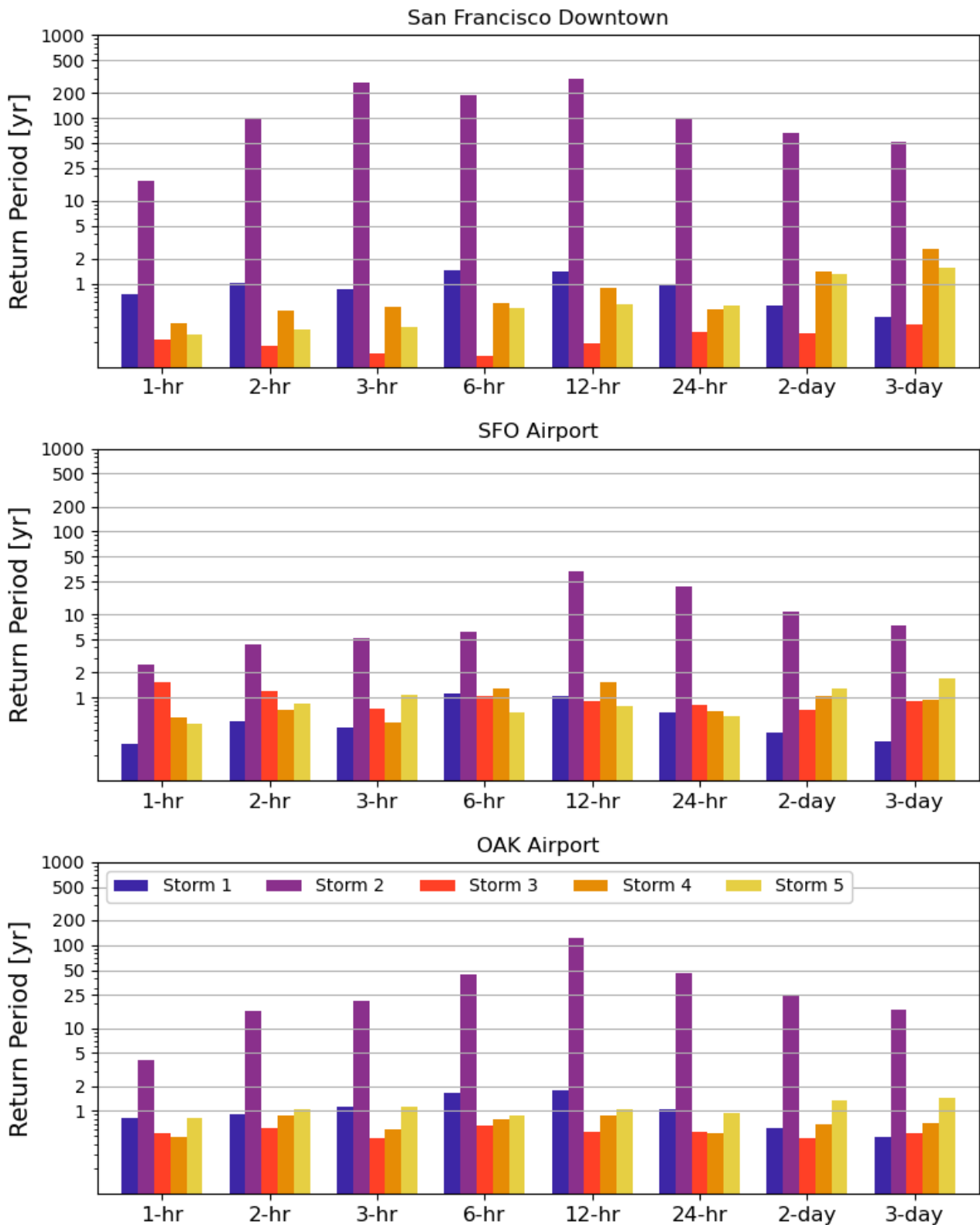


Figure 3. Rainfall totals by duration at three Bay Area rain gages: (A) SF Downtown, (B) SFO, and (C) OAK



Spotlight on Storm Duration

Looking more closely at Storm 2 at the SF Downtown gage, Figure 4 shows that the highest intensity of rainfall occurred during a strong burst towards the end of the event, during which 2.6 inches of precipitation fell within the peak 3-hour storm duration window. The peak 6-hour storm duration that yielded 3.4 inches of rain overlapped with the peak 3-hour storm duration, and these were both enveloped within the peak 24-hour storm duration, which registered 5.8 inches of rainfall accumulation. Storm durations refer to discrete periods within a storm, such as the 3-hour period with the maximum accumulation of rainfall, and not a discrete storm event that is 3-hours long.

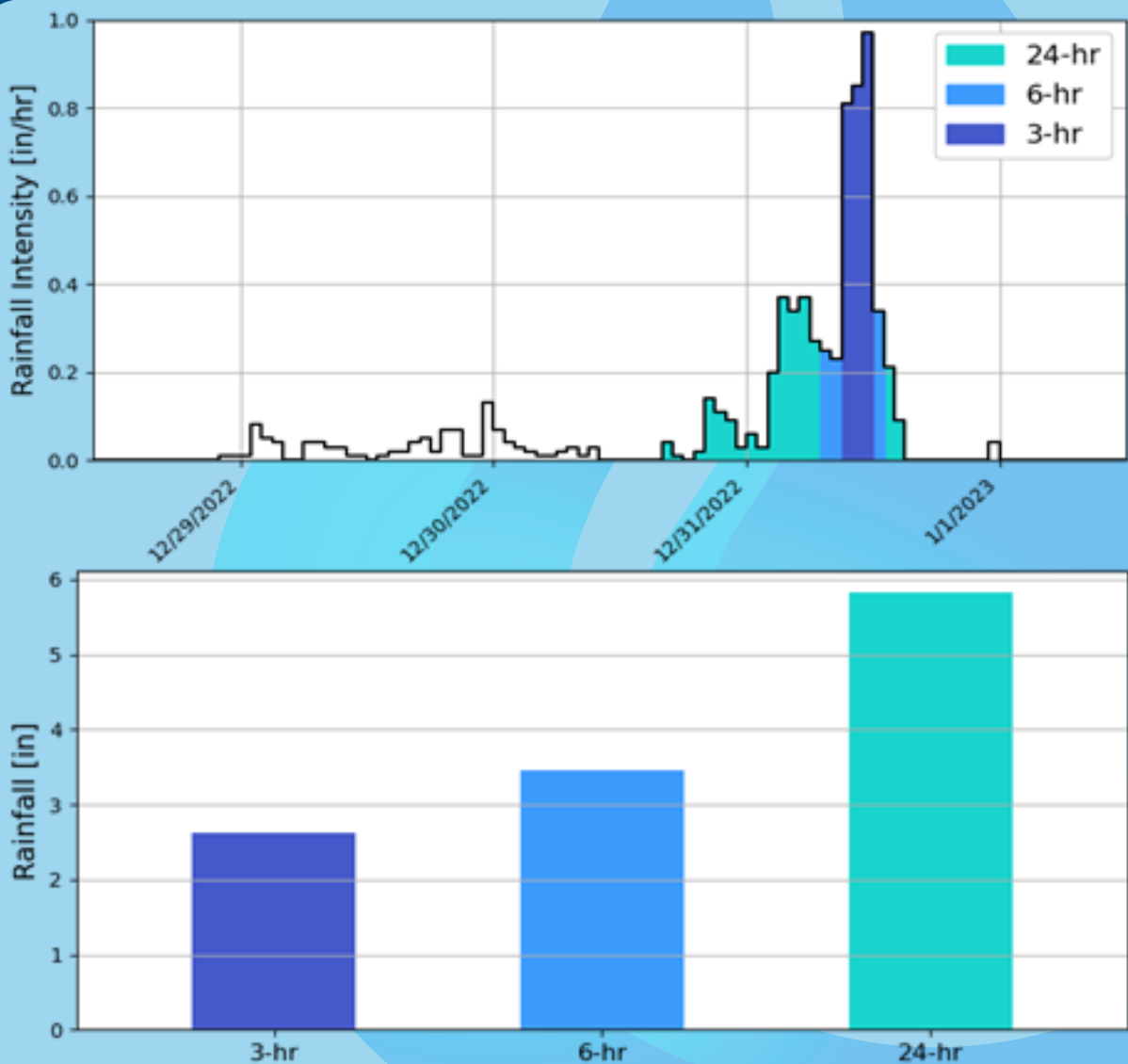


Figure 4. Storm 2 Intensity and Duration at the SF Downtown Gage



From Research to Application

Modeling Changes to Storms Intensity, Duration, and Frequency Under a Warming Planet

To understand how intensity, duration, and frequency may change in the future, and as described in Volume 1, LBNL modeled how six historical storms may change under a warmer future. Analysis of these simulations have provided insight into how storms may change from the short durations to the storm total precipitation. This information forms the foundation for developing future condition IDF curves.

What are IDF Curves?

IDF curves describe the relationship between the probability of a certain amount of rain falling (intensity), for a certain amount of time (duration), and how often this combination will impact their area of interest (frequency). IDF curves are used by a wide range of practitioners, including engineers, water resource managers, and planners to manage the impact and risks related to extreme rainfall, and in the design of hydrologic, hydraulic, and stormwater conveyance systems.

IDF curves rely on frequency analysis of historic rainfall observations; therefore, IDF curves are created for a specific location at a rain gage. The longer the historic record, the more robust or accurate the resulting IDF curves would be. IDF curves allow a practitioner to quickly estimate how much precipitation may fall in a given duration and return period, as well as how sensitive that estimate is to changes in duration or return period.

Most cities, municipalities, or sewer districts select a specific IDF combination as a LOS storm or design storm as the basis for designing and sizing flood risk reduction and stormwater conveyance systems. IDF curves support sensitivity testing and risk-based decisions, such as informing evaluations of system performance related to larger storms to assess if cost effective strategies could be implemented to reduce the likelihood of localized flooding. IDF curves also inform street design as some streets can convey stormwater within the curb line of the streets.

Existing IDF Curves for the Bay Area

In the U.S. , NOAA Atlas is the *de-facto* standard for designing, building, and operating utility infrastructure relative to precipitation (Ragno et al., 2018a; Smirnov et al., 2018; Tetra Tech Inc., 2015). For stormwater utilities, IDF curves are either based directly on NOAA Atlas 14, or the NOAA Atlas 14 curves are validated and/or adjusted to represent local conditions using local rain gage observations (Cheng & Aghakouchak, 2014; Ragno et al., 2018a; Smirnov et al., 2018). The SFPUC regularly validates their IDF curves and design storm with the observational record (May & Mak, 2013).

Precipitation frequency point estimates for the state of California in Atlas 14 Volume 6 were developed by the National Weather Service (NWS) and NOAA in 2011. NWS analyzed annual maxima time series at rain gages throughout the state to develop IDF curves as precipitation frequency point estimates for 5-minute through 60-day durations, and recurrence intervals of 1-year through 1,000-year. Precipitation frequency estimates for Atlas 14 were derived from 8,278 rain gages from multiple sources.

Figure 5 shows the NOAA Atlas 14 Volume 6 IDF Curve for Downtown San Francisco. Projected precipitation accumulation, or depth as a proxy for intensity (I), is presented on the y-axis in inches. Storm durations (D) are included along the x-axis, ranging from the 15-min to 24-hour storm durations. The different colored curved lines represent different storm return frequencies (F), ranging from the 1-yr to the 500-yr return interval. Table 3 provides the same information as Figure 5 in tabular format so that practitioners can quickly select the projected rainfall accumulation for their storm of interest, design storm, or level of service.

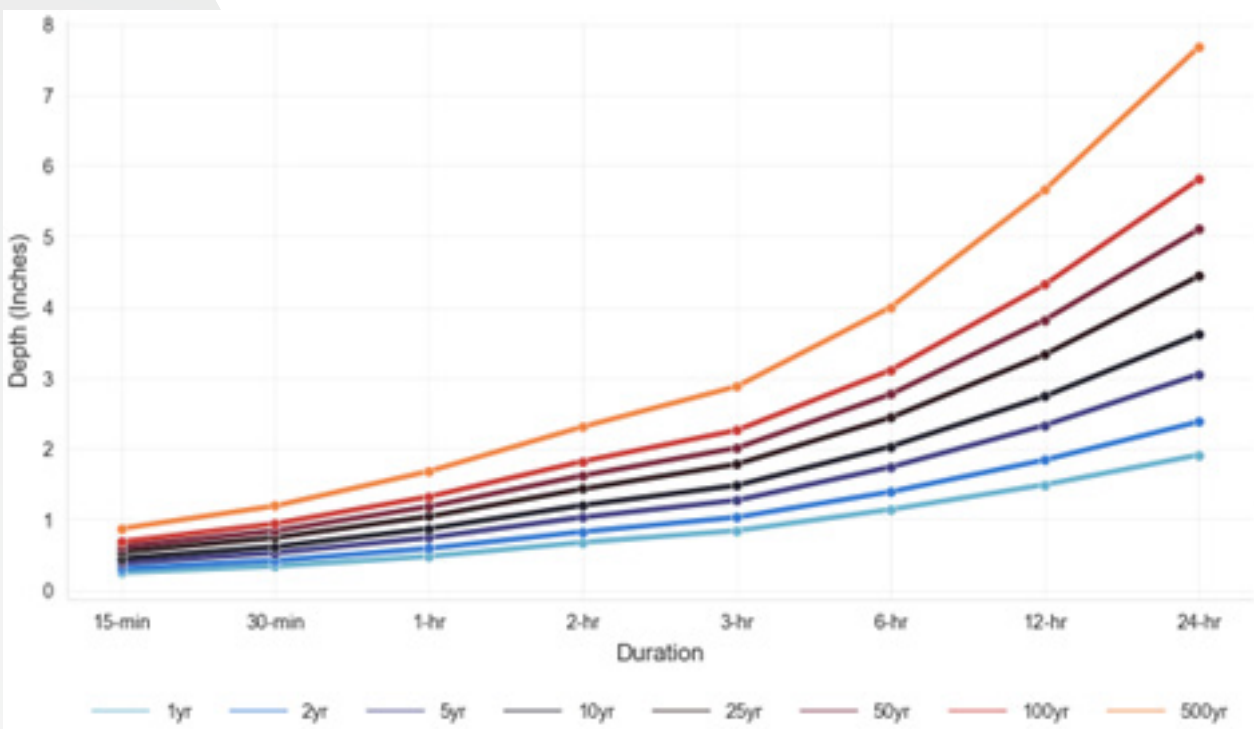



Figure 5. NOAA Atlas 14 Volume 6 IDF Curves for Downtown San Francisco.

RP	1-yr	2-yr	5-yr	10-yr	25-yr	50-yr	100-yr	500-yr
	Inches							
15-min	0.3	0.3	0.4	0.5	0.5	0.6	0.7	0.9
30-min	0.3	0.4	0.5	0.6	0.7	0.8	0.9	1.2
60-min	0.5	0.6	0.7	0.9	1.0	1.2	1.3	1.7
3-hr	0.8	1.0	1.3	1.5	1.8	2.0	2.3	2.9
6-hr	1.1	1.4	1.7	2.0	2.4	2.8	3.1	4.0
12-hr	1.5	1.8	2.3	2.7	3.3	3.8	4.3	5.7
24-hr	1.9	2.4	3.1	3.6	4.4	5.1	5.8	7.7

Table 3. NOAA Atlas 14 Point Precipitation Frequency Estimates – San Francisco Downtown (04-7772).



An annual maxima time series is a list of the largest storms that occurred each year. For example, when developing a 3-hour storm, the annual maximum series will contain a list of the largest 3-hour rainfall amounts that occurred each year to provide a more accurate estimate than would be obtained using annual maxima precipitation values.

Application of Research to Develop Future Conditions San Francisco IDF Curves



Although NOAA Atlas 14 is the de-facto standard, the IDF curves are based on historical observations using the assumption of a stationary climate. NOAA Atlas 14 does not account for the increasing frequency and intensity of extreme precipitation events already occurring, nor does it account for future increases associated with additional warming. Many communities have observed extreme storms that exceed NOAA Atlas 14 projections, and are seeking methods to develop updated existing condition and forward looking future condition IDF curves that consider increasing precipitation (Finzi Hart et al., 2022).

The simplest method for scaling existing IDF curves relies on the Clausius-Clapeyron (C-C) relationship. However, research of recent extreme storms has shown that the C-C relationship likely underestimates the projected increase in precipitation (Molnar et al., 2015; Pall et al., 2007, 2017; Patricola et al., 2022; Pendergrass, 2018; Risser & Wehner, 2017).

Another common method for scaling existing IDF curves relies on using a scaling relationship derived from the statistically downscaled GCM output from the Localized Constructed Analogs (LOCA) ensemble (CIRCA, 2019; Kunkel et al., 2020; Mauger et al., 2018; Obeysekera et al., 2021; Pierce et al., 2014; Pierce & Cayan, 2017; Ragno et al., 2018b). However, in areas with complex topography that drive complex weather patterns such as the SF Bay Area, reliance solely on LOCA may underestimate projected increases in extreme precipitation (DeGaetano & Castellano, 2017; Miro et al., 2021; Wang et al., 2020). Similar to using the C-C relationship, this approach derives a constant scaling parameter for application across all durations under the assumption that short durations and long durations will change similarly as temperatures increase.



Clausius-Clapeyron Relationship

Named after Rudolf Clausius and Benoît Paul Émile Clapeyron in the 1800's, the Clausius-Clapeyron (C-C) relationship specifies the temperature dependence of pressure, most importantly vapor pressure or the water-holding capacity of the atmosphere. A common approximation for this relationship is that the saturation vapor pressure of air increases by about 7 percent per degree Celsius increase in temperature. For example, in a world that is 2.5 °C warmer than pre-industrial conditions, the C-C relationship estimates that the water holding capacity of the atmosphere would increase by 17.5 percent. Future condition IDF curves are created by scaling the historical condition IDF curves by 17.5%. However, recent research has shown that the C-C relationship underestimates the projected increase in precipitation.



The Weather Research and Forecasting Model, or WRF, is a regional climate model that simulates weather and climate over a discrete portion of the globe. This is in contrast to global climate models which simulate climate over the entire globe.

In a review of existing approaches by other utilities or municipalities for developing future condition IDF curves, no approaches were considered satisfactory for application in the Bay Area and San Francisco. As commissioned by SFPUC, SFO, Port, and ORCP, the study team instead pursued a rigorous approach using the Weather Research and Forecasting (WRF) regional climate modeling presented in Volume 1 as a foundation. The following sections describe how the WRF simulations, coupled with additional climate data sets, were used to develop state-of-the-art future condition IDF curves for San Francisco.

Table 4 summarizes the additional sources that inform the future condition IDF curves, including a subset of climate models from the Coupled Model Intercomparison Project Phase 6 (CMIP6) and the downscaled LOCA ensemble. These datasets provide the temporal data needs for high resolution future condition IDF curves while also increasing the confidence and robustness through cross-validation. The use of multiple climate data sets that rely on the strengths of each data set helps to reduce the uncertainties inherent in relying on a single data source (Lopez-Cantu et al., 2020).

Data Needed for IDF	WRF	Supplement to WRF modeling	
		CMIP6 (Multi GCM)	LOCA (Multi GCM)
Convection Scale	✓		
Hourly/Sub-Hourly	✓		
Sub-Daily	✓	✓	
Multi-Model		✓	✓
Long-Term		✓	✓
Vertical levels	✓	✓	
Fine Spatial Resolution	✓		✓
RCP8.5/SSP5-8.5	✓	✓	✓

Table 4. Summary of criteria needs for development of future condition IDF curves.

The future IDF curves are represented through changes in the three dimensions of precipitation characteristics – changes in duration, frequency, and time. The equation below shows how the three climate model datasets (WRF, LOCA, and CMIP6) inform the three primary dimensions of the future condition IDF curves.

$$Rainfall\ Intensity = F(\overset{WRF}{\boxed{duration}}, \overset{LOCA}{\boxed{frequency}}, \overset{WRF, CMIP6}{\boxed{time}})$$

The hybrid approach of using multiple modeling sources (WRF, LOCA, CMIP6 models) and climate variables (precipitation and temperature) in aggregate meets all the climate data criteria for scaling IDF curves. Details of the supporting analysis are presented in the following sections.

WRF Regional Climate Model (Volume 1 Recap)



LBNL used WRF to simulate how extreme historic storms that impacted Bay Area may change under a warming climate. Six historical storms, which occurred between 1982 and 2014 were selected for analysis. The storms were modeled under their historical conditions and under two future time periods, 2050 and 2100, using the high greenhouse gas emissions scenario (RCP8.5 / SSP5-8.5).

The following storms were selected (Table 4a):

Storm Number	Event Dates	Storm Type
Storm 1a	Dec. 2 – 6, 2014	AR + ETC
Storm 1b	Dec. 11 – 12, 2014	AR + ETC
Storm 2	Jan. 3 – 5, 1982	AR
Storm 3	Nov. 4 – 7, 1994	AR
Storm 4	Jan. 31 – Feb. 8, 1998	AR + ETC
Storm 5	Dec. 10 – 13, 1995	AR + ETC

Table 4a. Summary table of selected storms, dates, and storm type.

The WRF simulations provide high resolution (3 km spatially, and 15 min temporally) model outputs for the six storm events in their historical (as they occurred) and future (as they could be) condition. This provides a high accuracy, but narrow snapshot, of the future intensity and duration of future extreme storms in the Bay Area.

Each storm event is simulated 10 times with slight perturbations in time, providing an ensemble of the event in both historical and the two future periods. The WRF model output provides climate variables necessary for evaluating precipitation trends, including temperature, specific humidity, and wind speeds at 44 pressure-based model levels (which can be translated to absolute elevation).

A key finding from LBNL’s storm total precipitation analysis was the difference in storm response to a warming climate. Among the six storms simulated WRF storms, those that occurred only as ARs showed a weak or even negative future trend, indicating a minimal change in response to a warming climate. However, storms that were ARs combined with ETCs showed a strong increase in storm total precipitation across all simulations (Table 4b). The storm totals presented in Volume 1 and Volume 2 may differ from those presented in Patricola et al. (2020) due to differences in size of the domain use to calculate storm totals. Patricola et al. (2020) used a larger domain to better understand the response of the storm across its entire breadth, whereas this study focused more specifically on the Bay Area.

Storm Type	2050	2100
AR + ETC	+7% to +17%	+26% to +37%
AR Only	-8% to +5%	-11% to +2%

Table 4b. Summary of Analysis by Storm Type
Source: Patricola et al. 2022

IDF Curve Duration – WRF

The WRF simulations provide the foundation for understanding how the different storm types evolve with climate change, primarily informing the future IDF trends across the time dimension. Patricola et al. (2022) focused on changes in multi-day storm totals across the six modeled storms. Additional analysis of the WRF simulations assessed the climate change response to the shorter durations. The analysis of shorter durations (down to 15-min) applied a moving time window (aligned to each duration of interest) to the continuous precipitation output at each WRF grid cell in the study domain, and the temporal maximum was assigned as the specified duration precipitation depth. The results of this analysis were then averaged spatially across the entire study domain and the percentage of change between the historical and future condition runs were calculated. Figure 6 shows the expected percent increases in precipitation from short to longer durations within the WRF simulated storms in 2050 and 2100.

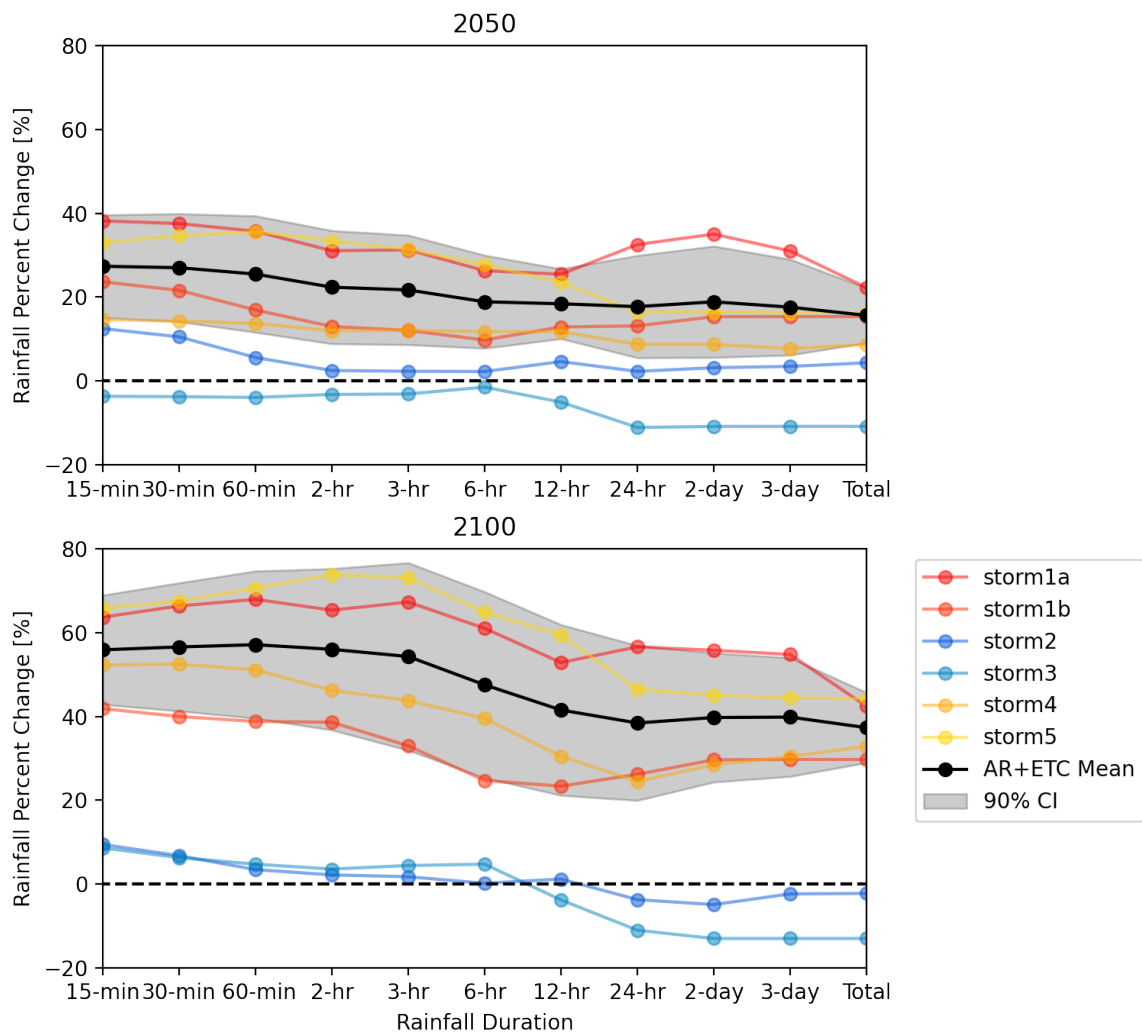


Figure 6. Analysis of Shorter Duration Trends in 2050 and 2100. Storms 1a, 1b, 4, and 5 (warm colors) are AR+ETC storms while storms 2 and 3 (cool colors) are AR only.

Across all durations, the expected changes in the combined AR and ETC storms are significant (Storm 1, 2, 4 and 5), but weekly defined for the AR only storms (Storm 2 and 3) and is consistent with the findings in Patricola et al. (2022). Additionally, this assessment identified a consistent trend of amplified precipitation changes relative to storm total in the shorter durations, regardless of storm type. The amplified change in the shorter durations is detectable due to the high temporal resolution of the WRF simulations down to the 15-minute duration. Ayat et al. (2022) confirmed similar findings based on observational data, providing confidence in these findings.

Storm mechanics suggest that the most likely explanation for the differences in storm response to warming between AR only and AR+ETC storms is the presence of ETC induced convection, which forces the additional moisture to precipitate out. Thus, the fundamental factor influencing whether a storm will worsen in a warmer climate is the presence of an ETC, which makes it logical that ETC only events would track similarly as AR+ETC events in a warming climate. To account for storm type considerations, the IDF scaling associated with the WRF simulations was adjusted by 91% (the ETC + AR+ETC storm percentage identified by Zhang et al. (2019) to account for the 9% of AR only events that will likely remain unchanged in a warming climate.

IDF Curve Frequency – LOCA

The statistically downscaled climate projections from the LOCA ensemble are used to inform the frequency dimension of the future IDF curves. The LOCA ensemble provides temperature and precipitation data at a six km horizontal resolution for 32 global climate models from the CMIP5 archive (Pierce & Cayan, 2017). The spatial resolution of the LOCA grid cells is improved over the native coarse resolution GCM; however, the Bay Area's complex topographic drivers of precipitation patterns and magnitudes are still highly smoothed in the downscaled data set.

Historical to future period analysis of the LOCA dataset focused on a subset of 10 GCMs recommended by the California Department of Water Resources for water resources planning and evaluation (based on performance metrics evaluated at a global scale, western U.S. scale, and locally across California considering both temporal and spatial patterns in the historical climate) (Bedsworth et al., 2018; Pierce et al., 2016). Using the daily precipitation output from the LOCA GCMs for the historical to future periods, percent change for the 1-year through 500-year return periods (24-hour duration) were calculated following a traditional an extreme value analysis (EVA). Analysis shows a definitive increase in 24-hour precipitation by mid-century (2050) and a strengthening of that trend by the end of century (2100). There is also a trend of larger storms having amplified percent changes relative to the smaller storms (e.g., the percent change in the 100-year depth by 2050 and 2100 is greater than the percent change in the 5-year depth across same time horizons).

The LOCA analysis EVA is stable; however, the percent change derived from LOCA are not directly used to inform future IDF curves because: 1) downscaling of GCMs can underestimate extreme events, 2) LOCA projections are not available at subdaily durations, and 3) WRF simulations have higher spatial and temporal resolution than the LOCA data. The WRF simulations also better capture the physical processes influencing extreme precipitation in the Bay Area. However, the WRF findings cannot inform the frequency (i.e., return period) dimension of the future IDF curves; therefore, the long-term simulations from the LOCA ensemble supplement the short-term WRF simulations. The relative changes for all return periods for 2050 and 2100 are applied to the historical return period of the WRF storm events, yielding a future scaling factor for every duration and return period.



Comparison of WRF Scaling to Clausius-Clapeyron Scaling

Changes in the WRF precipitation results (from historical to future condition for 2050 and 2100) were compared with the classic C-C relationship at the surface and multiple elevations aloft. The changes for both the WRF simulated precipitation and the C-C relationship were calculated as a ratio (future/historical) and then these two values compared as a ratio of those ratios. The results at 700 mb aloft are shown in Figure 7, with values above 1 denoting higher precipitation changes than would be expected from the classic C-C relationship (super C-C) and values below 1 denoting lower precipitation changes than expected. The results for the 700 mb pressure level were selected as the best elevation of those considered, since it shows an expected C-C ratio of 1 for the longer durations and storm totals, but a super C-C ratio of greater than 1 for the shorter durations. These findings are consistent at both 2050 and 2100, with the shorter durations super C-C ratio increasing from 2050 to 2100.

This dynamic fits with the current understanding of storm mechanics where the dynamic effect of the shorter durations are the main factor driving super C-C precipitation, but across the full storm duration those effects average out leading to storm totals that fit the classic C-C relationship (shown a ratio of 1 on Figure 7).

These findings also illustrate that developing IDF curves solely using the classic C-C relationship will underestimate the increases in the shorter durations, further supporting an approach that considers multiple data sources that address these accelerating increases in short duration precipitation. Increases in the short durations are more likely to cause flash flooding, sometimes with little time to prepare ahead of the event (Ayat et al., 2022)

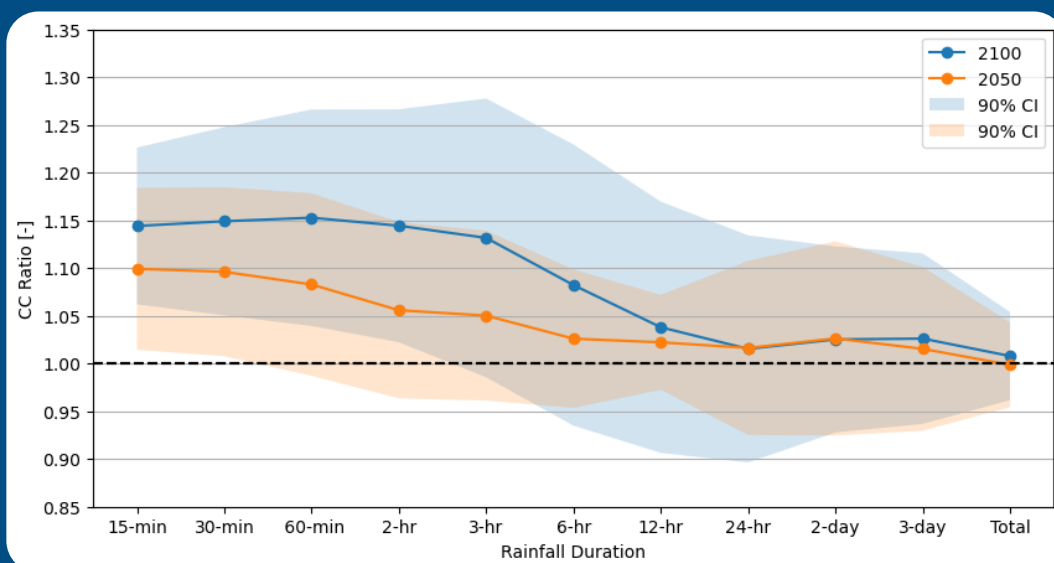


Figure 7. Trends in C-C Scaling (AR+ETC storms only at 700mb height)

IDF Curve Time – WRF and CMIP6

The final data set used in this assessment is state-of-the-art GCM output from the CMIP6 ensemble, which supports the most recent IPCC AR6 (IPCC, 2021; Stockhouse & Lautenschlager, 2017). While the WRF simulations support the development of the future IDF curves for 2050 and 2100 for the SSP5-8.5 climate scenario, the temperature and precipitation projections from the CMIP6 models are needed to develop future IDF curves for other time horizons and warming scenarios (i.e., alternate future scenarios).

To pair with the WRF findings on the C-C ratio for the discrete storms, temperature data from the CMIP6 model ensemble was evaluated to find its corresponding C-C change in the CMIP6 models across each year from 2006 to 2100. To account for bias in C-C change due to the strong seasonal variation in temperature changes and Bay Area storm dynamics in which storms predominantly occur during the colder months, a wet season weighting was applied to calculate the annual C-C change. The annual wet season weighted C-C change value was found by taking the monthly average temperature and the monthly average precipitation, then calculating an average weighted by the monthly fraction of the annual precipitation.

The CMIP6 GCMs were used to validate the study findings against the latest science. The CMIP6 dataset became available after the initiation of this study, and the integration of this dataset helps support the validity of the findings as CMIP6 will become the de-facto standard in the years to come. Climate variables necessary for evaluating precipitation trends, including precipitation, temperature, and specific humidity were extracted at multiple vertical pressure levels. For future condition IDF curve generation, the analysis of CMIP6 ensemble projections focused on SSP5-8.5. A subset of 18 CMIP6 models were selected for analysis, filtered to include only models with a Transient Climate Response (TCR) in the 'likely' (66% likelihood) range reported by AR6. This was done to avoid undue influence of overly hot outliers on the model mean (Hausfather et al., 2022). Additional investigation of CMIP6 data across all SSPs was performed using the 1850-1900 baseline for pre-industrial conditions, for which global temperature projections are published in AR6.

In summary, the evaluation of multiple modeling sources for San Francisco allows for the scaling of IDF curves using a hybrid method that draws from the elements of each source that best meet the climate data criteria defined in Table 4. In aggregate, this robust method provides the most confidence in scaling future precipitation events across intensity, duration, and frequency dimensions.

Combined Analysis Findings

The first step in developing future condition IDF curves is selecting or developing an IDF curve that represents historical conditions. This historical condition IDF curve can then be scaled or transformed using future condition scaling factors that are appropriate for the location of interest. For this study, the existing NOAA’s Atlas 14 IDF curves for SF Downtown (San Francisco Downtown Station #04-7772) published in Atlas 14 Volume 6 were selected to represent the historical condition IDF curves. Additional NOAA Atlas 14 IDF curves were selected for SFO and OAK for comparison purposes.

Spotlight on Confidence Intervals

A confidence interval is a range of values that describes the uncertainty surrounding an estimate. We indicate a confidence interval by its endpoints; for example, the 90% confidence interval for the number of people, of all ages, in poverty in the United States in 1995 (based on the March 1996 Current Population Survey) is “35,534,124 to 37,315,094.” A confidence interval is also itself an estimate. It is made using a model of how sampling, interviewing, measuring, and modeling contribute to uncertainty about the relation between the true value of the quantity we are estimating and our estimate of that value.

Source: <https://www.census.gov/programs-surveys/saipe/guidance/confidence-intervals.html>

One of the most important findings from this study is that both short-term and long-term storm durations are expected to increase in intensity, with short term durations increasing faster than longer durations (Table 6 and Table 7). Relative to historical storms, by 2050, the 5-year, 24-hour storm could increase an average of ~17% by 2050 and ~41% by 2100; similarly, the 100-year, 24-hour storm could increase by ~22% by 2050 and ~51% by 2100.

In Figure 9, the 5-year, 3-hour storm may increase by ~20% by 2050 and by ~56% by 2100; similarly, the 100-year, 3-hour storm could increase by ~26% by 2050 and by ~67% by 2100. These are substantial increases in projected short- and long-term rain intensities, which could have significant impacts on existing city infrastructure.

		5-yr, 24-hr	100-yr, 24-hr
Historical		+0%	+0%
		-10 to +13%	-17 to +23%
2050		+17%	+22%
	90% CI	+7 to +27%	+12 to 32%
2100		+41%	+51%
	90% CI	+26 to +57%	+35 to +67%

Table 6. Historical and Future Return Frequency for 24-hour Duration with 90% Confidence

		5-yr, 3-hr	100-yr, 3-hr
Historical		+0%	+0%
		-11% to 14%	-20% to 27%
2050		+20%	+26%
	90% CI	+12 to +30%	+16 to 35%
2100		+56%	+67%
	90% CI	+38 to +75%	+47% to +87%

Table 7. Historical and Future Return Frequency for 3-hour Duration with 90% Confidence Interval

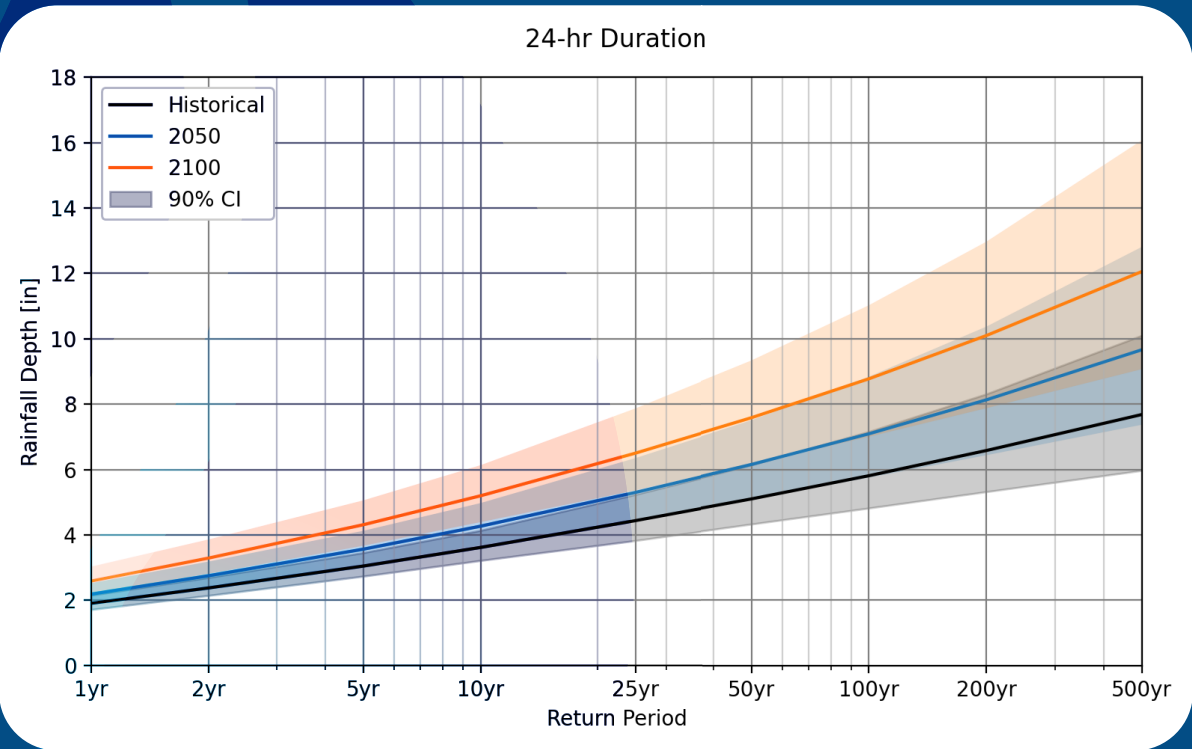


Figure 8. Historical and Future Return Period Verses Rainfall Depth for 24-hour Duration

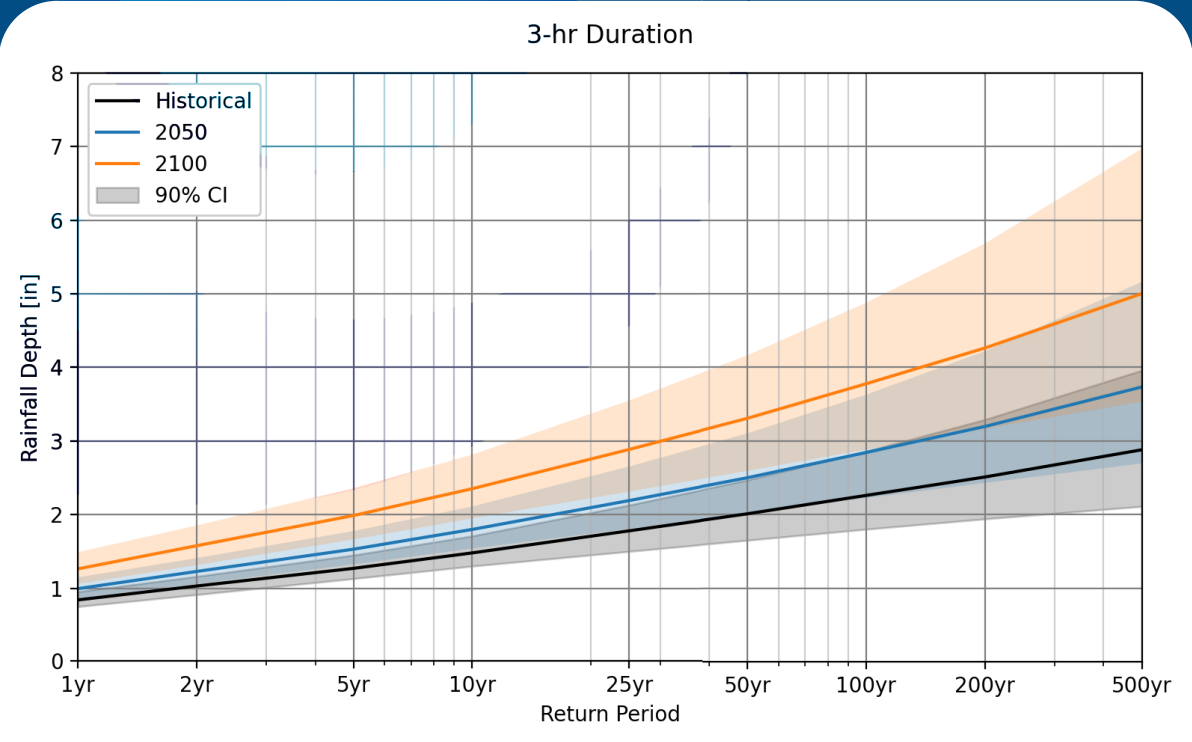


Figure 9. Changes in rainfall depth (with 90% confidence intervals) for 3-hour duration storm

Another important takeaway from Figures 8 and 9 is that the 90% confidence intervals increase with return period, and the 90% confidence interval for the historical NOAA Atlas 14 values is similar to that for the 2050 projections. Often, the perception is that projections of future conditions have a larger uncertainty range than past events. However, the NOAA Atlas 14 values are derived from statistical analysis of historical observations, which also carries a degree of uncertainty. The 90% confidence intervals provided in NOAA Atlas 14 are often not used by practitioners; therefore, the uncertainty in the NOAA Atlas 14 values is overlooked or not considered in

Future Condition IDF Curves for 2050 and 2100

San Francisco IDF Curves for 2050 and 2100

Figure 10 and Table 8 present the San Francisco IDF curves for 2050, using the hybrid approach applied to the historical NOAA Atlas 14 IDF curves for the SF Downtown Station (details in Appendix A). Figure 11 and Table 9 present the San Francisco IDF curves for 2100.

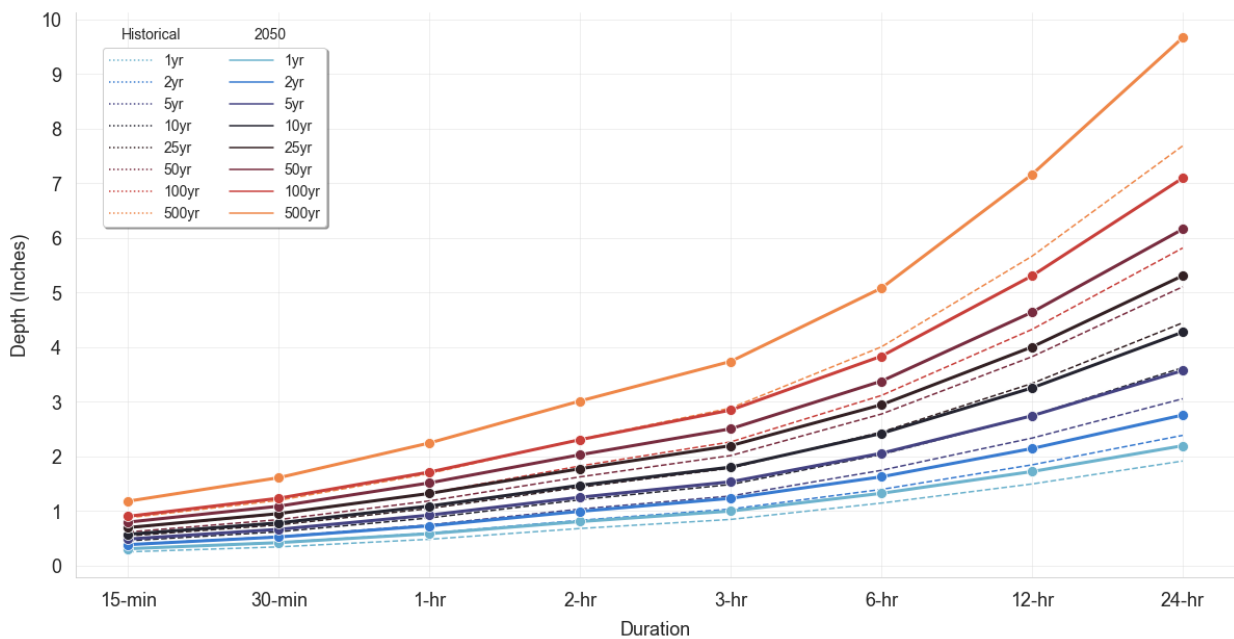


Figure 10. 2050 IDF Curves for Downtown San Francisco (SSP5-8.5)

RP	1-yr	2-yr	5-yr	10-yr	25-yr	50-yr	100-yr	500-yr
	Inches							
15-min	0.3	0.4	0.5	0.6	0.7	0.8	0.9	1.2
30-min	0.4	0.5	0.7	0.8	0.9	1.1	1.2	1.6
60-min	0.6	0.7	0.9	1.1	1.3	1.5	1.7	2.2
2-hr	0.8	1.0	1.2	1.5	1.8	2.0	2.3	3.0
3-hr	1.0	1.2	1.5	1.8	2.2	2.5	2.8	3.7
6-hr	1.3	1.6	2.1	2.4	2.9	3.4	3.8	5.1
12-hr	1.7	2.1	2.7	3.2	4.0	4.6	5.3	7.2
24-hr	2.2	2.8	3.6	4.3	5.3	6.2	7.1	9.7

Table 8. 2050 IDF Curves for Downtown San Francisco (SSP5-8.5)

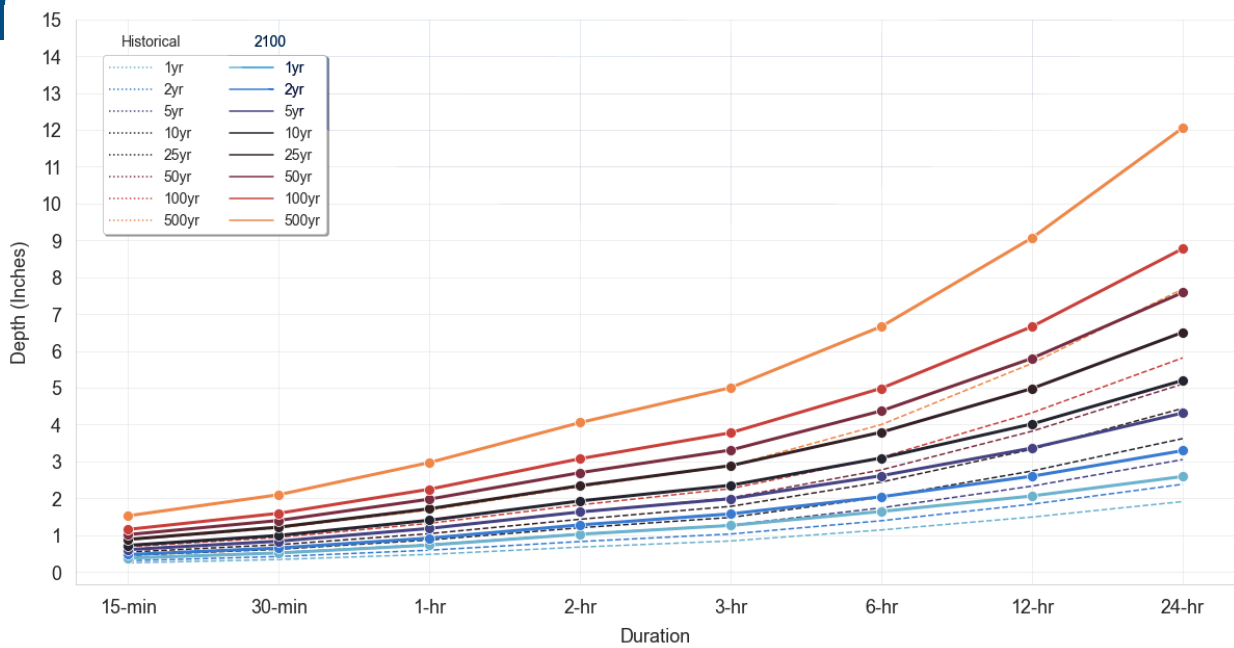


Figure 11. 2100 IDF Curves for Downtown San Francisco (SSP5-8.5)

RP	1-yr	2-yr	5-yr	10-yr	25-yr	50-yr	100-yr	500-yr
	Inches							
15-min	0.4	0.5	0.6	0.7	0.9	1.0	1.2	1.5
30-min	0.5	0.7	0.8	1.0	1.2	1.4	1.6	2.1
60-min	0.7	0.9	1.2	1.4	1.7	2.0	2.2	3.0
2-hr	1.0	1.3	1.6	1.9	2.3	2.7	3.1	4.1
3-hr	1.3	1.6	2.0	2.4	2.9	3.3	3.8	5.0
6-hr	1.6	2.0	2.6	3.1	3.8	4.4	5.0	6.7
12-hr	2.1	2.6	3.4	4.0	5.0	5.8	6.7	9.1
24-hr	2.6	3.3	4.3	5.2	6.5	7.6	8.8	12.1

Table 9. 2100 IDF Curves for Downtown San Francisco (SSP5-8.5)

SFO IDF Curves for 2050 and 2100

Figure 12 and Table 10 present the SFO IDF curves for 2050, using the hybrid approach applied to the historical NOAA Atlas 14 IDF curves for the SFO Station (details in Appendix A). Figure 13 and Table 11 present the SFO IDF curves for 2100.

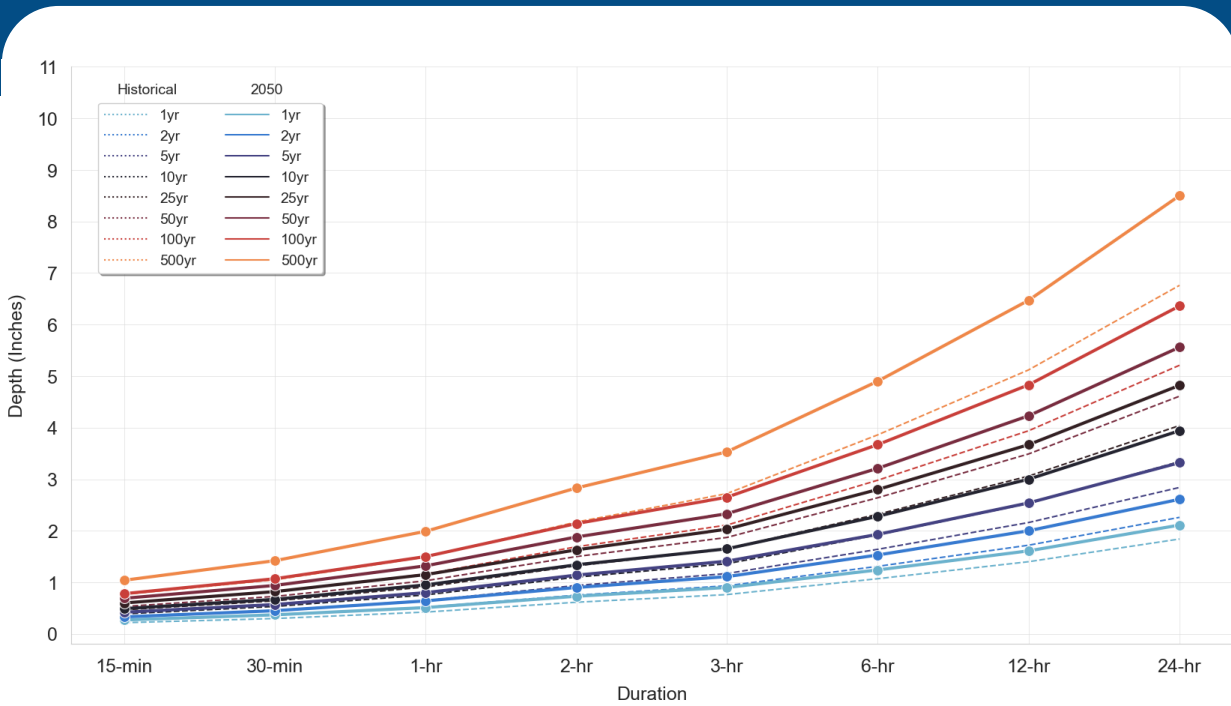


Figure 12. 2050 IDF Curves for SFO (SSP5-8.5)

RP	1-yr	2-yr	5-yr	10-yr	25-yr	50-yr	100-yr	500-yr
Inches								
15-min	0.3	0.3	0.4	0.5	0.6	0.7	0.8	1.0
30-min	0.4	0.5	0.6	0.7	0.8	0.9	1.1	1.4
60-min	0.5	0.6	0.8	1.0	1.2	1.3	1.5	2.0
2-hr	0.7	0.9	1.1	1.3	1.6	1.9	2.1	2.8
3-hr	0.9	1.1	1.4	1.7	2.0	2.3	2.7	3.5
6-hr	1.2	1.5	1.9	2.3	2.8	3.2	3.7	4.9
12-hr	1.6	2.0	2.5	3.0	3.7	4.2	4.8	6.5
24-hr	2.1	2.6	3.3	3.9	4.8	5.6	6.4	8.5

Table 10. 2050 IDF Curves for SFO (SSP5-8.5)

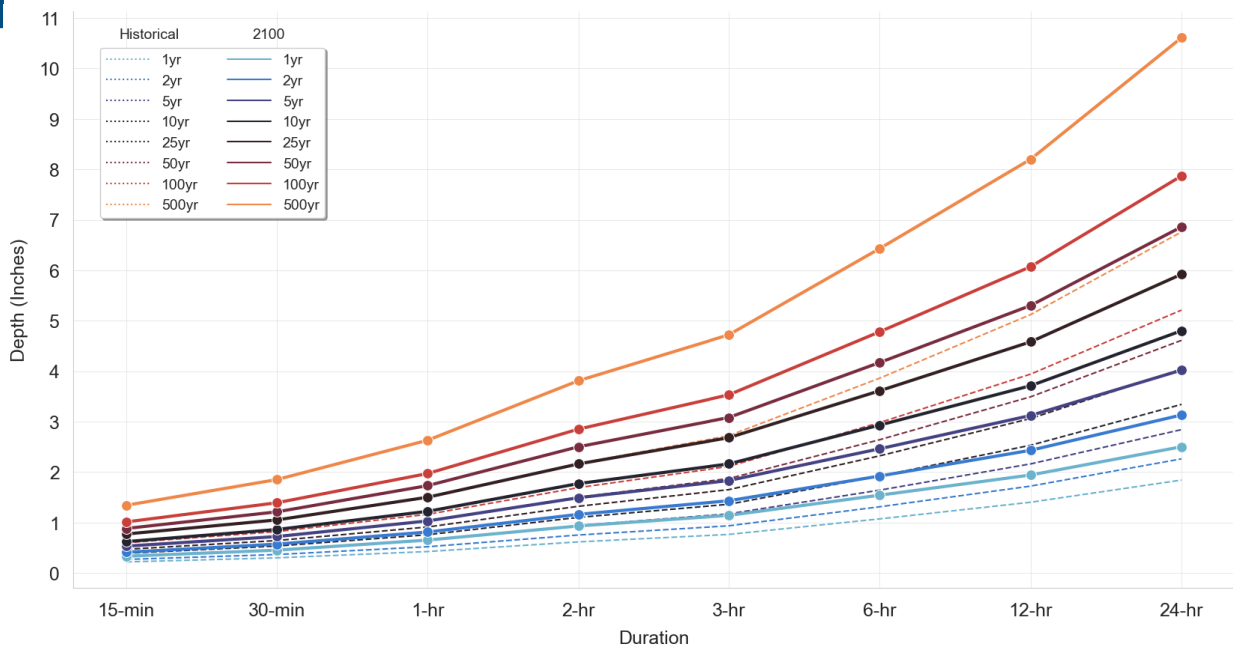


Figure 13. 2100 IDF Curves for SFO (SSP5-8.5)

RP	1-yr	2-yr	5-yr	10-yr	25-yr	50-yr	100-yr	500-yr
	Inches							
15-min	0.3	0.4	0.5	0.6	0.8	0.9	1.0	1.3
30-min	0.5	0.6	0.7	0.9	1.1	1.2	1.4	1.9
60-min	0.7	0.8	1.0	1.2	1.5	1.7	2.0	2.6
2-hr	0.9	1.2	1.5	1.8	2.2	2.5	2.9	3.8
3-hr	1.1	1.4	1.8	2.2	2.7	3.1	3.5	4.7
6-hr	1.5	1.9	2.5	2.9	3.6	4.2	4.8	6.4
12-hr	1.9	2.4	3.1	3.7	4.6	5.3	6.1	8.2
24-hr	2.5	3.1	4.0	4.8	5.9	6.9	7.9	10.6

Table 11. 2100 IDF Curves for SFO (SSP5-8.5)

The future condition IDF curves allow for evaluating changes in storm intensity and duration, but the standard presentation of IDF curves does not readily highlight the projected changes in storm frequency with climate change.

Figure 14 shows the projected change in storm frequency from historical conditions to 2100. Rare storms (based on historical benchmarks) will become increasingly more frequent. In San Francisco, a storm delivering the rainfall of a historical 1000-year event (0.01% chance of occurring in any given year) may correspond to a 100-year return period (1% chance of occurring in any given year) by 2100. Similarly, the historical 100-year event will become increasingly more frequent. The historical 100-year event may correspond to a 40-year event (2.5% chance of occurring in any given year) by 2050, and the 20-year event (5% chance of occurring in any given year) by 2100. Even smaller storms (e.g., the 5-year event) will occur more frequently, and become 3-year events by 2050, and 2-year events by 2100. When these changes in storm frequency are coupled with projected sea level rise, the potential for compound flooding due to high tide flooding and extreme Bay water levels further increases (Bevacqua et al., 2020; Fant et al., 2021; Rahimi et al., 2020; Sweet et al., 2018).

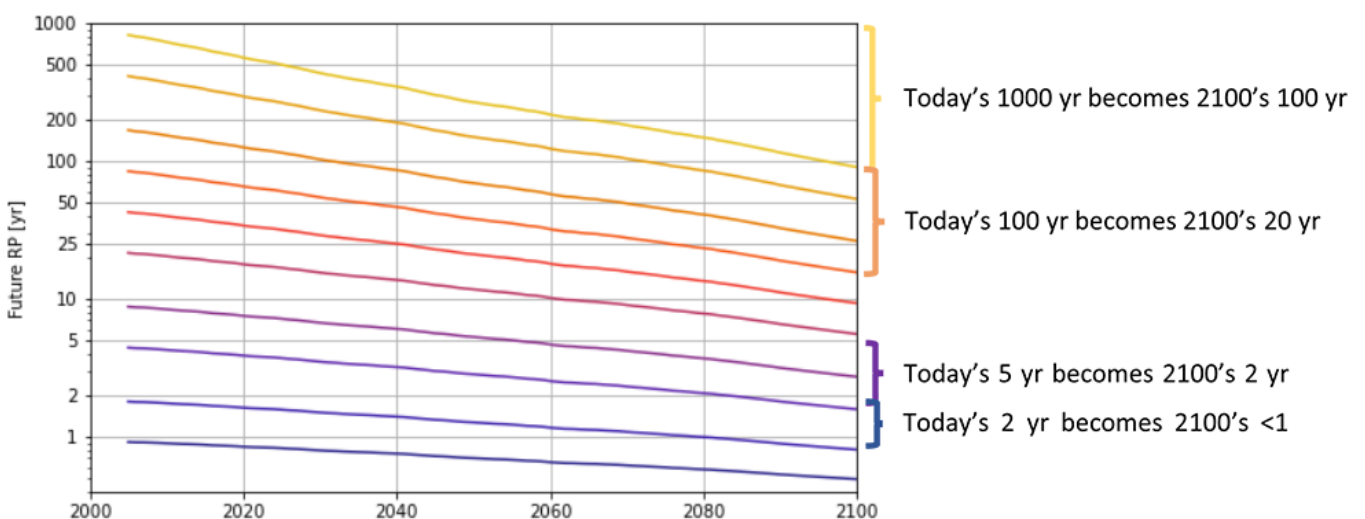


Figure 14. Expected Change in Storm Frequency from Historical Conditions to 2100



Steps for Scaling IDF Curves and Supporting Scaling Factors (for 2050 and 2100)

Future condition IDF curves were developed for San Francisco based on the SF Downtown station and for SFO based on SFO's station. However, the percent change factors derived in our analysis are applicable to the Bay Area and may be applied to existing IDF curves developed for other stations to develop future condition IDF curves for 2050 and 2100. These scaling factors can be applied to NOAA Atlas 14 projections for the Bay Area, allowing this research to support climate change assessments related to extreme precipitation well beyond San Francisco and SFO. At this time, the applicability of the scaling factors outside of the Bay Area has not been verified.

Scaling factor tables, for each return period and storm duration, are provided in Table 12 and Table 13. In this Guidebook, the full tables with confidence intervals are presented for the SF Downtown and SFO stations. The methodology for applying the scaling factors to other locations is presented on page 37, and the methodology for scaling the IDF curves to other time horizons and climate scenarios is presented on page 38.

Scaling Factor Tables

Duration	Return Period							
	1-yr	2-yr	5-yr	10-yr	25-yr	50-yr	100-yr	500-yr
15-min	23.3%	24.3%	25.7%	26.8%	28.4%	29.8%	31.2%	35.2%
90% CI	14.6-31.9%	15.6-33.1%	16.9-34.5%	17.9-35.7%	19.4-37.4%	20.6-38.9%	22.0-40.5%	25.7-44.7%
30-min	23.0%	24.0%	25.4%	26.5%	28.1%	29.4%	30.9%	34.9%
90% CI	13.9-32.0%	14.9-33.1%	16.2-34.6%	17.2-35.8%	18.7-37.5%	19.9-38.9%	21.3-40.5%	25.0-44.8%
60-min	21.6%	22.6%	24.0%	25.0%	26.6%	28.0%	29.4%	33.4%
90% CI	11.8-31.3%	12.8-32.4%	14.0-33.9%	15.0-35.1%	16.5-36.8%	17.7-38.2%	19.0-39.8%	22.7-44.1%
2-hr	18.8%	19.8%	21.1%	22.2%	23.7%	25.0%	26.4%	30.3%
90% CI	9.4-28.2%	10.3-29.3%	11.5-30.7%	12.5-31.8%	13.9-33.5%	15.1-34.9%	16.4-36.4%	20.0-40.6%
3-hr	18.2%	19.2%	20.5%	21.6%	23.1%	24.4%	25.8%	29.6%
90% CI	9.1-27.2%	10.1-28.3%	11.3-29.7%	12.2-30.9%	13.7-32.5%	14.9-33.9%	16.2-35.4%	19.7-39.6%
6-hr	15.7%	16.6%	17.9%	19.0%	20.5%	21.7%	23.1%	26.9%
90% CI	8.3-23.0%	9.2-24.0%	10.5-25.4%	11.4-26.5%	12.8-28.1%	14.0-29.5%	15.3-30.9%	18.8-34.9%
12-hr	15.3%	16.2%	17.5%	18.6%	20.1%	21.3%	22.7%	26.5%
90% CI	10.3-20.2%	11.2-21.3%	12.5-22.6%	13.4-23.7%	14.9-25.2%	16.1-26.6%	17.4-28.0%	21.0-31.9%
24-hr	14.7%	15.6%	16.9%	17.9%	19.4%	20.7%	22.1%	25.8%
90% CI	5.3-24.0%	6.2-25.1%	7.3-26.5%	8.3-27.6%	9.7-29.2%	10.8-30.6%	12.1-32.0%	15.5-36.1%
2-day	15.7%	16.7%	18.0%	19.0%	20.5%	21.8%	23.2%	26.9%
90% CI	5.2-26.2%	6.1-27.3%	7.3-28.7%	8.2-29.8%	9.6-31.4%	10.7-32.8%	12.0-34.3%	15.4-38.4%
3-day	14.6%	15.5%	16.8%	17.8%	19.3%	20.6%	21.9%	25.7%
90% CI	5.7-23.4%	6.6-24.4%	7.8-25.8%	8.7-26.9%	10.1-28.5%	11.3-29.9%	12.5-31.3%	16.0-35.4%

Table 12. Percent Change in Precipitation Depth from Historical Atlas 14 to 2050
(Based on CMIP6 C-C Trend for 2050 applied to WRF C-C Scale Factor and SSP5-8.5)

Duration	Return Period							
	1-yr	2-yr	5-yr	10-yr	25-yr	50-yr	100-yr	500-yr
15-min	51.7%	54.7%	58.2%	60.6%	63.8%	66.3%	68.9%	75.5%
90% CI	41.6-61.9%	44.4-65.1%	47.6-68.7%	49.9-71.4%	52.9-74.8%	55.2-77.4%	57.6-80.2%	63.8-87.2%
30-min	52.3%	55.3%	58.8%	61.3%	64.5%	67.0%	69.6%	76.2%
90% CI	40.1-64.5%	42.9-67.8%	46.1-71.5%	48.3-74.2%	51.3-77.7%	53.6-80.4%	56.0-83.2%	62.1-90.3%
60-min	52.8%	55.8%	59.3%	61.8%	65.0%	67.5%	70.1%	76.7%
90% CI	38.7-66.8%	41.5-70.1%	44.7-73.9%	46.9-76.6%	49.8-80.1%	52.1-82.9%	54.5-85.7%	60.5-93.0%
2-hr	51.7%	54.7%	58.2%	60.6%	63.9%	66.3%	68.9%	75.5%
90% CI	36.7-66.8%	39.4-70.1%	42.5-73.9%	44.7-76.6%	47.6-80.1%	49.8-82.9%	52.1-85.7%	58.1-93.0%
3-hr	50.1%	53.1%	56.5%	59.0%	62.1%	64.6%	67.2%	73.7%
90% CI	32.1-68.2%	34.7-71.6%	37.7-75.4%	39.8-78.1%	42.6-81.6%	44.8-84.4%	47.0-87.3%	52.8-94.6%
6-hr	44.0%	46.8%	50.1%	52.4%	55.5%	57.8%	60.3%	66.6%
90% CI	25.7-62.2%	28.2-65.4%	31.1-69.1%	33.1-71.8%	35.8-75.2%	37.8-77.8%	40.0-80.6%	45.5-87.7%
12-hr	38.5%	41.2%	44.4%	46.6%	49.5%	51.8%	54.2%	60.2%
90% CI	22.2-54.7%	24.6-57.8%	27.4-61.3%	29.4-63.8%	32.0-67.1%	34.0-69.6%	36.1-72.3%	41.4-79.0%
24-hr	35.7%	38.3%	41.4%	43.6%	46.5%	48.7%	51.0%	56.9%
90% CI	21.0-50.3%	23.4-53.3%	26.1-56.7%	28.1-59.2%	30.6-62.3%	32.6-64.8%	34.7-67.4%	39.9-73.9%
2-day	36.9%	39.6%	42.7%	44.9%	47.8%	50.1%	52.4%	58.4%
90% CI	24.9-48.9%	27.3-51.9%	30.2-55.2%	32.2-57.6%	34.8-60.8%	36.9-63.2%	39.0-65.8%	44.4-72.3%
3-day	37.0%	39.7%	42.8%	45.0%	47.9%	50.2%	52.5%	58.5%
90% CI	26.0-48.0%	28.5-50.9%	31.3-54.3%	33.4-56.7%	36.0-59.8%	38.1-62.3%	40.2-64.8%	45.7-71.2%

Table 13. Percent Change in Precipitation Depth from Historical Atlas 14 to 2100
(Based on CMIP6 C-C Trend for 2050 applied to WRF C-C Scale Factor and SSP5-8.5)

SF Downtown IDF Curves with Confidence Intervals

Duration	Return Period							
	1-yr	2-yr	5-yr	10-yr	25-yr	50-yr	100-yr	500-yr
15-min	0.30	0.38	0.48	0.57	0.69	0.79	0.90	1.18
90% CI	0.26-0.35	0.33-0.44	0.42-0.56	0.49-0.66	0.57-0.84	0.64-0.98	0.71-1.15	0.85-1.63
30-min	0.42	0.52	0.66	0.78	0.95	1.08	1.23	1.61
90% CI	0.36-0.48	0.45-0.60	0.57-0.76	0.67-0.91	0.78-1.15	0.87-1.35	0.96-1.57	1.16-2.22
60-min	0.58	0.72	0.92	1.09	1.32	1.51	1.71	2.24
90% CI	0.50-0.67	0.62-0.84	0.79-1.07	0.93-1.27	1.09-1.60	1.22-1.88	1.35-2.19	1.61-3.11
2-hr	0.80	0.99	1.25	1.47	1.77	2.03	2.30	3.01
90% CI	0.69-0.93	0.85-1.14	1.07-1.44	1.25-1.71	1.46-2.15	1.63-2.51	1.80-2.93	2.17-4.17
3-hr	0.99	1.23	1.53	1.80	2.19	2.50	2.84	3.73
90% CI	0.86-1.15	1.06-1.41	1.32-1.78	1.54-2.11	1.81-2.65	2.01-3.10	2.22-3.63	2.70-5.16
6-hr	1.32	1.62	2.05	2.42	2.94	3.37	3.83	5.08
90% CI	1.16-1.51	1.42-1.87	1.78-2.36	2.08-2.80	2.45-3.55	2.73-4.17	3.02-4.88	3.69-7.02
12-hr	1.72	2.14	2.74	3.25	4.00	4.63	5.30	7.16
90% CI	1.52-1.96	1.89-2.44	2.40-3.13	2.83-3.75	3.35-4.82	3.77-5.71	4.21-6.74	5.22-9.87
24-hr	2.19	2.75	3.57	4.27	5.30	6.15	7.09	9.66
90% CI	1.91-2.53	2.40-3.19	3.10-4.13	3.68-4.98	4.45-6.35	5.10-7.51	5.75-8.84	7.37-12.80
2-day	2.75	3.44	4.42	5.27	6.51	7.54	8.66	11.70
90% CI	2.38-3.19	2.98-4.00	3.82-5.15	4.53-6.17	5.45-7.83	6.20-9.22	6.98-10.81	8.89-15.51
3-day	3.09	3.85	4.92	5.83	7.17	8.28	9.47	12.69
90% CI	2.70-3.56	3.36-4.45	4.29-5.68	5.05-6.79	6.06-8.58	6.87-10.08	7.70-11.78	9.71-16.83

Table 14. 2050 IDF Curves for San Francisco (SSP5-8.5) with 90% Confidence Intervals

Duration	Return Period							
	1-yr	2-yr	5-yr	10-yr	25-yr	50-yr	100-yr	500-yr
15-min	0.37	0.47	0.61	0.72	0.88	1.01	1.16	1.53
90% CI	0.33-0.43	0.41-0.54	0.53-0.70	0.62-0.84	0.73-1.07	0.82-1.26	0.91-1.47	1.11-2.11
30-min	0.51	0.65	0.84	0.99	1.22	1.40	1.59	2.10
90% CI	0.45-0.59	0.56-0.75	0.72-0.97	0.85-1.16	1.00-1.48	1.12-1.74	1.25-2.04	1.52-2.91
60-min	0.73	0.92	1.18	1.40	1.72	1.98	2.25	2.97
90% CI	0.62-0.85	0.79-1.07	1.01-1.38	1.19-1.65	1.41-2.10	1.58-2.46	1.76-2.89	2.13-4.13
2-hr	1.02	1.28	1.63	1.93	2.34	2.69	3.07	4.05
90% CI	0.87-1.19	1.09-1.49	1.38-1.90	1.62-2.27	1.91-2.87	2.14-3.37	2.38-3.94	2.89-5.63
3-hr	1.26	1.58	1.99	2.35	2.89	3.31	3.78	5.00
90% CI	1.06-1.49	1.32-1.85	1.66-2.36	1.95-2.82	2.31-3.55	2.59-4.16	2.88-4.88	3.54-6.97
6-hr	1.64	2.04	2.61	3.09	3.79	4.37	4.99	6.66
90% CI	1.37-1.94	1.70-2.42	2.17-3.10	2.55-3.70	3.03-4.68	3.41-5.51	3.79-6.46	4.71-9.32
12-hr	2.06	2.60	3.36	4.02	4.98	5.80	6.66	9.07
90% CI	1.73-2.43	2.18-3.07	2.81-3.97	3.34-4.78	4.01-6.14	4.55-7.28	5.11-8.61	6.42-12.64
24-hr	2.59	3.29	4.31	5.20	6.50	7.58	8.77	12.05
90% CI	2.21-3.03	2.81-3.86	3.67-5.06	4.39-6.13	5.37-7.87	6.17-9.34	7.00-11.02	9.07-16.07
2-day	3.26	4.12	5.35	6.42	7.98	9.29	10.71	14.60
90% CI	2.82-3.77	3.58-4.78	4.63-6.22	5.52-7.51	6.70-9.59	7.66-11.35	8.66-13.37	11.11-19.34
3-day	3.70	4.65	6.01	7.18	8.89	10.32	11.85	16.01
90% CI	3.22-4.26	4.06-5.38	5.23-6.96	6.21-8.37	7.50-10.65	8.54-12.56	9.61-14.74	12.23-21.24

Table 15. 2100 IDF Curves for San Francisco (SSP5-8.5) with 90% Confidence Intervals

SFO IDF Curves with Confidence Intervals

Duration	Return Period							
	1-yr	2-yr	5-yr	10-yr	25-yr	50-yr	100-yr	500-yr
15-min	0.27	0.33	0.42	0.49	0.60	0.69	0.78	1.04
90% CI	0.23-0.31	0.28-0.39	0.36-0.49	0.42-0.58	0.49-0.74	0.55-0.87	0.60-1.02	0.73-1.47
30-min	0.37	0.45	0.57	0.67	0.82	0.94	1.07	1.42
90% CI	0.31-0.43	0.39-0.53	0.49-0.67	0.57-0.80	0.67-1.01	0.75-1.19	0.82-1.40	1.00-2.01
60-min	0.51	0.64	0.80	0.95	1.15	1.32	1.50	1.99
90% CI	0.44-0.60	0.54-0.74	0.68-0.94	0.80-1.12	0.93-1.42	1.04-1.67	1.15-1.96	1.40-2.83
2-hr	0.73	0.90	1.14	1.34	1.63	1.88	2.14	2.83
90% CI	0.62-0.85	0.77-1.05	0.97-1.33	1.13-1.59	1.33-2.01	1.48-2.37	1.64-2.78	2.00-4.02
3-hr	0.90	1.11	1.41	1.65	2.03	2.33	2.65	3.53
90% CI	0.77-1.05	0.95-1.30	1.20-1.65	1.40-1.96	1.64-2.50	1.84-2.94	2.04-3.45	2.48-4.99
6-hr	1.24	1.53	1.93	2.28	2.80	3.21	3.67	4.90
90% CI	1.07-1.44	1.32-1.78	1.66-2.25	1.94-2.69	2.28-3.42	2.56-4.04	2.84-4.77	3.47-6.93
12-hr	1.61	2.00	2.54	3.00	3.67	4.23	4.83	6.47
90% CI	1.41-1.87	1.74-2.31	2.20-2.94	2.58-3.51	3.03-4.49	3.39-5.32	3.76-6.26	4.61-9.16
24-hr	2.11	2.61	3.32	3.94	4.82	5.56	6.36	8.50
90% CI	1.85-2.42	2.29-3.00	2.91-3.82	3.42-4.56	4.08-5.77	4.60-6.79	5.14-7.94	6.42-11.36
2-day	2.70	3.36	4.29	5.09	6.23	7.17	8.18	10.85
90% CI	2.35-3.10	2.93-3.88	3.74-4.96	4.40-5.92	5.23-7.47	5.91-8.76	6.58-10.23	8.16-14.48
3-day	3.07	3.86	4.94	5.87	7.18	8.25	9.39	12.39
90% CI	2.70-3.51	3.39-4.42	4.34-5.68	5.12-6.78	6.08-8.56	6.84-10.04	7.60-11.70	9.37-16.57

Table 16. 2050 IDF Curves for SFO (SSP5-8.5) with 90% Confidence Intervals

Duration	Return Period							
	1-yr	2-yr	5-yr	10-yr	25-yr	50-yr	100-yr	500-yr
15-min	0.33	0.41	0.53	0.62	0.77	0.88	1.01	1.34
90% CI	0.28-0.38	0.35-0.48	0.45-0.61	0.53-0.74	0.62-0.94	0.70-1.11	0.78-1.31	0.95-1.90
30-min	0.45	0.57	0.72	0.86	1.05	1.21	1.39	1.85
90% CI	0.39-0.53	0.48-0.66	0.62-0.85	0.72-1.02	0.85-1.30	0.96-1.54	1.06-1.81	1.30-2.62
60-min	0.65	0.81	1.03	1.22	1.50	1.73	1.97	2.63
90% CI	0.55-0.76	0.68-0.95	0.87-1.22	1.02-1.46	1.21-1.86	1.36-2.19	1.51-2.58	1.85-3.76
2-hr	0.93	1.16	1.49	1.77	2.16	2.50	2.85	3.81
90% CI	0.79-1.10	0.98-1.37	1.25-1.75	1.47-2.11	1.74-2.68	1.95-3.17	2.17-3.73	2.67-5.43
3-hr	1.14	1.43	1.83	2.16	2.68	3.08	3.53	4.72
90% CI	0.95-1.36	1.18-1.70	1.51-2.19	1.78-2.61	2.11-3.34	2.38-3.94	2.65-4.63	3.26-6.73
6-hr	1.54	1.92	2.46	2.93	3.61	4.17	4.78	6.43
90% CI	1.27-1.84	1.59-2.31	2.02-2.95	2.38-3.54	2.84-4.51	3.20-5.33	3.57-6.30	4.42-9.18
12-hr	1.94	2.43	3.12	3.71	4.58	5.30	6.07	8.20
90% CI	1.61-2.31	2.02-2.89	2.58-3.72	3.05-4.46	3.63-5.71	4.09-6.77	4.57-7.98	5.67-11.72
24-hr	2.50	3.13	4.02	4.80	5.92	6.86	7.87	10.61
90% CI	2.14-2.90	2.68-3.64	3.45-4.69	4.08-5.63	4.91-7.15	5.58-8.44	6.26-9.90	7.90-14.25
2-day	3.19	4.02	5.19	6.20	7.64	8.84	10.12	13.54
90% CI	2.79-3.66	3.51-4.63	4.53-5.99	5.36-7.20	6.43-9.16	7.29-10.79	8.15-12.64	10.20-18.05
3-day	3.67	4.67	6.04	7.22	8.91	10.27	11.74	15.63
90% CI	3.22-4.20	4.09-5.35	5.29-6.95	6.28-8.35	7.52-10.63	8.51-12.52	9.49-14.65	11.80-20.91

Table 17. 2100 IDF Curves for SFO (SSP5-8.5) with 90% Confidence Intervals

Developing Future Condition IDF Curves for Other Locations

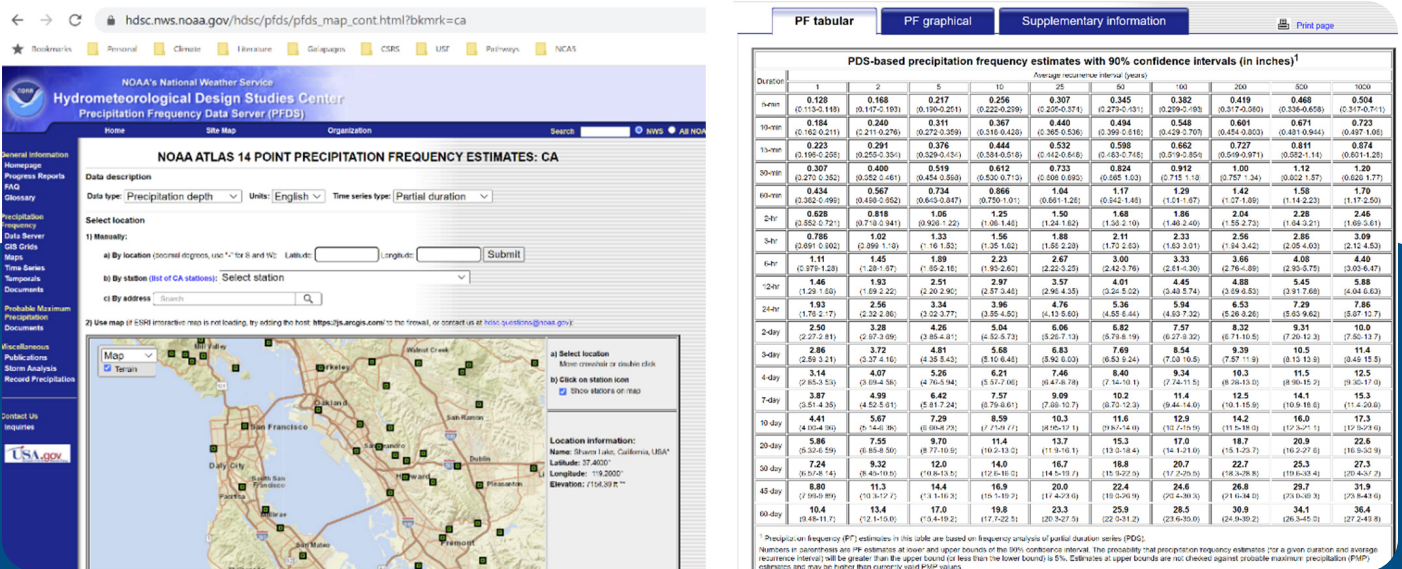


Figure 15. Example NOAA Atlas 14 Web Interface and Tabular Existing IDF Curve
Source: https://hdsc.nws.noaa.gov/hdsc/pfds/pfds_map_cont.html?bkmrk=ca

The Scaling Factor Tables (Table 12 and Table 13) were developed to help other communities in the Bay Area use the findings from San Francisco’s Extreme Precipitation Study. With these factors, any community in the Bay Area can use existing NOAA Atlas 14 projections to create future condition IDF curves. The factors can be applied to the NOAA Atlas 14 projections from the 15-minute to the 3-day duration, and from the 1-year to the 500-year return periods. Alternatively, the scaling factors can be applied to select design or level of service storms of interest within this range.

Step-by-step Process to Scale Historical IDF to Future Condition IDF Projection

Access the NOAA Atlas 14 Point Precipitation Frequency estimates by going to the NOAA National Weather Service Hydrometeorological Design Studies Center site:

https://hdsc.nws.noaa.gov/hdsc/pfds/pfds_map_cont.html?bkmrk=ca
 Select by entering an address or selecting a station. In this example, we selected, “Oakland Museum.”

Either download the entire table or select your storm of interest.

For this example, we selected the 5-yr, 3-hr storm.

Take NOAA Atlas 14 estimate of rainfall depth (in inches) and multiply by the scaling factor from Table 12 or 13.

Developing Future Conditions IDF Curves for other Time Horizons and Climate Scenarios

The future condition IDF Curves were developed for the 2050 and 2100 time horizon, assuming an SSP5-8.5 climate future, which is the highest greenhouse gas emissions scenario considered by IPCC (IPCC, 2021). However, the findings can be scaled to other time horizons or climate scenarios, such as SSP4-7.0, SSP2-7.0, and SSP2-4.5, if required for risk-based decision making or sensitivity analysis.

To facilitate this scaling, IDF curve percent change scale factors are provided under SSP5-8.5 in 5-year intervals from 2020 to 2100 in Appendix B. These values were derived from applying an interpolated C-C ratio to the estimated CMIP6 C-C change for the given years. C-C ratios were interpolated between the WRF and LOCA results between 2050 and 2100 and an assumed C-C ratio of 1 at 2005, the beginning of the analysis period.

Scale factors for given years along SSP5-8.5 can be equated to global warming targets as published by the IPCC’s AR6 Report (IPCC, 2021). These global warming values can be in turn matched with the corresponding year that level of warming would occur along another IPCC climate scenario of interest. Table 18 provides a synthesis of these results, showing the target temperature values associated with SSP2-4.5, the other most common IPCC climate scenario used by San Francisco agencies, and SSP3-7.0, an intermediate climate scenario. However, this same approach can transform the results to other IPCC climate scenarios if needed. Figure 16 presents this same information in a graphical form.

SSP5-8.5 year	Temperature change [C]	SSP3-7.0 year	SSP2-4.5 year
2020	1.25	2021.3	2020.9
2027	1.48	2029.5	2029.7
2028	1.51	2030.7	2031.1
2030	1.58	2033.1	2034.2
2040	1.93	2044.8	2049.5
2042	2.01	2047.2	2052.7
2044	2.09	2049.8	2056.5
2050	2.35	2057.4	2069.9
2056	2.62	2064.9	2087.4
2058	2.71	2067.5	2095.2
2064	2.99	2075.0	
2068	3.18	2080.0	
2080	3.78	2095.7	
2082	3.89	2098.4	
2084	3.99		
2099	4.73		

Table 18. Crosswalk for Translating from SSP5-8.5 to other Scenarios based on Degree of Warming

For example, if a practitioner is interested in how extreme precipitation or a design storm may change with 3°C in warming, the temperature change Figure 16b and in Table 12 highlight that this degree of warming occurs at about 2064 for SSP5-8.5. Using the tables in Appendix B, a practitioner can estimate the percent increase in precipitation at 2064, which would match their 3°C warming target. From Figure 16a, we can see that a practitioner interested in results for 2075 under SSP3-7.0 would similarly find that the year 2064 for SSP5-8.5 best matches this target.

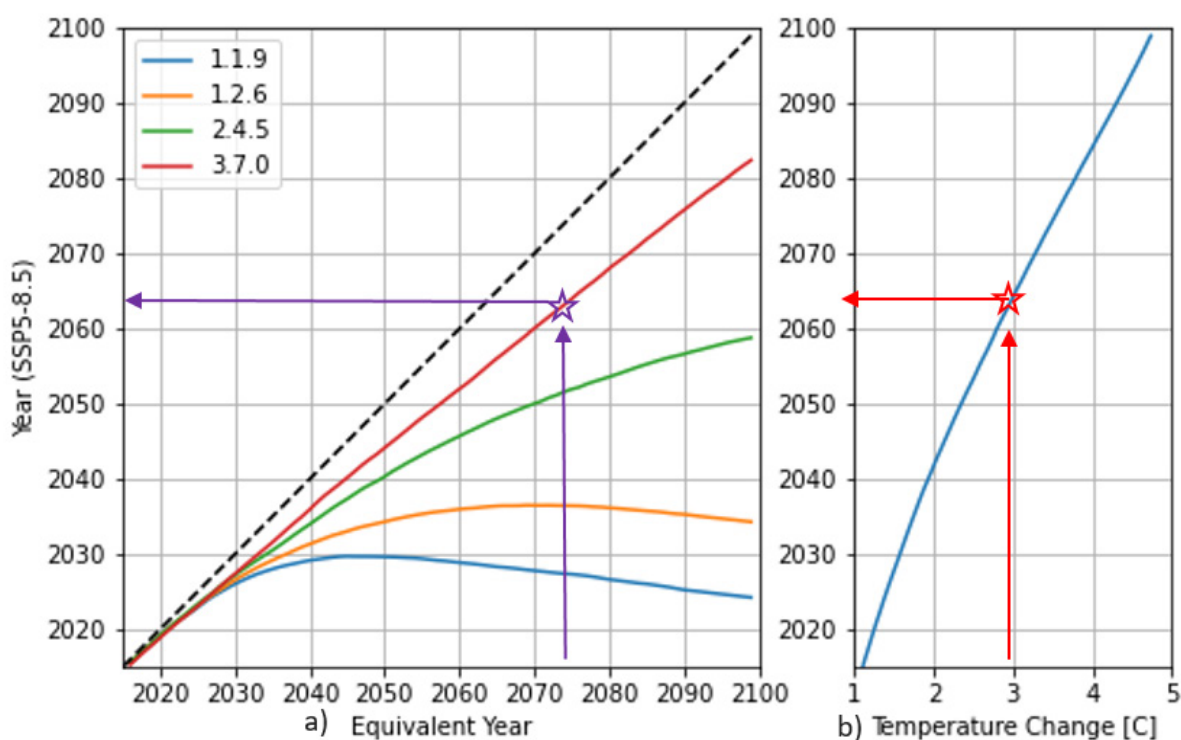


Figure 16. Alternative Approach for Scaling IDF Change Factors based on Temperature Change

Other Climate Variables

When evaluating changing climate conditions and the potential for flooding, it is useful to consider more than one climate variable of interest. Compound flooding, or flooding that occurs due to multiple sources, such as storm surge and sea level rise, groundwater rise, and precipitation, is becoming more common (Bevacqua et al., 2020; Rahimi et al., 2020; Sweet et al., 2018). Therefore, for instance, when evaluating flooding associated with an extreme precipitation event in 2050, the corresponding amount of sea level rise and storm surge should be considered.

In this section, we discuss how to consider or pair the future condition IDF curves with other climate variables.

Back-to-Back Events

In December 2022 to January 2023, the Bay Area experienced nine back-to-back events consisting of both an AR family (Fish et al., 2022) and a series of ETCs (Dacre & Pinto, 2020). The low-pressure conditions associated with the ETCs resulted in elevated Bay water levels (Figure 17). And the combination of ARs and ETCs created bomb cyclone conditions on January 5, 2023 (characterized by a rapid pressure drop) that elevated Bay water levels and brought heavy rainfall, high winds, and damaging waves along the open Pacific coast.

While the recent series of storms may seem unusual, the Bay Area has long experienced successive storms, or storms that occur one after the other in a series over multiple days to weeks (May et al., 2016). For example, a series of storms between December 18 and 27, 1955, February 11 and 21, 1986, and March 9 to 16, 2016 all coupled higher than average Bay water levels with heavy precipitation, resulting in flooding in low-lying areas across the Bay Area (May et al., 2016). The December 2014 storms selected for modeling as part of this study included a long series of storms, requiring the simulation period to be split into two and modeled as two separate events.

In the past, the storm events that caused the most flooding across the Bay Area occurred during El Niño years when Bay water levels could be elevated by a foot more even in the absence of low-pressure driven storm surge. The elevated Bay water levels impact stormwater drainage to the Bay and exacerbate inland flooding. However, due to accelerating sea level rise, recent storm events occurring during La Niña years are causing Bay Area flooding that rivals the historic El Niño storm events. The December 2022 to January 2023 series of storms occurred during a La Niña year.

Recent research has shown that successive ARs, known as AR families, can result in prolonged flooding and impacts with little recovery time between events (Fish et al., 2022). AR families that occur in La Niña years are associated with higher average precipitation across California. AR families that occur during El Niño years are characterized by lower precipitation intensities; however, the AR families persist for longer durations and could achieve similar storm totals (Fish et al., 2022). AR events are also notable as they bring the majority of California’s precipitation in only 10 to 100 hours per year, and a single storm event can bring up to 30% of a specific location’s annual precipitation (Lamjiri et al., 2018). These characteristics were evident in the recent Bay Area storms, with 18 inches of rain recorded at the SF Downtown rain gage, across the 9 storms, and with much of the precipitation falling during one storm event (Figure 17). Combined, over 75% of San Francisco’s average rainfall fell over a relatively short duration.

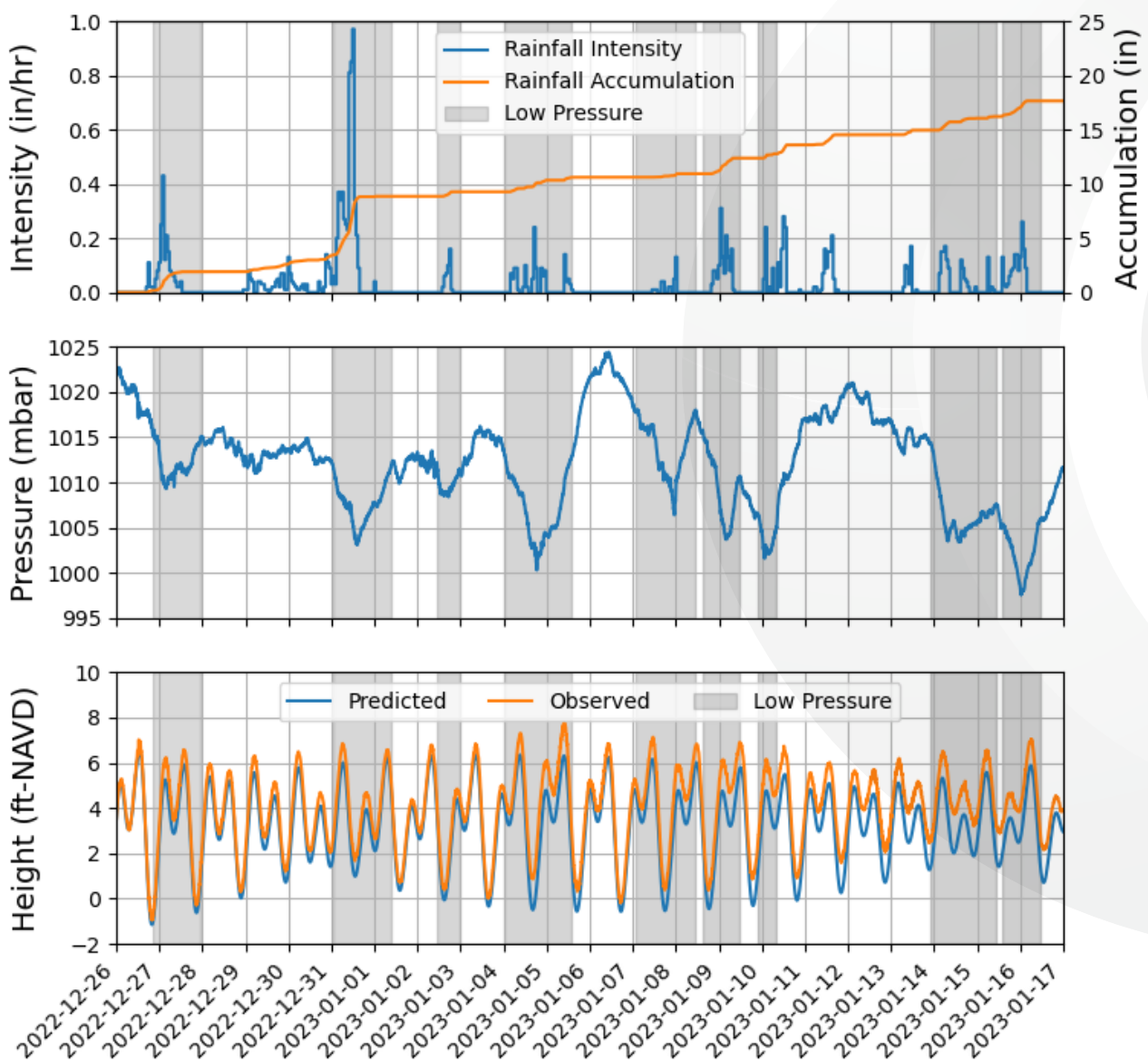


Figure 17. Total rainfall accumulation over the storm series at the SF Downtown Station, Barometric pressure, Observed and Predicted water levels at the Presidio Tide Gauge

Changes in Storm Surge

In San Francisco Bay and the Pacific Ocean offshore of San Francisco, elevated water levels associated with storm surge is driven by low atmospheric pressure. The maximum storm surge associated with low atmospheric pressure is about 10 to 12 inches. The WRF simulations did not reveal any significant changes atmospheric pressure across the modeled storms (Figure 18). However, the WRF simulations were optimized to assess changes in precipitation; therefore, the lack of a change in atmospheric pressure across the six storms evaluated is insufficient to rule out a potential increase in pressure drop with similar storm events in the future. Explosive cyclogenesis is driven by a rapid drop in pressure within the ETC, and this rapid pressure drop is required to

classify the storm as a bomb cyclone. It is possible pressure drops that exceed historic conditions could occur in the future.

Many other processes are associated with elevated Bay water levels, such as El Niño conditions, which can elevate coastal water levels by 12 inches or more (USGS, 1999). El Niño can also bring extreme weather conditions and heavy precipitation (Barnard et al., 2015; DeFlorio et al., 2013; Goddard & Gershunov, 2020; Griggs, 1998). On the West Coast, it is challenging to relate an increase in Bay water levels above predicted tides to one factor, such as changes in atmospheric pressure.

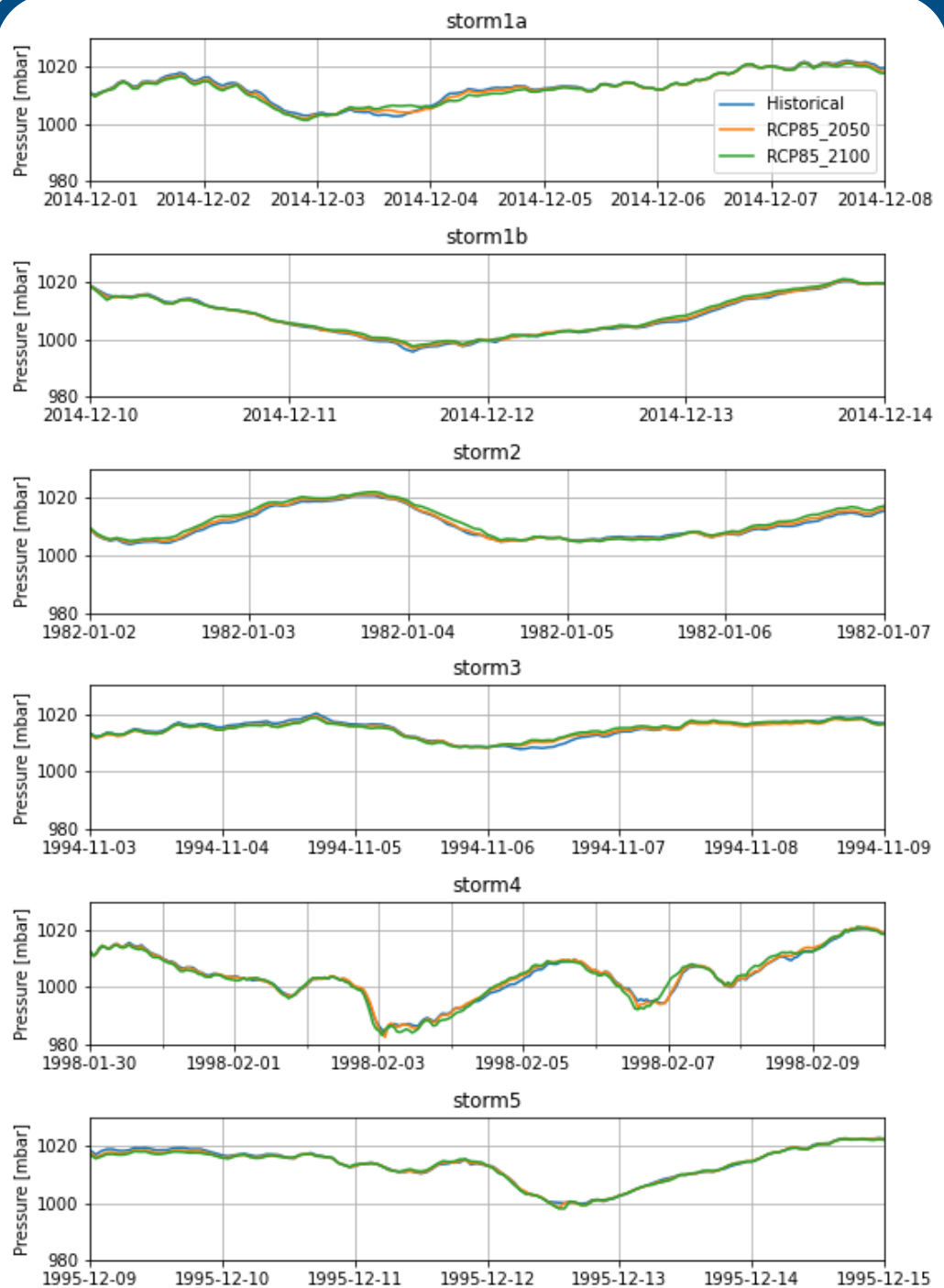


Figure 18. Change in Surface Pressure for the Modeled Storms

Changes in Storm Surge

The windspeeds within the WRF simulations were evaluated to assess if increasing windspeeds occurred in response to the warming climate. Increased windspeeds could drive local wind-wave generation and wave runup along the shoreline, and high windspeeds can impact SFO and Port operations. However, there are no observable changes in windspeeds across the simulations. Slight changes are evident above 10 km (Figure 19), the mean height associated with moisture transport. However, near the ground, no discernable changes in windspeeds are evident (Figure 20). Although there is no evidence of changes in extreme windspeeds across the simulations, changes in windspeeds to climate change cannot be definitively ruled out. It is possible the windspeeds that exceed historic conditions could occur in the future with AR and ETC events.

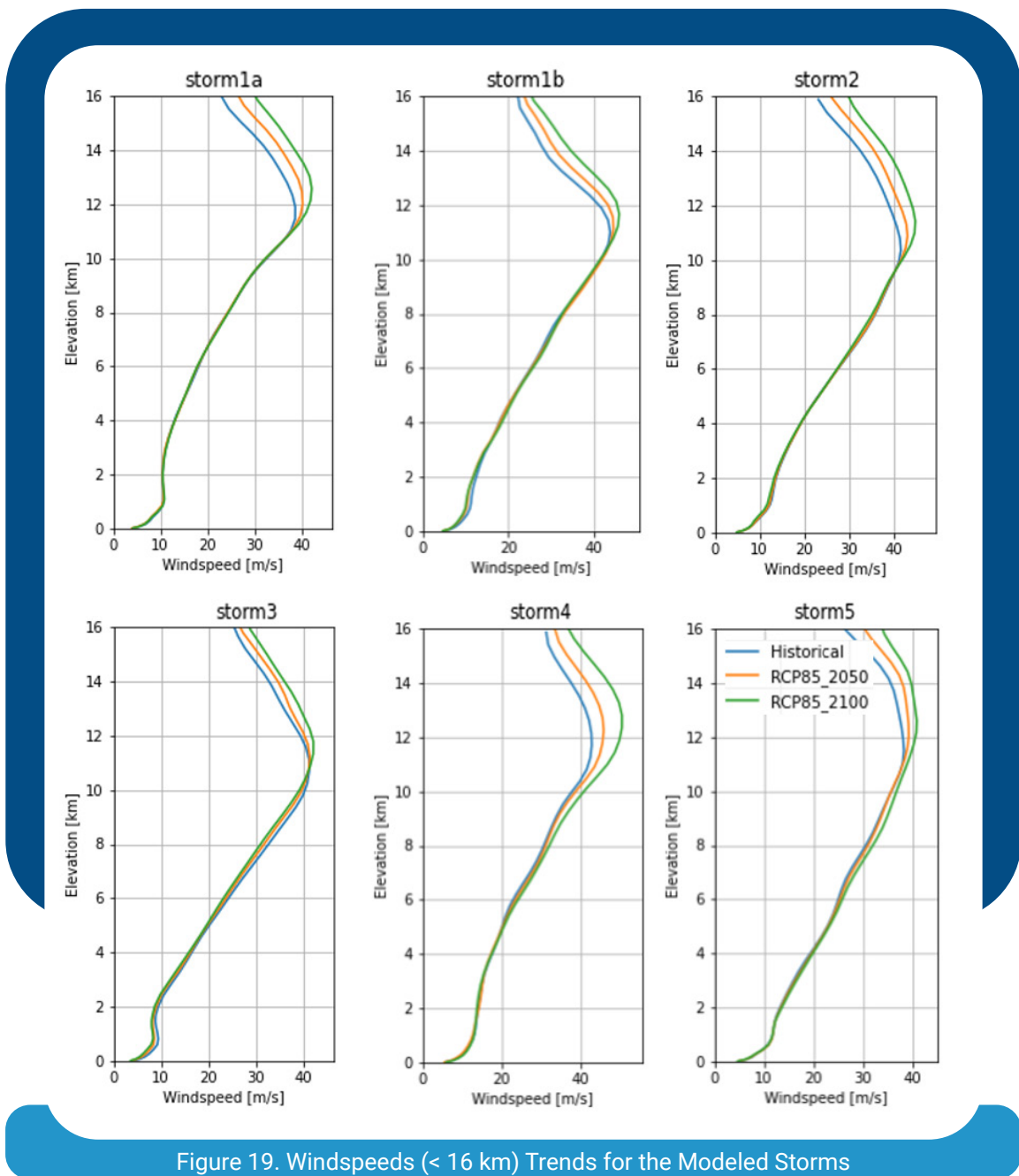


Figure 19. Windspeeds (< 16 km) Trends for the Modeled Storms

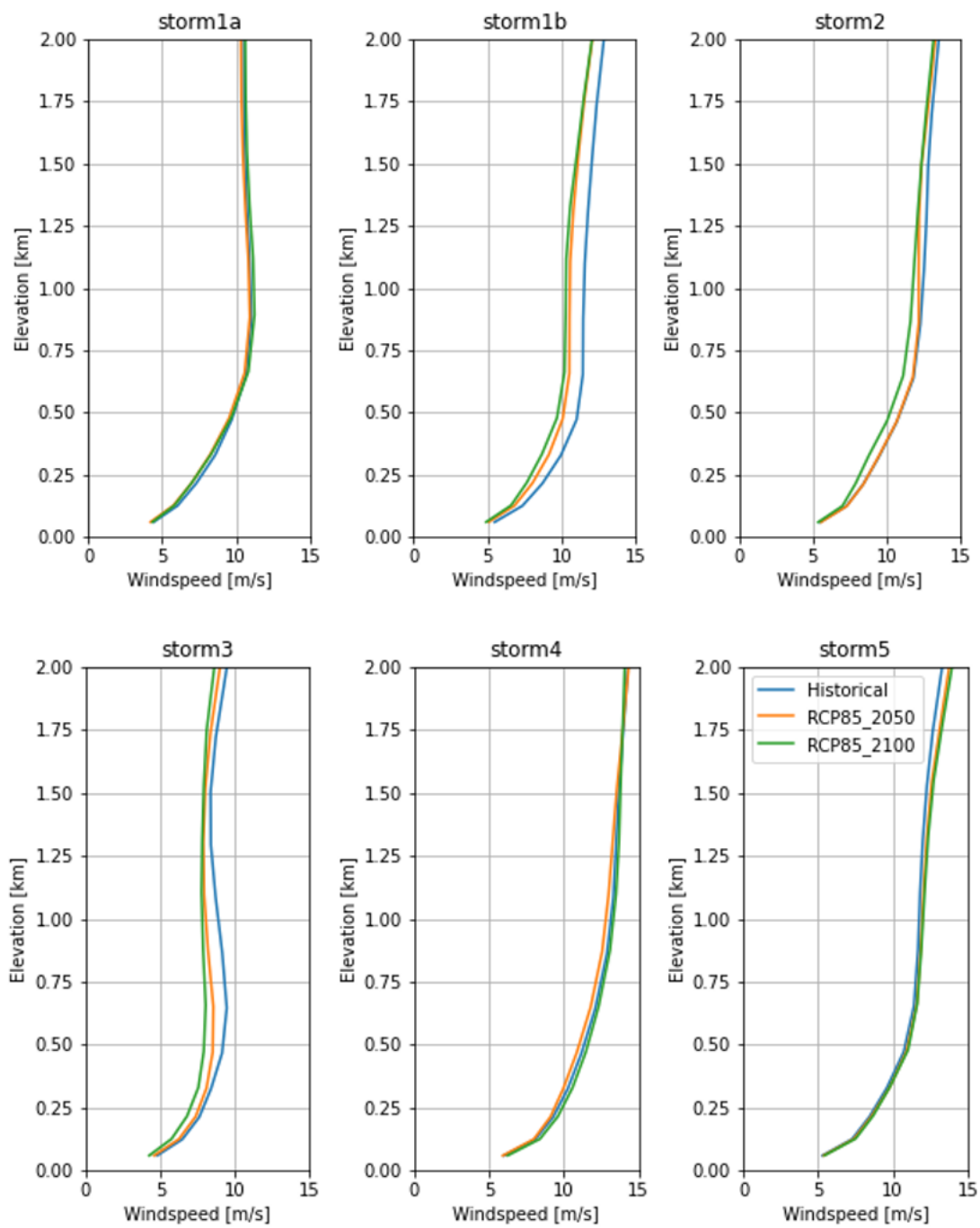


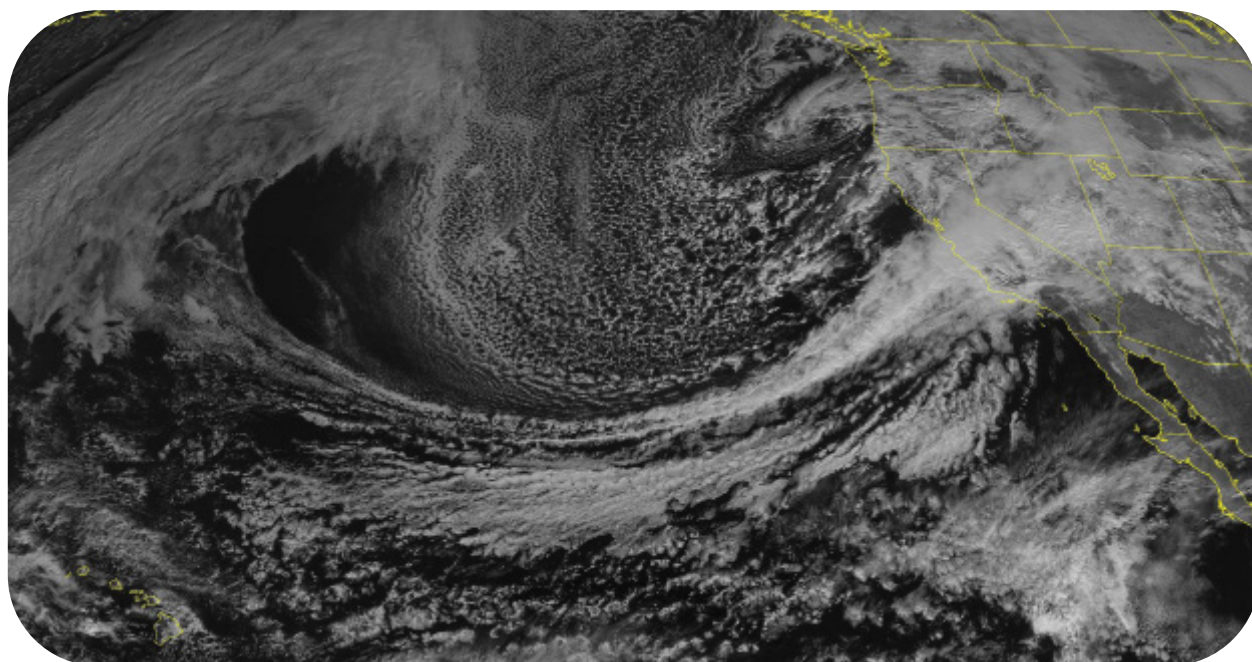
Figure 20. Near Ground (< 2 km) Windspeed Trends for Modeled Storms

Closing Thoughts

The Bay Area has experienced flooding from numerous extreme storm events that delivered heavy precipitation and other severe storm conditions (e.g., high winds and storm surge). However, San Francisco has not experienced devastating or catastrophic flooding and the associated consequences that have impacted so many other cities around the U.S. and the world.

Over ~18 inches of rain were recorded at the San Francisco Downtown rain gage between December 26, 2022 to January 16, 2023. In a mere 21 days, the storms produced more than 75% of San Francisco's annual average rainfall amount. Historically, San Francisco's receives about 23 inches of rainfall with 68 days per year of measurable rain. As our climate continues to warm, San Francisco's average annual rainfall may not change significantly, although more rain will fall across shorter durations, leading to fewer and fewer days with measurable rainfall. San Francisco will continue to experience a climate that oscillates between prolonged periods of drought with below average annual precipitation, and extreme wet years with annual precipitation well above average conditions.

In the Bay Area, storms will continue to increase in intensity and severity irrespective of the future emissions trajectory. The findings from this Extreme Precipitation Study, both Volume 1 and Volume 2, provide scientific analysis that helps various stakeholders and interested parties understand how large storms might change under a warming climate, which can facilitate preparation for future extreme precipitation.



References

1. Ayat, H., Evans, J. P., Sherwood, S. C., & Soderholm, J. (2022). Intensification of subhourly heavy rainfall. *Science*, 378(6620), 655–659. https://doi.org/10.1126/SCIENCE.ABN8657/SUPPL_FILE/SCIENCE.ABN8657_SM.PDF
2. Barnard, P. L., Short, A. D., Harley, M. D., Splinter, K. D., Vitousek, S., Turner, I. L., Allan, J., Banno, M., Bryan, K. R., Doria, A., Hansen, J. E., Kato, S., Kuriyama, Y., Randall-Goodwin, E., Ruggiero, P., Walker, I. J., & Heathfield, D. K. (2015). Coastal vulnerability across the Pacific dominated by El Niño/Southern Oscillation. *Nature Geoscience*, 8, 801–807.
3. Bedsworth, L., Cayan, D., Guido, Franco, L. F., & Ziaja, S. (2018). Statewide Summary Report, In: California’s Fourth Climate Change Assessment (p. 133). Published by California Governor’s Office of Planning and Research, Scripps Institution of Oceanography, California Energy Commission, California Public Utilities Commission. Publication number: SUM-CCCa4-2018-03. <http://www.climateassessment.ca.gov/state/index.html>
4. Bevacqua, E., Vousdoukas, M. I., Zappa, G., Hodges, K., Shepherd, T. G., Maraun, D., Mentaschi, L., & Feyen, L. (2020). More meteorological events that drive compound coastal flooding are projected under climate change. *Communications Earth & Environment*, 1(1), Article 1. <https://doi.org/10.1038/s43247-020-00044-z>
5. Cheng, L., & Aghakouchak, A. (2014). Nonstationary precipitation intensity-duration-frequency curves for infrastructure design in a changing climate. *Scientific Reports*, 1–6. <https://doi.org/10.1038/srep07093>
6. CIRCA. (2019). Connecticut Physical Climate Science Assessment Report (PCSAR): Observed trends if projections of temperature and precipitation (Issue August). Sponsored by a grant from the Connecticut Institute for Resilience and Climate Adaptation (CIRCA).
7. Collini, R., Carter, J., Auermuller, L., Engeman, L., Hintzen, K., Gambill, J., Johnson, R., Miller, I., Schafer, C., & Stiller, H. (2022). Application Guide for the 2022 Sea Level Rise Technical Report. National Oceanic and Atmospheric Administration Office for Coastal Management, Mississippi–Alabama Sea Grant Consortium (MASGP-22-028), and Florida Sea Grant (SGEB 88).
8. CPC. (2020). Guidance for Incorporating Sea Level Rise into Capital Planning, Assessing Vulnerability and Risk to Support Adaptation (p. 55). City and County of San Francisco, Capital Planning Committee, adopted September 22, 2014, revised and adopted December 14, 2015. <https://onesanfrancisco.org/sea-level-rise-guidance/>
9. Dacre, H. F., & Pinto, J. G. (2020). Serial clustering of extratropical cyclones: A review of where, when and why it occurs. *Npj Climate and Atmospheric Science*, 3(1). <https://doi.org/10.1038/s41612-020-00152-9>

10. DeFlorio, M. J., Pierce, D. W., Cayan, D. R., & Miller, A. J. (2013). Western U.S. extreme precipitation events and their relation to ENSO and PDO in CCSM4. *Journal of Climate*, 26(12), 4231–4243. <https://doi.org/10.1175/JCLI-D-12-00257.1>
11. DeGaetano, A. T., & Castellano, C. M. (2017). Future projections of extreme precipitation intensity-duration-frequency curves for climate adaptation planning in New York State. *Climate Services*, 5, 23–35. <https://doi.org/10.1016/j.cliser.2017.03.003>
12. Fant, C., Jacobs, J. M., Chinowsky, P., Sweet, W., Weiss, N., Sias, J. E., Martinich, J., & Neumann, J. E. (2021). Mere Nuisance or Growing Threat? The Physical and Economic Impact of High Tide Flooding on US Road Networks. *Journal of Infrastructure Systems*, 27(4), 04021044. [https://doi.org/10.1061/\(ASCE\)IS.1943-555X.0000652](https://doi.org/10.1061/(ASCE)IS.1943-555X.0000652)
13. Finzi Hart, J., May, C. L., Mak, M., Ramirez Lopez, D., Cohn, A., Rockwell, J., & Anbessie, T. (2022). *Climate Projections for Stormwater and Wastewater Resilience Planning*. Pathways Climate Institute.
14. Fish, M. A., Done, J. M., Swain, D. L., Wilson, A. M., Michaelis, A. C., Gibson, P. B., & Ralph, M. (2022). Large-Scale Environments of Successive Atmospheric River Events Leading to Compound Precipitation Extremes in California. *Journal of Climate*, 35(5), 1515–1536. <https://doi.org/10.1175/JCLI-D-21-0168.1>
15. Goddard, L., & Gershunov, A. (2020). Impact of El Niño on Weather and Climate Extremes. *Geophysical Monograph Series*, 253, 361–375. <https://doi.org/10.1002/9781119548164.CH16>
16. Griggs, G. B. (1998). California’s Coastline: El Nino, Erosion, and Protection. In *California’s Coastal Natural Hazards*, CSBPA Conference (pp. 36–55).
17. Hausfather, Z., Marvel, K., Schmidt, G. A., Nielsen-Gammon, J. W., & Zelinka, M. (2022). Climate simulations: Recognize the ‘hot model’ problem. *Nature*, 605(7908), 26–29. <https://doi.org/10.1038/d41586-022-01192-2>
18. Huang, X., & Swain, D. L. (2022). Climate change is increasing the risk of a California megaflood. *Science Advances*, 8(32). https://doi.org/10.1126/SCIADV.ABQ0995/SUPPL_FILE/SCIADV.ABQ0995_MOVIES_S1_AND_S2.ZIP
19. IPCC. (2021). Summary for Policymakers. In: *Climate Change 2021: The Physical Science Basis. Contribution of Working Group I to the Sixth Assessment Report of the Intergovernmental Panel on Climate Change* [Masson-Delmotte, V., P. Zhai, A. Pirani, S. L. Connors, C. Péan. <https://www.ipcc.ch/report/ar6/wg1/>
20. Kunkel, K. E., Esterling, T. R., Karl, J. C., Biard, S. M., Champion, B. E., Gleason, K. M., Johnson, A., Li, S., Stegall, L. E., Stevens, S. E., M, S., L, S., & X, Y. (2020). *Incorporation of the Effects of Future Anthropogenically Forced Climate Change in Intensity-Duration-Frequency Design Values: Final Report* (p. 123). North Carolina Institute for Climate Studies, North Carolina State University.

21. Lamjiri, M. A., Dettinger, M. D., Ralph, F. M., Oakley, N. S., & Rutz, J. J. (2018). Hourly Analyses of the Large Storms and Atmospheric Rivers that Provide Most of California's Precipitation in Only 10 to 100 Hours per Year. *San Francisco Estuary and Watershed Science*, 16(4), 1–17. <https://doi.org/10.15447/sfews.2018v16iss4art1>
22. Lopez-Cantu, T., Prein, A. F., & Samaras, C. (2020). Uncertainties in Future U.S. Extreme Precipitation From Downscaled Climate Projections. *Geophysical Research Letters*, 47(e2019GL08679). <https://doi.org/10.1029/2019GL086797>
23. Mauger, G. S., Won, J. S., Hegewisch, K., Lynch, C., & ... (2018). New Projections of Changing Heavy Precipitation in King County (Issue May).
24. May, C., & Mak, M. (2013). Climate Change Adaptation Task 1: Review of Design Storms (p. 52). Prepared for the San Francisco Public Utilities Commission Sewer System Improvement Program.
25. May, C., Mak, M., Harris, E., Lightner, M., Guyenet, J., Vandever, J., Kassem, S., & Adleman, L. (2016). Extreme Storms in San Francisco Bay – Past to Present (p. 48). Federal Emergency Management Agency.
26. Miro, M. E., Degaetano, A. T., López-cantú, T., Samaras, C., & Webber, M. (2021). Developing Future Projected Intensity-Duration-Frequency (IDF) Curves (p. 62).
27. Molnar, P., Fatichi, S., Gaál, L., Szolgay, J., & Burlando, P. (2015). Storm type effects on super Clausius-Clapeyron scaling of intense rainstorm properties with air temperature. *Hydrology and Earth System Sciences*, 19(4), 1753–1766. <https://doi.org/10.5194/hess-19-1753-2015>
28. Obeysekera, J., Sukop, M. C., Troxler, T. G., & Anupama, J. (2021). Updating the Statewide Extreme Rainfall Projections. Prepared for the Sea Level Solutions Center, Institute of Environment, Florida International University.
29. OPC & CNRA. (2018). State of California Sea Level Rise Guidance (p. 84). Prepared by the California Ocean Protection Council and the California National Resources Agency.
30. Pall, P., Allen, M. R., & Stone, D. A. (2007). Testing the Clausius-Clapeyron constraint on changes in extreme precipitation under CO₂ warming. *Climate Dynamics*, 28(4), 351–363. <https://doi.org/10.1007/s00382-006-0180-2>
31. Pall, P., Patricola, C. M., Wehner, M. F., Stone, D. A., Paciorek, C. J., & Collins, W. D. (2017). Diagnosing conditional anthropogenic contributions to heavy Colorado rainfall in September 2013. *Weather and Climate Extremes*, 17, 1–6. <https://doi.org/10.1016/j.wace.2017.03.004>
32. Patricola, C. M., Wehner, M. F., Bercos-Hickey, E., Maciel, F. V., May, C., Mak, M., Yip, O., Roche, A., & Leal, S. (2022). Future Changes in Extreme Precipitation over the San Francisco Bay Area: Dependence on Atmospheric River and Extratropical Cyclone Events. *Weather and Climate Extremes*, 36. <https://doi.org/10.1016/j.wace.2022.100440>

33. Pendergrass, A. G. (2018). What precipitation is extreme? *Science*, 360(6393), 1072–1073. <https://doi.org/10.1126/science.aat1871>
34. Pierce, D., & Cayan, D. (2017). High-Resolution LOCA Downscaled Climate Projections Aim to Better Represent Extreme Weather Events.
35. Pierce, D., Cayan, D., & Thrasher, B. (2014). Statistical downscaling using localized constructed analogs (LOCA). *Journal of Hydrometeorology*, 15(6), 2558–2585. <https://doi.org/10.1175/JHM-D-14-0082.1>
36. Pierce, D. W., Cayan, D. R., & Dehann, L. (2016). Creating Climate projections to support the 4th California Climate Assessment (pp. 1–20). Division of Climate, Atmospheric Sciences, and Physical Oceanography, Scripps Institution of Oceanography.
37. Ragno, E., AghaKouchak, A., Love, C. A., Cheng, L., Vahedifard, F., & Lima, C. H. R. (2018a). Quantifying Changes in Future Intensity-Duration-Frequency Curves Using Multimodel Ensemble Simulations. *Water Resources Research*, 54(3), 1751–1764. <https://doi.org/10.1002/2017WR021975>
38. Ragno, E., AghaKouchak, A., Love, C. A., Cheng, L., Vahedifard, F., & Lima, C. H. R. (2018b). Quantifying Changes in Future Intensity-Duration-Frequency Curves Using Multimodel Ensemble Simulations. *Water Resources Research*, 54(3), 1751–1764. <https://doi.org/10.1002/2017WR021975>
39. Rahimi, R., Tavakol-Davani, H., Graves, C., Gomez, A., & Valipour, M. F. (2020). Compound inundation impacts of coastal climate change: Sea-level rise, groundwater rise, and coastal precipitation. *Water (Switzerland)*, 12(10). <https://doi.org/10.3390/w12102776>
40. Ralph, M. F., Rutz, J. J., Cordeira, J. M., Dettinger, M., Anderson, M., Reynolds, D., Schick, L. J., & Smallcomb, C. (2019). A Scale to Characterize the Strength and Impacts of Atmospheric Rivers. *Bulletin of the American Meteorological Society*, 100(2), 269–289. <https://doi.org/10.1175/BAMS-D-18-0023.1>
41. Rhoades, A. M., Jones, A. D., Srivastava, A., Huang, H., O'Brien, T. A., Patricola, C. M., Ullrich, P. A., Wehner, M., & Zhou, Y. (2020). The Shifting Scales of Western U.S. Landfalling Atmospheric Rivers Under Climate Change. *Geophysical Research Letters*, 47(17), e2020GL089096. <https://doi.org/10.1029/2020GL089096>
42. Risser, M. D., & Wehner, M. F. (2017). Attributable Human-Induced Changes in the Likelihood and Magnitude of the Observed Extreme Precipitation during Hurricane Harvey. *Geophysical Research Letters*, 44, 12457–12464. <https://doi.org/10.1002/2017GL075888>
43. Sanders, F., & Gyakum, J. R. (1980). Synoptic-Dynamic Climatology of the “Bomb.” *Monthly Weather Review*, 10, 1589–1606. [https://doi.org/10.1175/1520-0493\(1980\)108<1589:SDCOT>2.0.CO;2](https://doi.org/10.1175/1520-0493(1980)108<1589:SDCOT>2.0.CO;2)

44. Smirnov, D., Giovannettone, J., Lawler, S., Sreetharan, M., Plummer, J., Workman, B., Batten, B., Rosenberg, S., & Mcglone, D. (2018). Analysis of Historical and Future Heavy Precipitation: City of Virginia Beach, Virginia.
45. Stockhause, M., & Lautenschlager, M. (2017). CMIP6 Data Citation of Evolving Data. *Data Science Journal*, 16, 30. <https://doi.org/10.5334/dsj-2017-030>
46. Swain, D. L., Langenbrunner, B., Neelin, J. D., & Hall, A. (2018). Increasing precipitation volatility in twenty-first-century California. *Nature Climate Change*, 8(5), 427–433. <https://doi.org/10.1038/s41558-018-0140-y>
47. Sweet, W., Dusek, G., Obeysekera, J., & Marra, J. (2018). Patterns and Projections of High Tide Flooding Along the U.S. Coastline Using a Common Impact Threshold (Issue February, p. 44). National Oceanic and Atmospheric Administration, U.S. Department of Commerce, National Ocean Service, and the Center for Operational Oceanographic Products and Services.
48. Sweet, W. V., Hamlington, B. D., Kopp, R. E., Weaver, C. P., Barnard, P. L., Bekaert, D., Brooks, W., Craghan, M., Dusek, G., Frederikse, T., Garner, G., Genz, A. S., Krasting, J. P., Larour, E., Marcy, D., Marra, J. J., Obeysekera, J., Osler, M., Pendleton, M., ... Zuzak, C. (2022). Global and Regional Sea Level Rise Scenarios for the United States: Updated Mean Projections and Extreme Water Level Probabilities Along U.S. Coastlines (p. 95). NOAA Technical Report NOS 01.
49. Tetra Tech Inc. (2015). Hydrologic Design Standards under Future Climate for Grand Rapids, Michigan (p. 44).
50. USGS. (1999). El Nino sea-level rise wreaks havoc on California's San Francisco Bay region. *Spring*, 175–199.
51. Wang, G., Kirchhoff, C. J., Seth, A., Abatzoglou, J. T., Livneh, B., Pierce, D. W., Fomenko, L., & Ding, T. (2020). Projected changes of precipitation characteristics depend on downscaling method and training data: Maca versus loca using the u.s. Northeast as an example. *Journal of Hydrometeorology*, 21(12), 2739–2758. <https://doi.org/10.1175/JHM-D-19-0275.1>
52. Zhang, Z., Ralph, F. M., & Zheng, M. (2019). The Relationship Between Extratropical Cyclone Strength and Atmospheric River Intensity and Position. *Geophysical Research Letters*, 10. <https://doi.org/10.1029/2018GL079071>
53. Zhu, Y., & Newell, R. E. (1994). Atmospheric rivers and bombs. *Geophysical Research Letters*, 21(18), 1999–2002. <https://doi.org/10.1029/94GL01710>

Appendix A

Steps for Scaling IDF Curves and Supporting Scaling Factors (for 2050 and 2100)

The following summarizes the methodology used to transform the WRF, LOCA, and CMIP6 ensemble climate models to derive the future conditions IDF curves for 2050 and 2100.

- WRF (AR+ETC) 2050 and 2100 C-C ratios: Use WRF simulations to derive Clausius- Clapeyron ratios for individual temporal durations. Apply the AR+ETC storm weighting adjustment factor, then calculate the C-C ratios for each temporal duration (15-min through 24-hour) for 2050 and 2100. This partially provides the IDF scaling along the duration dimension.
- WRF (AR+ETC) historical return period: Estimate the average return period of the historical AR+ETC storms modeled in WRF (resulting in an average return period of 2 years across multiple durations).
- WRF-LOCA C-C scale factors (normalized percent change): Using the percent change factors for each return period (1-year through 500-year) calculated using the LOCA ensemble, normalize the percent change factors to the estimated return period of the combined AR+ETC storm events modeled in WRF. This returns adjustment factors to scale the C-C ratios for each temporal duration from the estimated return period of the combined AR+ETC storms to other return periods (1-, 2-, 5-, 10-, 25-, 50-, 100-, and 500-year). This partially provides the IDF scaling along the frequency dimension.
- CMIP6 2050 and 2100 C-C percent change: Using the historical to future percent change factors for the C-C ratios obtained from the CMIP6 models, apply the percent change factors to the WRF-LOCA scaled C-C ratios for 2050 and 2100.
 - CMIP6 C-C change factor for 2050 = 1.15 (+15.3%)
 - CMIP6 C-C change factor for 2100 = 1.40 (+39.7%)

This results in the percent change factors to apply to the NOAA Atlas 14 precipitation depths for all temporal durations and return periods.

Appendix B

The following tables provide estimated percent change scaling factors for converting historical Atlas 14 IDF curves to the given year along SSP5-8.5. Values have been calculated by interpolating WRF-LOCA C-C scale factors to the given year and then apply those to the corresponding CMIP6 C-C percent change for the given year. Tables of the final estimated percent change are provided for every 5 years between 2020 and 2100, a high enough frequency that further interpolation of these tables to intermediate years should be reasonable.

Duration	Return Period							
	1-yr	2-yr	5-yr	10-yr	25-yr	50-yr	100-yr	500-yr
15-min	8.9%	9.2%	9.6%	10.0%	10.5%	10.9%	11.3%	12.6%
90% CI	6.2-11.6%	6.5-11.9%	6.9-12.4%	7.2-12.7%	7.7-13.2%	8.1-13.7%	8.5-14.2%	9.7-15.5%
30-min	8.8%	9.1%	9.5%	9.9%	10.4%	10.8%	11.2%	12.5%
90% CI	6.0-11.6%	6.3-11.9%	6.7-12.4%	7.0-12.7%	7.5-13.3%	7.9-13.7%	8.3-14.2%	9.4-15.5%
60-min	8.4%	8.7%	9.1%	9.4%	9.9%	10.3%	10.8%	12.0%
90% CI	5.4-11.4%	5.7-11.7%	6.0-12.2%	6.4-12.5%	6.8-13.0%	7.2-13.5%	7.6-14.0%	8.7-15.3%
2-hr	7.5%	7.8%	8.2%	8.5%	9.0%	9.4%	9.9%	11.0%
90% CI	4.6-10.4%	4.9-10.7%	5.3-11.2%	5.6-11.5%	6.0-12.0%	6.4-12.5%	6.8-12.9%	7.9-14.2%
3-hr	7.3%	7.6%	8.0%	8.4%	8.8%	9.2%	9.7%	10.9%
90% CI	4.5-10.1%	4.8-10.4%	5.2-10.9%	5.5-11.2%	5.9-11.7%	6.3-12.2%	6.7-12.6%	7.8-13.9%
6-hr	6.5%	6.9%	7.2%	7.6%	8.0%	8.4%	8.8%	10.0%
90% CI	4.3-8.8%	4.6-9.1%	4.9-9.6%	5.2-9.9%	5.7-10.4%	6.0-10.8%	6.4-11.2%	7.5-12.5%
12-hr	6.4%	6.7%	7.1%	7.4%	7.9%	8.3%	8.7%	9.9%
90% CI	4.9-8.0%	5.2-8.3%	5.6-8.7%	5.9-9.0%	6.3-9.5%	6.7-9.9%	7.1-10.3%	8.2-11.5%
24-hr	6.2%	6.5%	6.9%	7.2%	7.7%	8.1%	8.5%	9.7%
90% CI	3.4-9.1%	3.6-9.5%	4.0-9.9%	4.3-10.2%	4.7-10.7%	5.1-11.1%	5.4-11.6%	6.5-12.8%
2-day	6.6%	6.9%	7.3%	7.6%	8.0%	8.4%	8.9%	10.0%
90% CI	3.3-9.8%	3.6-10.1%	4.0-10.6%	4.3-10.9%	4.7-11.4%	5.0-11.8%	5.4-12.3%	6.5-13.6%
3-day	6.2%	6.5%	6.9%	7.2%	7.7%	8.1%	8.5%	9.6%
90% CI	3.5-8.9%	3.8-9.2%	4.1-9.7%	4.4-10.0%	4.8-10.5%	5.2-10.9%	5.6-11.4%	6.6-12.6%

Table B1. Percent Change in Precipitation Depth for Scaling Historical Atlas 14 to 2020 under SSP5-8.5 (Based on CMIP6 C-C Trend for 2020 applied to interpolated WRF C-C Scale Factor)

Duration	Return Period							
	1-yr	2-yr	5-yr	10-yr	25-yr	50-yr	100-yr	500-yr
15-min	10.8%	11.3%	11.8%	12.3%	13.0%	13.5%	14.1%	15.8%
90% CI	7.2-14.4%	7.6-14.9%	8.2-15.5%	8.6-16.0%	9.2-16.7%	9.7-17.3%	10.3-18.0%	11.9-19.7%
30-min	10.7%	11.1%	11.7%	12.2%	12.8%	13.4%	14.0%	15.6%
90% CI	7.0-14.4%	7.4-14.9%	7.9-15.5%	8.3-16.0%	8.9-16.7%	9.4-17.3%	10.0-18.0%	11.5-19.7%
60-min	10.1%	10.6%	11.1%	11.6%	12.2%	12.8%	13.4%	15.0%
90% CI	6.1-14.2%	6.5-14.6%	7.0-15.2%	7.4-15.7%	8.0-16.4%	8.5-17.0%	9.1-17.7%	10.6-19.4%
2-hr	9.0%	9.4%	9.9%	10.4%	11.0%	11.5%	12.1%	13.7%
90% CI	5.1-12.9%	5.5-13.3%	6.0-13.9%	6.4-14.4%	7.0-15.1%	7.4-15.6%	8.0-16.3%	9.5-18.0%
3-hr	8.7%	9.1%	9.7%	10.1%	10.8%	11.3%	11.9%	13.5%
90% CI	5.0-12.5%	5.4-12.9%	5.9-13.5%	6.3-14.0%	6.8-14.7%	7.3-15.2%	7.9-15.9%	9.4-17.6%
6-hr	7.7%	8.1%	8.6%	9.0%	9.7%	10.2%	10.8%	12.3%
90% CI	4.6-10.7%	5.0-11.2%	5.5-11.7%	5.9-12.2%	6.5-12.8%	7.0-13.4%	7.5-14.0%	9.0-15.7%
12-hr	7.5%	7.9%	8.5%	8.9%	9.5%	10.0%	10.6%	12.1%
90% CI	5.4-9.6%	5.8-10.0%	6.3-10.6%	6.8-11.0%	7.4-11.6%	7.9-12.2%	8.4-12.8%	9.9-14.4%
24-hr	7.3%	7.7%	8.2%	8.6%	9.2%	9.8%	10.3%	11.9%
90% CI	3.4-11.1%	3.7-11.6%	4.2-12.2%	4.6-12.6%	5.2-13.3%	5.7-13.8%	6.2-14.5%	7.6-16.1%
2-day	7.7%	8.1%	8.6%	9.1%	9.7%	10.2%	10.8%	12.3%
90% CI	3.3-12.0%	3.7-12.5%	4.2-13.1%	4.6-13.5%	5.2-14.2%	5.6-14.8%	6.2-15.4%	7.6-17.1%
3-day	7.2%	7.6%	8.1%	8.6%	9.2%	9.7%	10.3%	11.8%
90% CI	3.6-10.9%	3.9-11.3%	4.4-11.9%	4.8-12.3%	5.4-13.0%	5.9-13.6%	6.4-14.2%	7.8-15.8%

Table B2. Percent Change in Precipitation Depth for Scaling Historical Atlas 14 to 2025 under SSP5-8.5 (Based on CMIP6 C-C Trend for 2025 applied to interpolated WRF C-C Scale Factor)

Duration	Return Period							
	1-yr	2-yr	5-yr	10-yr	25-yr	50-yr	100-yr	500-yr
15-min	13.3%	13.9%	14.6%	15.2%	16.0%	16.7%	17.5%	19.6%
90% CI	8.8-17.9%	9.3-18.5%	10.0-19.3%	10.5-19.9%	11.3-20.8%	11.9-21.5%	12.7-22.4%	14.6-24.6%
30-min	13.2%	13.7%	14.4%	15.0%	15.9%	16.6%	17.3%	19.4%
90% CI	8.4-17.9%	8.9-18.5%	9.6-19.3%	10.1-19.9%	10.9-20.8%	11.6-21.6%	12.3-22.4%	14.2-24.6%
60-min	12.4%	13.0%	13.7%	14.3%	15.1%	15.8%	16.6%	18.6%
90% CI	7.3-17.6%	7.8-18.1%	8.5-18.9%	9.0-19.5%	9.8-20.4%	10.4-21.2%	11.1-22.0%	13.0-24.3%
2-hr	11.0%	11.5%	12.2%	12.7%	13.6%	14.2%	15.0%	17.0%
90% CI	6.0-15.9%	6.5-16.5%	7.1-17.2%	7.7-17.8%	8.4-18.7%	9.0-19.4%	9.7-20.2%	11.6-22.4%
3-hr	10.7%	11.2%	11.9%	12.4%	13.2%	13.9%	14.7%	16.7%
90% CI	5.9-15.4%	6.4-16.0%	7.0-16.7%	7.5-17.3%	8.3-18.2%	8.9-18.9%	9.6-19.7%	11.5-21.9%
6-hr	9.3%	9.8%	10.5%	11.1%	11.9%	12.5%	13.3%	15.2%
90% CI	5.5-13.2%	6.0-13.7%	6.6-14.5%	7.1-15.0%	7.8-15.9%	8.5-16.6%	9.1-17.4%	11.0-19.5%
12-hr	9.1%	9.6%	10.3%	10.9%	11.6%	12.3%	13.0%	15.0%
90% CI	6.5-11.7%	7.0-12.3%	7.6-13.0%	8.2-13.5%	8.9-14.4%	9.6-15.1%	10.2-15.8%	12.1-17.9%
24-hr	8.8%	9.3%	10.0%	10.5%	11.3%	12.0%	12.7%	14.6%
90% CI	3.9-13.7%	4.3-14.3%	5.0-15.0%	5.4-15.6%	6.2-16.4%	6.8-17.2%	7.4-17.9%	9.2-20.1%
2-day	9.3%	9.9%	10.5%	11.1%	11.9%	12.5%	13.3%	15.2%
90% CI	3.8-14.9%	4.3-15.4%	4.9-16.2%	5.4-16.8%	6.1-17.6%	6.7-18.3%	7.4-19.1%	9.2-21.3%
3-day	8.7%	9.3%	9.9%	10.5%	11.2%	11.9%	12.6%	14.6%
90% CI	4.1-13.4%	4.6-13.9%	5.2-14.7%	5.7-15.2%	6.4-16.1%	7.0-16.8%	7.7-17.6%	9.5-19.7%

Table B3. Percent Change in Precipitation Depth for Scaling Historical Atlas 14 to 2030 under SSP5-8.5 (Based on CMIP6 C-C Trend for 2030 applied to interpolated WRF C-C Scale Factor)

Duration	Return Period							
	1-yr	2-yr	5-yr	10-yr	25-yr	50-yr	100-yr	500-yr
15-min	15.5%	16.2%	17.1%	17.8%	18.8%	19.7%	20.6%	23.2%
90% CI	10.0-21.1%	10.6-21.8%	11.4-22.7%	12.1-23.5%	13.1-24.6%	13.8-25.5%	14.7-26.5%	17.1-29.2%
30-min	15.3%	16.0%	16.9%	17.6%	18.6%	19.5%	20.4%	22.9%
90% CI	9.6-21.1%	10.2-21.8%	11.0-22.7%	11.7-23.5%	12.6-24.6%	13.4-25.5%	14.3-26.5%	16.6-29.3%
60-min	14.4%	15.1%	16.0%	16.7%	17.7%	18.5%	19.5%	22.0%
90% CI	8.2-20.7%	8.8-21.4%	9.6-22.3%	10.3-23.1%	11.2-24.2%	12.0-25.1%	12.8-26.1%	15.2-28.8%
2-hr	12.7%	13.3%	14.1%	14.8%	15.8%	16.6%	17.5%	20.0%
90% CI	6.7-18.7%	7.2-19.4%	8.0-20.3%	8.7-21.0%	9.6-22.1%	10.3-23.0%	11.2-23.9%	13.4-26.6%
3-hr	12.3%	12.9%	13.8%	14.4%	15.4%	16.2%	17.1%	19.6%
90% CI	6.5-18.1%	7.1-18.8%	7.9-19.7%	8.5-20.4%	9.4-21.4%	10.2-22.3%	11.0-23.3%	13.3-25.9%
6-hr	10.7%	11.3%	12.1%	12.8%	13.7%	14.6%	15.4%	17.8%
90% CI	6.0-15.4%	6.6-16.0%	7.3-16.9%	8.0-17.6%	8.9-18.6%	9.6-19.5%	10.4-20.4%	12.7-23.0%
12-hr	10.4%	11.0%	11.9%	12.5%	13.5%	14.3%	15.2%	17.6%
90% CI	7.2-13.6%	7.8-14.3%	8.6-15.1%	9.3-15.8%	10.2-16.8%	10.9-17.6%	11.8-18.6%	14.1-21.0%
24-hr	10.0%	10.7%	11.5%	12.1%	13.1%	13.9%	14.8%	17.1%
90% CI	4.0-16.0%	4.6-16.7%	5.4-17.6%	6.0-18.3%	6.8-19.3%	7.6-20.2%	8.4-21.1%	10.6-23.7%
2-day	10.7%	11.3%	12.1%	12.8%	13.8%	14.6%	15.5%	17.9%
90% CI	4.0-17.4%	4.6-18.1%	5.3-19.0%	5.9-19.7%	6.8-20.7%	7.5-21.6%	8.3-22.6%	10.5-25.2%
3-day	10.0%	10.6%	11.4%	12.1%	13.0%	13.8%	14.7%	17.1%
90% CI	4.3-15.6%	4.9-16.3%	5.7-17.1%	6.3-17.9%	7.1-18.9%	7.9-19.7%	8.7-20.7%	10.9-23.2%

Table B4. Percent Change in Precipitation Depth for Scaling Historical Atlas 14 to 2035 under SSP5-8.5 (Based on CMIP6 C-C Trend for 2035 applied to interpolated WRF C-C Scale Factor)

Duration	Return Period							
	1-yr	2-yr	5-yr	10-yr	25-yr	50-yr	100-yr	500-yr
15-min	17.7%	18.4%	19.5%	20.3%	21.5%	22.5%	23.6%	26.7%
90% CI	11.1-24.2%	11.9-25.0%	12.8-26.1%	13.6-27.0%	14.7-28.3%	15.7-29.4%	16.7-30.6%	19.5-33.8%
30-min	17.4%	18.2%	19.2%	20.1%	21.3%	22.3%	23.4%	26.4%
90% CI	10.6-24.2%	11.4-25.1%	12.3-26.2%	13.1-27.1%	14.2-28.3%	15.1-29.4%	16.2-30.6%	18.9-33.9%
60-min	16.4%	17.1%	18.2%	19.0%	20.2%	21.2%	22.3%	25.3%
90% CI	9.0-23.7%	9.7-24.6%	10.7-25.7%	11.4-26.5%	12.5-27.8%	13.5-28.9%	14.5-30.1%	17.2-33.3%
2-hr	14.3%	15.0%	16.0%	16.8%	18.0%	19.0%	20.0%	22.9%
90% CI	7.2-21.3%	7.9-22.2%	8.8-23.2%	9.5-24.1%	10.6-25.3%	11.5-26.4%	12.5-27.6%	15.2-30.7%
3-hr	13.8%	14.6%	15.6%	16.4%	17.5%	18.5%	19.6%	22.5%
90% CI	7.0-20.6%	7.7-21.4%	8.6-22.5%	9.3-23.4%	10.4-24.6%	11.3-25.7%	12.3-26.8%	15.0-29.9%
6-hr	11.9%	12.7%	13.6%	14.4%	15.5%	16.5%	17.5%	20.4%
90% CI	6.4-17.4%	7.1-18.2%	8.0-19.3%	8.7-20.1%	9.8-21.3%	10.7-22.3%	11.7-23.4%	14.3-26.4%
12-hr	11.6%	12.4%	13.3%	14.1%	15.2%	16.2%	17.2%	20.0%
90% CI	7.9-15.4%	8.6-16.1%	9.5-17.1%	10.3-18.0%	11.3-19.1%	12.2-20.1%	13.2-21.2%	15.9-24.2%
24-hr	11.2%	11.9%	12.9%	13.6%	14.8%	15.7%	16.7%	19.5%
90% CI	4.1-18.2%	4.8-19.0%	5.7-20.1%	6.4-20.9%	7.4-22.1%	8.3-23.1%	9.2-24.3%	11.8-27.3%
2-day	11.9%	12.7%	13.7%	14.4%	15.6%	16.5%	17.6%	20.4%
90% CI	4.0-19.8%	4.7-20.7%	5.6-21.7%	6.3-22.6%	7.3-23.8%	8.2-24.8%	9.2-26.0%	11.7-29.1%
3-day	11.1%	11.8%	12.8%	13.6%	14.7%	15.6%	16.6%	19.5%
90% CI	4.4-17.7%	5.1-18.5%	6.0-19.6%	6.7-20.4%	7.7-21.6%	8.6-22.6%	9.6-23.7%	12.2-26.7%

Table B5. Percent Change in Precipitation Depth for Scaling Historical Atlas 14 to 2040 under SSP5-8.5 (Based on CMIP6 C-C Trend for 2040 applied to interpolated WRF C-C Scale Factor)

Duration	Return Period							
	1-yr	2-yr	5-yr	10-yr	25-yr	50-yr	100-yr	500-yr
15-min	20.6%	21.6%	22.8%	23.7%	25.1%	26.3%	27.6%	31.1%
90% CI	13.0-28.2%	13.9-29.2%	15.0-30.5%	15.9-31.5%	17.2-33.0%	18.3-34.3%	19.5-35.7%	22.8-39.4%
30-min	20.4%	21.3%	22.5%	23.4%	24.8%	26.0%	27.3%	30.8%
90% CI	12.4-28.3%	13.3-29.2%	14.4-30.5%	15.3-31.6%	16.6-33.1%	17.7-34.3%	18.9-35.7%	22.1-39.5%
60-min	19.1%	20.0%	21.2%	22.2%	23.6%	24.7%	26.0%	29.5%
90% CI	10.6-27.7%	11.4-28.7%	12.5-29.9%	13.4-31.0%	14.7-32.5%	15.7-33.7%	16.9-35.1%	20.1-38.8%
2-hr	16.7%	17.6%	18.7%	19.7%	21.0%	22.1%	23.4%	26.8%
90% CI	8.4-24.9%	9.3-25.9%	10.3-27.1%	11.2-28.1%	12.4-29.6%	13.5-30.8%	14.6-32.2%	17.7-35.8%
3-hr	16.2%	17.0%	18.2%	19.1%	20.5%	21.6%	22.8%	26.2%
90% CI	8.2-24.1%	9.0-25.0%	10.1-26.3%	11.0-27.3%	12.2-28.7%	13.3-30.0%	14.4-31.3%	17.5-34.9%
6-hr	14.0%	14.8%	16.0%	16.9%	18.2%	19.3%	20.5%	23.8%
90% CI	7.5-20.4%	8.3-21.3%	9.4-22.5%	10.2-23.5%	11.5-24.9%	12.5-26.1%	13.7-27.3%	16.7-30.8%
12-hr	13.6%	14.5%	15.6%	16.5%	17.8%	18.9%	20.1%	23.4%
90% CI	9.3-18.0%	10.1-18.9%	11.2-20.0%	12.0-21.0%	13.3-22.4%	14.3-23.5%	15.5-24.8%	18.6-28.2%
24-hr	13.1%	13.9%	15.1%	16.0%	17.3%	18.4%	19.6%	22.8%
90% CI	4.9-21.3%	5.6-22.2%	6.7-23.4%	7.5-24.4%	8.7-25.8%	9.7-27.0%	10.8-28.3%	13.8-31.8%
2-day	14.0%	14.9%	16.0%	16.9%	18.2%	19.3%	20.5%	23.8%
90% CI	4.8-23.2%	5.6-24.1%	6.6-25.4%	7.4-26.3%	8.6-27.8%	9.6-29.0%	10.7-30.3%	13.7-33.9%
3-day	13.0%	13.8%	15.0%	15.9%	17.2%	18.3%	19.5%	22.7%
90% CI	5.3-20.7%	6.0-21.6%	7.1-22.8%	7.9-23.8%	9.1-25.2%	10.1-26.4%	11.2-27.7%	14.2-31.2%

Table B6. Percent Change in Precipitation Depth for Scaling Historical Atlas 14 to 2045 under SSP5-8.5 (Based on CMIP6 C-C Trend for 2045 applied to interpolated WRF C-C Scale Factor)

Duration	Return Period							
	1-yr	2-yr	5-yr	10-yr	25-yr	50-yr	100-yr	500-yr
15-min	23.3%	24.3%	25.7%	26.8%	28.4%	29.8%	31.2%	35.2%
90% CI	14.6-31.9%	15.6-33.1%	16.9-34.5%	17.9-35.7%	19.4-37.4%	20.6-38.9%	22.0-40.5%	25.7-44.7%
30-min	23.0%	24.0%	25.4%	26.5%	28.1%	29.4%	30.9%	34.9%
90% CI	13.9-32.0%	14.9-33.1%	16.2-34.6%	17.2-35.8%	18.7-37.5%	19.9-38.9%	21.3-40.5%	25.0-44.8%
60-min	21.6%	22.6%	24.0%	25.0%	26.6%	28.0%	29.4%	33.4%
90% CI	11.8-31.3%	12.8-32.4%	14.0-33.9%	15.0-35.1%	16.5-36.8%	17.7-38.2%	19.0-39.8%	22.7-44.1%
2-hr	18.8%	19.8%	21.1%	22.2%	23.7%	25.0%	26.4%	30.3%
90% CI	9.4-28.2%	10.3-29.3%	11.5-30.7%	12.5-31.8%	13.9-33.5%	15.1-34.9%	16.4-36.4%	20.0-40.6%
3-hr	18.2%	19.2%	20.5%	21.6%	23.1%	24.4%	25.8%	29.6%
90% CI	9.1-27.2%	10.1-28.3%	11.3-29.7%	12.2-30.9%	13.7-32.5%	14.9-33.9%	16.2-35.4%	19.7-39.6%
6-hr	15.7%	16.6%	17.9%	19.0%	20.5%	21.7%	23.1%	26.9%
90% CI	8.3-23.0%	9.2-24.0%	10.5-25.4%	11.4-26.5%	12.8-28.1%	14.0-29.5%	15.3-30.9%	18.8-34.9%
12-hr	15.3%	16.2%	17.5%	18.6%	20.1%	21.3%	22.7%	26.5%
90% CI	10.3-20.2%	11.2-21.3%	12.5-22.6%	13.4-23.7%	14.9-25.2%	16.1-26.6%	17.4-28.0%	21.0-31.9%
24-hr	14.7%	15.6%	16.9%	17.9%	19.4%	20.7%	22.1%	25.8%
90% CI	5.3-24.0%	6.2-25.1%	7.3-26.5%	8.3-27.6%	9.7-29.2%	10.8-30.6%	12.1-32.0%	15.5-36.1%
2-day	15.7%	16.7%	18.0%	19.0%	20.5%	21.8%	23.2%	26.9%
90% CI	5.2-26.2%	6.1-27.3%	7.3-28.7%	8.2-29.8%	9.6-31.4%	10.7-32.8%	12.0-34.3%	15.4-38.4%
3-day	14.6%	15.5%	16.8%	17.8%	19.3%	20.6%	21.9%	25.7%
90% CI	5.7-23.4%	6.6-24.4%	7.8-25.8%	8.7-26.9%	10.1-28.5%	11.3-29.9%	12.5-31.3%	16.0-35.4%

Table B7. Percent Change in Precipitation Depth for Scaling Historical Atlas 14 to 2050 under SSP5-8.5 (Based on CMIP6 C-C Trend for 2050 applied to interpolated WRF C-C Scale Factor)

Duration	Return Period							
	1-yr	2-yr	5-yr	10-yr	25-yr	50-yr	100-yr	500-yr
15-min	25.3%	26.5%	28.1%	29.3%	31.0%	32.4%	34.0%	38.2%
90% CI	16.5-34.1%	17.7-35.4%	19.1-37.0%	20.2-38.3%	21.8-40.2%	23.2-41.7%	24.6-43.4%	28.6-47.9%
30-min	25.1%	26.3%	27.8%	29.0%	30.8%	32.2%	33.8%	38.0%
90% CI	15.8-34.3%	16.9-35.6%	18.3-37.3%	19.5-38.6%	21.1-40.4%	22.4-42.0%	23.8-43.7%	27.7-48.2%
60-min	23.8%	25.0%	26.6%	27.8%	29.5%	30.9%	32.5%	36.6%
90% CI	13.8-33.9%	14.9-35.2%	16.3-36.9%	17.4-38.2%	18.9-40.0%	20.2-41.6%	21.7-43.2%	25.5-47.7%
2-hr	21.2%	22.4%	23.9%	25.0%	26.7%	28.1%	29.6%	33.7%
90% CI	11.3-31.0%	12.4-32.3%	13.8-33.9%	14.9-35.2%	16.4-37.0%	17.7-38.5%	19.1-40.2%	22.8-44.6%
3-hr	20.5%	21.7%	23.2%	24.3%	26.0%	27.4%	28.9%	33.0%
90% CI	10.7-30.3%	11.8-31.6%	13.2-33.2%	14.2-34.5%	15.8-36.3%	17.0-37.8%	18.4-39.4%	22.1-43.8%
6-hr	17.7%	18.8%	20.3%	21.4%	23.1%	24.4%	25.9%	29.8%
90% CI	9.5-25.9%	10.5-27.2%	11.9-28.7%	12.9-29.9%	14.4-31.7%	15.7-33.1%	17.0-34.7%	20.7-39.0%
12-hr	16.9%	18.0%	19.4%	20.6%	22.2%	23.5%	25.0%	28.9%
90% CI	11.0-22.8%	12.0-24.0%	13.4-25.5%	14.5-26.7%	16.0-28.4%	17.3-29.8%	18.6-31.3%	22.4-35.5%
24-hr	16.1%	17.2%	18.6%	19.7%	21.3%	22.7%	24.1%	28.0%
90% CI	6.3-25.9%	7.3-27.1%	8.6-28.6%	9.6-29.9%	11.1-31.6%	12.3-33.0%	13.6-34.6%	17.2-38.9%
2-day	17.1%	18.3%	19.7%	20.8%	22.4%	23.8%	25.3%	29.2%
90% CI	6.5-27.7%	7.6-29.0%	8.9-30.5%	9.9-31.8%	11.4-33.5%	12.6-35.0%	13.9-36.6%	17.5-40.9%
3-day	16.1%	17.2%	18.6%	19.8%	21.4%	22.7%	24.2%	28.1%
90% CI	7.1-25.1%	8.1-26.3%	9.5-27.8%	10.5-29.0%	12.0-30.8%	13.2-32.2%	14.5-33.8%	18.1-38.0%

Table B8. Percent Change in Precipitation Depth for Scaling Historical Atlas 14 to 2055 under SSP5-8.5 (Based on CMIP6 C-C Trend for 2055 applied to interpolated WRF C-C Scale Factor)

Duration	Return Period							
	1-yr	2-yr	5-yr	10-yr	25-yr	50-yr	100-yr	500-yr
15-min	28.0%	29.4%	31.1%	32.4%	34.3%	35.8%	37.5%	42.0%
90% CI	19.1-36.9%	20.4-38.4%	22.0-40.2%	23.2-41.6%	25.0-43.6%	26.4-45.3%	27.9-47.1%	32.1-51.8%
30-min	27.8%	29.2%	30.9%	32.3%	34.1%	35.7%	37.3%	41.8%
90% CI	18.3-37.4%	19.5-38.9%	21.1-40.7%	22.4-42.2%	24.1-44.2%	25.5-45.8%	27.1-47.6%	31.2-52.4%
60-min	26.8%	28.1%	29.8%	31.2%	33.0%	34.6%	36.2%	40.6%
90% CI	16.3-37.2%	17.5-38.7%	19.1-40.6%	20.3-42.0%	22.0-44.0%	23.4-45.7%	24.9-47.5%	29.0-52.2%
2-hr	24.3%	25.6%	27.3%	28.6%	30.4%	31.9%	33.5%	37.9%
90% CI	13.9-34.6%	15.1-36.1%	16.7-37.9%	17.9-39.3%	19.5-41.3%	20.9-42.9%	22.4-44.7%	26.3-49.4%
3-hr	23.5%	24.8%	26.5%	27.8%	29.6%	31.1%	32.7%	37.0%
90% CI	12.9-34.1%	14.1-35.5%	15.6-37.4%	16.8-38.8%	18.5-40.8%	19.8-42.4%	21.3-44.1%	25.2-48.8%
6-hr	20.4%	21.7%	23.3%	24.5%	26.3%	27.8%	29.3%	33.5%
90% CI	11.2-29.6%	12.4-31.0%	13.8-32.7%	15.0-34.1%	16.6-36.0%	17.9-37.6%	19.4-39.3%	23.2-43.8%
12-hr	19.1%	20.4%	22.0%	23.2%	24.9%	26.4%	27.9%	32.1%
90% CI	12.2-26.0%	13.4-27.4%	14.9-29.1%	16.0-30.4%	17.7-32.2%	19.0-33.8%	20.4-35.4%	24.3-39.8%
24-hr	18.1%	19.4%	21.0%	22.2%	23.9%	25.3%	26.8%	30.9%
90% CI	7.8-28.4%	9.0-29.8%	10.4-31.5%	11.5-32.8%	13.1-34.7%	14.4-36.2%	15.8-37.9%	19.5-42.4%
2-day	19.2%	20.4%	22.0%	23.3%	25.0%	26.5%	28.0%	32.1%
90% CI	8.4-29.9%	9.6-31.3%	11.0-33.0%	12.2-34.4%	13.8-36.3%	15.1-37.8%	16.5-39.5%	20.2-44.0%
3-day	18.2%	19.5%	21.1%	22.3%	24.1%	25.5%	27.0%	31.1%
90% CI	9.1-27.4%	10.2-28.8%	11.7-30.5%	12.8-31.8%	14.4-33.7%	15.7-35.2%	17.1-36.9%	20.9-41.3%

Table B9. Percent Change in Precipitation Depth for Scaling Historical Atlas 14 to 2060 under SSP5-8.5 (Based on CMIP6 C-C Trend for 2060 applied to interpolated WRF C-C Scale Factor)

Duration	Return Period							
	1-yr	2-yr	5-yr	10-yr	25-yr	50-yr	100-yr	500-yr
15-min	30.0%	31.6%	33.5%	34.9%	37.0%	38.6%	40.4%	45.0%
90% CI	21.0-39.0%	22.5-40.7%	24.3-42.7%	25.6-44.3%	27.5-46.4%	29.0-48.2%	30.6-50.1%	35.0-55.1%
30-min	30.0%	31.5%	33.4%	34.9%	36.9%	38.5%	40.3%	44.9%
90% CI	20.2-39.8%	21.6-41.4%	23.4-43.5%	24.7-45.1%	26.6-47.2%	28.1-49.0%	29.7-50.9%	34.0-55.9%
60-min	29.1%	30.6%	32.5%	34.0%	36.0%	37.6%	39.3%	44.0%
90% CI	18.3-39.9%	19.7-41.6%	21.4-43.6%	22.7-45.2%	24.6-47.4%	26.0-49.1%	27.6-51.0%	31.9-56.0%
2-hr	26.7%	28.3%	30.1%	31.5%	33.5%	35.1%	36.8%	41.4%
90% CI	15.9-37.6%	17.3-39.2%	19.0-41.3%	20.3-42.8%	22.1-44.9%	23.5-46.7%	25.1-48.5%	29.3-53.5%
3-hr	25.9%	27.4%	29.3%	30.7%	32.6%	34.2%	35.9%	40.4%
90% CI	14.5-37.2%	15.9-38.9%	17.6-40.9%	18.8-42.5%	20.6-44.6%	22.1-46.4%	23.6-48.2%	27.7-53.2%
6-hr	22.4%	23.9%	25.7%	27.1%	29.0%	30.5%	32.2%	36.6%
90% CI	12.3-32.6%	13.6-34.2%	15.3-36.1%	16.5-37.6%	18.2-39.7%	19.6-41.4%	21.1-43.2%	25.1-48.0%
12-hr	20.7%	22.1%	23.9%	25.2%	27.1%	28.6%	30.3%	34.6%
90% CI	12.8-28.6%	14.1-30.1%	15.8-32.0%	17.0-33.5%	18.7-35.5%	20.1-37.1%	21.7-38.9%	25.7-43.5%
24-hr	19.5%	20.9%	22.7%	24.0%	25.8%	27.3%	29.0%	33.2%
90% CI	8.8-30.2%	10.1-31.8%	11.7-33.7%	12.9-35.1%	14.5-37.2%	15.9-38.8%	17.4-40.6%	21.3-45.2%
2-day	20.6%	22.0%	23.8%	25.1%	27.0%	28.5%	30.1%	34.4%
90% CI	9.8-31.4%	11.1-33.0%	12.7-34.9%	13.9-36.4%	15.6-38.4%	17.0-40.0%	18.4-41.8%	22.4-46.5%
3-day	19.8%	21.2%	23.0%	24.3%	26.1%	27.7%	29.3%	33.6%
90% CI	10.4-29.2%	11.8-30.7%	13.4-32.6%	14.6-34.0%	16.3-36.0%	17.7-37.6%	19.2-39.4%	23.1-44.0%

Table B10. Percent Change in Precipitation Depth for Scaling Historical Atlas 14 to 2065 under SSP5-8.5 (Based on CMIP6 C-C Trend for 2065 applied to interpolated WRF C-C Scale Factor)

Duration	Return Period							
	1-yr	2-yr	5-yr	10-yr	25-yr	50-yr	100-yr	500-yr
15-min	32.2%	33.9%	36.0%	37.6%	39.8%	41.5%	43.3%	48.2%
90% CI	23.1-41.3%	24.7-43.2%	26.7-45.4%	28.1-47.1%	30.1-49.4%	31.7-51.2%	33.5-53.2%	38.0-58.4%
30-min	32.2%	34.0%	36.0%	37.6%	39.8%	41.5%	43.4%	48.3%
90% CI	22.2-42.3%	23.8-44.1%	25.7-46.4%	27.1-48.1%	29.1-50.4%	30.7-52.3%	32.4-54.3%	37.0-59.5%
60-min	31.5%	33.2%	35.3%	36.9%	39.0%	40.8%	42.6%	47.5%
90% CI	20.3-42.7%	21.9-44.5%	23.8-46.8%	25.2-48.5%	27.2-50.8%	28.8-52.7%	30.5-54.7%	34.9-60.0%
2-hr	29.3%	31.0%	33.1%	34.6%	36.8%	38.5%	40.3%	45.1%
90% CI	18.0-40.6%	19.6-42.5%	21.4-44.8%	22.8-46.4%	24.8-48.7%	26.3-50.6%	28.0-52.6%	32.3-57.8%
3-hr	28.4%	30.1%	32.1%	33.7%	35.8%	37.5%	39.3%	44.0%
90% CI	16.2-40.5%	17.8-42.4%	19.6-44.7%	21.0-46.3%	22.9-48.7%	24.4-50.5%	26.0-52.5%	30.3-57.7%
6-hr	24.6%	26.3%	28.2%	29.7%	31.7%	33.4%	35.1%	39.7%
90% CI	13.5-35.7%	15.0-37.5%	16.8-39.7%	18.1-41.3%	19.9-43.6%	21.4-45.4%	23.0-47.3%	27.2-52.3%
12-hr	22.4%	24.0%	26.0%	27.4%	29.4%	31.0%	32.7%	37.2%
90% CI	13.5-31.3%	15.0-33.1%	16.7-35.2%	18.1-36.7%	19.9-38.9%	21.4-40.6%	22.9-42.5%	27.1-47.3%
24-hr	21.0%	22.6%	24.5%	25.9%	27.9%	29.5%	31.2%	35.6%
90% CI	9.9-32.2%	11.3-33.9%	13.0-36.0%	14.3-37.6%	16.1-39.7%	17.5-41.5%	19.0-43.3%	23.1-48.2%
2-day	22.1%	23.7%	25.6%	27.1%	29.1%	30.7%	32.4%	36.9%
90% CI	11.2-33.1%	12.6-34.8%	14.4-36.9%	15.7-38.5%	17.5-40.6%	19.0-42.4%	20.5-44.2%	24.6-49.1%
3-day	21.4%	23.0%	24.9%	26.4%	28.3%	29.9%	31.6%	36.1%
90% CI	11.9-31.0%	13.4-32.7%	15.1-34.7%	16.5-36.3%	18.3-38.4%	19.7-40.1%	21.3-42.0%	25.4-46.8%

Table B11. Percent Change in Precipitation Depth for Scaling Historical Atlas 14 to 2070 under SSP5-8.5 (Based on CMIP6 C-C Trend for 2070 applied to interpolated WRF C-C Scale Factor)

Duration	Return Period							
	1-yr	2-yr	5-yr	10-yr	25-yr	50-yr	100-yr	500-yr
15-min	34.8%	36.7%	39.0%	40.7%	43.0%	44.9%	46.8%	52.0%
90% CI	25.6-44.1%	27.4-46.1%	29.5-48.6%	31.1-50.4%	33.2-52.8%	34.9-54.8%	36.8-56.9%	41.5-62.4%
30-min	34.9%	36.8%	39.1%	40.8%	43.1%	45.0%	46.9%	52.1%
90% CI	24.6-45.3%	26.3-47.3%	28.4-49.8%	30.0-51.6%	32.1-54.1%	33.8-56.1%	35.7-58.2%	40.4-63.8%
60-min	34.4%	36.3%	38.6%	40.3%	42.6%	44.4%	46.4%	51.5%
90% CI	22.8-45.9%	24.5-48.0%	26.6-50.5%	28.2-52.4%	30.3-54.9%	32.0-56.9%	33.8-59.0%	38.4-64.6%
2-hr	32.4%	34.3%	36.5%	38.2%	40.5%	42.3%	44.2%	49.3%
90% CI	20.5-44.2%	22.3-46.3%	24.3-48.8%	25.8-50.6%	27.9-53.1%	29.5-55.1%	31.3-57.2%	35.9-62.7%
3-hr	31.3%	33.2%	35.5%	37.1%	39.4%	41.2%	43.1%	48.1%
90% CI	18.3-44.4%	20.0-46.4%	22.0-48.9%	23.5-50.7%	25.5-53.2%	27.1-55.2%	28.9-57.3%	33.4-62.9%
6-hr	27.2%	29.0%	31.2%	32.8%	35.0%	36.7%	38.6%	43.4%
90% CI	15.1-39.4%	16.7-41.4%	18.6-43.8%	20.1-45.5%	22.0-48.0%	23.6-49.9%	25.2-51.9%	29.6-57.2%
12-hr	24.5%	26.3%	28.4%	30.0%	32.1%	33.8%	35.6%	40.3%
90% CI	14.6-34.5%	16.2-36.5%	18.1-38.8%	19.5-40.5%	21.4-42.8%	23.0-44.6%	24.6-46.6%	29.0-51.7%
24-hr	22.9%	24.7%	26.8%	28.3%	30.4%	32.1%	33.8%	38.5%
90% CI	11.3-34.6%	12.8-36.5%	14.7-38.8%	16.1-40.5%	18.0-42.8%	19.5-44.6%	21.1-46.6%	25.3-51.7%
2-day	24.1%	25.8%	27.9%	29.5%	31.6%	33.3%	35.1%	39.8%
90% CI	13.0-35.1%	14.6-37.0%	16.5-39.3%	17.9-41.0%	19.8-43.3%	21.4-45.2%	23.0-47.1%	27.3-52.2%
3-day	23.5%	25.2%	27.3%	28.9%	31.0%	32.7%	34.5%	39.1%
90% CI	13.8-33.2%	15.4-35.1%	17.3-37.4%	18.7-39.0%	20.7-41.3%	22.2-43.1%	23.9-45.0%	28.2-50.1%

Table B12. Percent Change in Precipitation Depth for Scaling Historical Atlas 14 to 2075 under SSP5-8.5 (Based on CMIP6 C-C Trend for 2075 applied to interpolated WRF C-C Scale Factor)

Duration	Return Period							
	1-yr	2-yr	5-yr	10-yr	25-yr	50-yr	100-yr	500-yr
15-min	37.5%	39.6%	42.1%	44.0%	46.4%	48.4%	50.4%	55.8%
90% CI	28.1-46.9%	30.1-49.2%	32.4-51.8%	34.1-53.8%	36.4-56.4%	38.3-58.5%	40.2-60.7%	45.2-66.5%
30-min	37.7%	39.8%	42.3%	44.2%	46.6%	48.6%	50.7%	56.1%
90% CI	27.1-48.4%	29.0-50.7%	31.3-53.4%	33.0-55.3%	35.3-58.0%	37.1-60.1%	39.0-62.3%	44.0-68.2%
60-min	37.4%	39.5%	42.0%	43.8%	46.3%	48.2%	50.3%	55.7%
90% CI	25.4-49.3%	27.3-51.7%	29.6-54.4%	31.2-56.4%	33.5-59.0%	35.3-61.2%	37.2-63.4%	42.1-69.3%
2-hr	35.5%	37.6%	40.1%	41.9%	44.4%	46.3%	48.3%	53.7%
90% CI	23.1-47.9%	25.0-50.2%	27.3-52.9%	28.9-54.9%	31.1-57.6%	32.9-59.7%	34.7-61.9%	39.6-67.8%
3-hr	34.4%	36.5%	38.9%	40.7%	43.1%	45.1%	47.1%	52.4%
90% CI	20.5-48.3%	22.4-50.6%	24.5-53.3%	26.1-55.3%	28.3-58.0%	30.0-60.1%	31.8-62.4%	36.5-68.2%
6-hr	29.9%	31.9%	34.3%	36.0%	38.3%	40.2%	42.2%	47.2%
90% CI	16.7-43.2%	18.5-45.4%	20.6-48.0%	22.1-49.9%	24.2-52.5%	25.8-54.6%	27.6-56.7%	32.1-62.4%
12-hr	26.7%	28.7%	31.0%	32.6%	34.9%	36.7%	38.6%	43.6%
90% CI	15.6-37.8%	17.4-40.0%	19.4-42.5%	21.0-44.3%	23.0-46.8%	24.6-48.8%	26.4-50.9%	30.9-56.3%
24-hr	24.9%	26.8%	29.1%	30.7%	33.0%	34.7%	36.6%	41.5%
90% CI	12.7-37.1%	14.4-39.2%	16.5-41.7%	17.9-43.5%	20.0-46.0%	21.5-47.9%	23.2-50.0%	27.6-55.3%
2-day	26.1%	28.0%	30.2%	31.9%	34.2%	36.0%	37.8%	42.8%
90% CI	14.8-37.3%	16.6-39.4%	18.7-41.8%	20.2-43.7%	22.2-46.1%	23.9-48.0%	25.6-50.1%	30.1-55.5%
3-day	25.6%	27.5%	29.8%	31.5%	33.7%	35.5%	37.4%	42.3%
90% CI	15.7-35.5%	17.4-37.6%	19.5-40.1%	21.1-41.9%	23.1-44.3%	24.8-46.2%	26.5-48.2%	31.0-53.5%

Table B13. Percent Change in Precipitation Depth for Scaling Historical Atlas 14 to 2080 under SSP5-8.5 (Based on CMIP6 C-C Trend for 2080 applied to interpolated WRF C-C Scale Factor)

Duration	Return Period							
	1-yr	2-yr	5-yr	10-yr	25-yr	50-yr	100-yr	500-yr
15-min	40.7%	43.0%	45.7%	47.7%	50.3%	52.4%	54.6%	60.2%
90% CI	31.1-50.2%	33.3-52.7%	35.8-55.6%	37.6-57.7%	40.1-60.5%	42.0-62.7%	44.1-65.1%	49.4-71.1%
30-min	41.0%	43.3%	46.0%	48.0%	50.6%	52.7%	54.9%	60.6%
90% CI	29.9-52.0%	32.1-54.5%	34.6-57.4%	36.4-59.5%	38.8-62.4%	40.8-64.6%	42.8-67.0%	48.0-73.1%
60-min	40.8%	43.1%	45.8%	47.8%	50.5%	52.5%	54.7%	60.4%
90% CI	28.3-53.2%	30.5-55.8%	32.9-58.7%	34.7-60.9%	37.1-63.8%	39.0-66.0%	41.0-68.4%	46.2-74.6%
2-hr	39.2%	41.5%	44.2%	46.1%	48.7%	50.8%	53.0%	58.6%
90% CI	26.1-52.2%	28.2-54.7%	30.7-57.6%	32.4-59.8%	34.8-62.7%	36.7-64.9%	38.6-67.3%	43.7-73.4%
3-hr	37.9%	40.2%	42.9%	44.8%	47.4%	49.4%	51.6%	57.2%
90% CI	23.1-52.8%	25.1-55.3%	27.5-58.3%	29.2-60.4%	31.5-63.3%	33.3-65.6%	35.2-68.0%	40.2-74.2%
6-hr	33.0%	35.2%	37.8%	39.7%	42.2%	44.1%	46.2%	51.6%
90% CI	18.7-47.4%	20.6-49.9%	22.9-52.8%	24.5-54.8%	26.7-57.6%	28.5-59.8%	30.3-62.1%	35.1-68.1%
12-hr	29.3%	31.4%	33.9%	35.7%	38.2%	40.1%	42.1%	47.3%
90% CI	17.0-41.6%	18.9-44.0%	21.2-46.7%	22.8-48.7%	24.9-51.4%	26.7-53.5%	28.5-55.7%	33.2-61.4%
24-hr	27.3%	29.4%	31.8%	33.6%	35.9%	37.8%	39.8%	44.9%
90% CI	14.5-40.0%	16.4-42.3%	18.6-45.0%	20.2-47.0%	22.3-49.6%	24.0-51.7%	25.7-53.8%	30.3-59.5%
2-day	28.4%	30.5%	33.0%	34.8%	37.2%	39.1%	41.1%	46.2%
90% CI	17.0-39.8%	19.0-42.1%	21.2-44.8%	22.8-46.7%	25.0-49.4%	26.7-51.4%	28.6-53.6%	33.3-59.2%
3-day	28.1%	30.2%	32.7%	34.5%	36.9%	38.7%	40.7%	45.9%
90% CI	17.9-38.3%	19.9-40.6%	22.1-43.2%	23.8-45.1%	26.0-47.7%	27.7-49.8%	29.6-51.9%	34.3-57.5%

Table B14. Percent Change in Precipitation Depth for Scaling Historical Atlas 14 to 2085 under SSP5-8.5 (Based on CMIP6 C-C Trend for 2085 applied to interpolated WRF C-C Scale Factor)

Duration	Return Period							
	1-yr	2-yr	5-yr	10-yr	25-yr	50-yr	100-yr	500-yr
15-min	44.5%	47.0%	50.0%	52.1%	54.9%	57.2%	59.5%	65.5%
90% CI	34.7-54.3%	37.1-57.0%	39.9-60.1%	41.8-62.4%	44.5-65.4%	46.5-67.8%	48.7-70.2%	54.3-76.6%
30-min	44.9%	47.4%	50.4%	52.5%	55.4%	57.6%	59.9%	65.9%
90% CI	33.5-56.3%	35.8-59.1%	38.6-62.3%	40.5-64.6%	43.1-67.6%	45.2-70.0%	47.3-72.5%	52.8-79.0%
60-min	44.9%	47.5%	50.4%	52.6%	55.4%	57.6%	60.0%	66.0%
90% CI	31.9-57.9%	34.3-60.7%	37.0-63.9%	38.9-66.3%	41.5-69.4%	43.5-71.8%	45.6-74.3%	51.1-80.9%
2-hr	43.5%	46.0%	48.9%	51.1%	53.9%	56.1%	58.4%	64.3%
90% CI	29.8-57.2%	32.1-59.9%	34.7-63.2%	36.6-65.5%	39.2-68.6%	41.2-71.0%	43.2-73.5%	48.6-80.0%
3-hr	42.1%	44.6%	47.5%	49.6%	52.4%	54.6%	56.9%	62.8%
90% CI	26.2-58.0%	28.4-60.8%	31.0-64.1%	32.9-66.4%	35.3-69.5%	37.3-71.9%	39.3-74.5%	44.5-81.1%
6-hr	36.8%	39.2%	42.0%	44.1%	46.7%	48.8%	51.0%	56.7%
90% CI	21.2-52.5%	23.3-55.2%	25.8-58.3%	27.5-60.6%	29.9-63.6%	31.7-65.9%	33.7-68.4%	38.7-74.7%
12-hr	32.5%	34.8%	37.6%	39.5%	42.1%	44.1%	46.2%	51.7%
90% CI	18.9-46.1%	21.0-48.7%	23.4-51.7%	25.2-53.8%	27.5-56.7%	29.3-58.9%	31.2-61.3%	36.1-67.4%
24-hr	30.2%	32.5%	35.2%	37.1%	39.6%	41.6%	43.7%	49.1%
90% CI	16.8-43.6%	18.9-46.1%	21.2-49.1%	22.9-51.2%	25.2-54.0%	27.0-56.2%	28.9-58.5%	33.7-64.4%
2-day	31.4%	33.7%	36.4%	38.3%	40.9%	42.9%	45.0%	50.4%
90% CI	19.8-43.0%	21.9-45.5%	24.3-48.4%	26.1-50.5%	28.4-53.3%	30.3-55.5%	32.2-57.8%	37.1-63.7%
3-day	31.2%	33.5%	36.2%	38.1%	40.7%	42.7%	44.8%	50.2%
90% CI	20.8-41.7%	22.9-44.2%	25.3-47.1%	27.1-49.1%	29.5-51.9%	31.3-54.1%	33.3-56.3%	38.2-62.2%

Table B15. Percent Change in Precipitation Depth for Scaling Historical Atlas 14 to 2090 under SSP5-8.5 (Based on CMIP6 C-C Trend for 2090 applied to interpolated WRF C-C Scale Factor)

Duration	Return Period							
	1-yr	2-yr	5-yr	10-yr	25-yr	50-yr	100-yr	500-yr
15-min	48.1%	50.8%	54.0%	56.3%	59.3%	61.7%	64.1%	70.4%
90% CI	38.1-58.0%	40.7-61.0%	43.7-64.4%	45.8-66.8%	48.6-70.0%	50.8-72.5%	53.1-75.2%	59.0-81.9%
30-min	48.6%	51.4%	54.6%	56.9%	59.9%	62.2%	64.7%	71.0%
90% CI	36.8-60.4%	39.3-63.4%	42.3-66.8%	44.4-69.3%	47.2-72.6%	49.3-75.1%	51.6-77.8%	57.4-84.6%
60-min	48.8%	51.6%	54.8%	57.1%	60.1%	62.5%	65.0%	71.3%
90% CI	35.3-62.3%	37.8-65.4%	40.8-68.9%	42.9-71.4%	45.6-74.7%	47.8-77.3%	50.0-79.9%	55.7-86.8%
2-hr	47.6%	50.3%	53.5%	55.8%	58.8%	61.1%	63.6%	69.9%
90% CI	33.2-61.9%	35.7-65.0%	38.6-68.5%	40.6-71.0%	43.3-74.3%	45.4-76.9%	47.6-79.5%	53.3-86.4%
3-hr	46.1%	48.8%	52.0%	54.2%	57.2%	59.5%	62.0%	68.2%
90% CI	29.1-63.1%	31.5-66.1%	34.3-69.7%	36.3-72.2%	38.9-75.5%	41.0-78.1%	43.1-80.8%	48.6-87.7%
6-hr	40.4%	43.0%	46.0%	48.2%	51.1%	53.3%	55.6%	61.6%
90% CI	23.4-57.3%	25.8-60.2%	28.4-63.7%	30.3-66.1%	32.8-69.3%	34.8-71.8%	36.8-74.4%	42.0-81.1%
12-hr	35.5%	38.0%	40.9%	43.0%	45.8%	47.9%	50.2%	55.9%
90% CI	20.6-50.4%	22.8-53.2%	25.4-56.4%	27.3-58.8%	29.7-61.8%	31.6-64.2%	33.6-66.7%	38.7-73.1%
24-hr	32.9%	35.4%	38.3%	40.3%	43.0%	45.1%	47.3%	53.0%
90% CI	18.9-47.0%	21.1-49.7%	23.7-52.9%	25.5-55.1%	27.9-58.1%	29.8-60.5%	31.7-62.9%	36.8-69.1%
2-day	34.1%	36.6%	39.5%	41.6%	44.3%	46.4%	48.7%	54.3%
90% CI	22.3-46.0%	24.6-48.7%	27.2-51.8%	29.1-54.1%	31.6-57.0%	33.5-59.3%	35.6-61.8%	40.7-67.9%
3-day	34.1%	36.6%	39.5%	41.6%	44.3%	46.4%	48.6%	54.3%
90% CI	23.4-44.8%	25.7-47.5%	28.3-50.7%	30.2-52.9%	32.7-55.8%	34.7-58.1%	36.7-60.5%	42.0-66.7%

Table B16. Percent Change in Precipitation Depth for Scaling Historical Atlas 14 to 2095 under SSP5-8.5 (Based on CMIP6 C-C Trend for 2095 applied to interpolated WRF C-C Scale Factor)

Duration	Return Period							
	1-yr	2-yr	5-yr	10-yr	25-yr	50-yr	100-yr	500-yr
15-min	51.7%	54.7%	58.2%	60.6%	63.8%	66.3%	68.9%	75.5%
90% CI	41.6-61.9%	44.4-65.1%	47.6-68.7%	49.9-71.4%	52.9-74.8%	55.2-77.4%	57.6-80.2%	63.8-87.2%
30-min	52.3%	55.3%	58.8%	61.3%	64.5%	67.0%	69.6%	76.2%
90% CI	40.1-64.5%	42.9-67.8%	46.1-71.5%	48.3-74.2%	51.3-77.7%	53.6-80.4%	56.0-83.2%	62.1-90.3%
60-min	52.8%	55.8%	59.3%	61.8%	65.0%	67.5%	70.1%	76.7%
90% CI	38.7-66.8%	41.5-70.1%	44.7-73.9%	46.9-76.6%	49.8-80.1%	52.1-82.9%	54.5-85.7%	60.5-93.0%
2-hr	51.7%	54.7%	58.2%	60.6%	63.9%	66.3%	68.9%	75.5%
90% CI	36.7-66.8%	39.4-70.1%	42.5-73.9%	44.7-76.6%	47.6-80.1%	49.8-82.9%	52.1-85.7%	58.1-93.0%
3-hr	50.1%	53.1%	56.5%	59.0%	62.1%	64.6%	67.2%	73.7%
90% CI	32.1-68.2%	34.7-71.6%	37.7-75.4%	39.8-78.1%	42.6-81.6%	44.8-84.4%	47.0-87.3%	52.8-94.6%
6-hr	44.0%	46.8%	50.1%	52.4%	55.5%	57.8%	60.3%	66.6%
90% CI	25.7-62.2%	28.2-65.4%	31.1-69.1%	33.1-71.8%	35.8-75.2%	37.8-77.8%	40.0-80.6%	45.5-87.7%
12-hr	38.5%	41.2%	44.4%	46.6%	49.5%	51.8%	54.2%	60.2%
90% CI	22.2-54.7%	24.6-57.8%	27.4-61.3%	29.4-63.8%	32.0-67.1%	34.0-69.6%	36.1-72.3%	41.4-79.0%
24-hr	35.7%	38.3%	41.4%	43.6%	46.5%	48.7%	51.0%	56.9%
90% CI	21.0-50.3%	23.4-53.3%	26.1-56.7%	28.1-59.2%	30.6-62.3%	32.6-64.8%	34.7-67.4%	39.9-73.9%
2-day	36.9%	39.6%	42.7%	44.9%	47.8%	50.1%	52.4%	58.4%
90% CI	24.9-48.9%	27.3-51.9%	30.2-55.2%	32.2-57.6%	34.8-60.8%	36.9-63.2%	39.0-65.8%	44.4-72.3%
3-day	37.0%	39.7%	42.8%	45.0%	47.9%	50.2%	52.5%	58.5%
90% CI	26.0-48.0%	28.5-50.9%	31.3-54.3%	33.4-56.7%	36.0-59.8%	38.1-62.3%	40.2-64.8%	45.7-71.2%

Table B17. Percent Change in Precipitation Depth for Scaling Historical Atlas 14 to 2100 under SSP5-8.5 (Based on CMIP6 C-C Trend for 2100 applied to interpolated WRF C-C Scale Factor)